ADDIS ABABA UNIVERSITY

COLLEGE OF HEALTH SCIENCES

SCHOOL OF PHARMACY

DEPARTMENT OF PHARMACEUTICS AND SOCIAL PHARMACY

Preparation and Characterization of Cellulose from Bamboo Wood and Eucalyptus Sawdust, and Evaluation of the Derivative Sodium Carboxymethyl Celluloses as Suspending Agents

Sine Gebreegziabher

September, 2024

Addis Ababa, Ethiopia

Preparation and Characterization of Cellulose from Bamboo Wood and Eucalyptus Sawdust, and Evaluation of the Derivative Sodium Carboxymethyl Celluloses as Suspending Agents

A Thesis Submitted to the School of Pharmacy, Addis Ababa University, Department of Pharmaceutics and Social Pharmacy, in Partial Fulfillment of the Requirements for the Degree of Master of Science in Pharmaceutics.

Sine Gebreegziabher

Under the Supervision of Prof. Tsige Gebre-Mariam and Prof. Anteneh Belete, Department of Pharmaceutics and Social Pharmacy, School of Pharmacy, Addis Ababa University

September, 2024

Addis Ababa, Ethiopia

Addis Ababa University

School of Pharmacy

This is to certify that the thesis undertaken by Sine Gebreegziabher, entitled "Preparation and Characterization of Cellulose from Bamboo Wood and Eucalyptus Sawdust, and Evaluation of the Derivative Sodium Carboxymethyl Celluloses as Suspending Agents" and submitted in partial fulfilment of the requirements for the Degree of Master of Science in Pharmaceutics complies with the regulations of the University and meets the accepted standards with respect to originality and quality.

Approved and Signed by the Examining Committee:

Name	**Signature**	**Date**
Prof. Tsige Gebre-Mariam (Advisor)	_____	_____
Prof. Anteneh Belete (Advisor)	_____	_____
Dr. Admassu Assen (External Examiner)	_____	_____
Mr. Muluken Nigatu (Internal Examiner)	_____	_____

_____

Head, Department of Pharmaceutics and Social Pharmacy, School of Pharmacy, Addis Ababa University

Acknowledgments

First of all, I would like to thank almighty God for giving me strength and patience throughout the entire situation and challenge that I faced for successful completion of this study. I express my deep sense of gratitude to my research supervisors Prof. Tsige Gebre-Mariam and Prof. Anteneh Belete for their assistance, invaluable comments, constructive suggestions and excellent supervision throughout my research work.

I would also like to acknowledge Cadila Pharmaceuticals Ethiopia PLC for FTIR study and Ethiopian Pharmaceutical Factory Sh. Co (EPHARM), for providing the model paracetamol drug. My special thanks also go to Adama Science and Technology University, Department of Materials Science Engineering, for XRD study and Leather Industry Development Institute for thermal analysis.

I would also like to thank Dr. Tesfaye Gabriel for supporting me during my research work and Mr. Fekade Tefera and Mr. Abraham Temesgen for their technical support in the laboratory. I am highly indebted to all other staff members of the Department of Pharmaceutics and Social Pharmacy. Furthermore, I would like to thank my family and all my friends who provided me with all-rounded support throughout my study. Finally, I would like to acknowledge Addis Ababa University for sponsoring my postgraduate studies.

Abstract

Cellulose has gained a great deal of interest from researchers due to its high demand in paper, food, cosmetics, textile and pharmaceutical industries. Woody plants and cotton are the major sources of cellulose and its derivatives such as sodium carboxymethyl cellulose, microcrystalline cellulose, cellulose acetate and hydroxypropyl cellulose. However, overutilization of these sources has raised huge economic and environmental concerns forcing researchers and stakeholders to look for other potential substitutes. In Ethiopia, bamboo wood (BW) and eucalyptus sawdust (ES) are abundant and can be exploited as potential raw materials for cellulose extraction.

The aim of this study was therefore to extract and characterize native cellulose from BW and ES, and evaluate the derivatives BW-SCMC and ES-SCMC as suspending agents in suspension formulations. In this study, cellulose fibers were extracted from the aforementioned sources by steam explosion method. SCMC was obtained from the extracted cellulose fibers, following alkalinization and etherification steps using sodium hydroxide and monochloroacetic acid (MCA) in isopropyl alcohol. Central composite design (CCD) with three coded values was employed. The amount of MCA, duration of etherification and temperature of etherification were selected as independent variables; and the degree of substitution (DS) was taken as the response variable during optimization. By comparing several statistical parameters, two quadratic models were selected as best fit for DS of BW-SCMC and ES-SCMC. The adequacy of the models as per ANOVA revealed that both models have significant values indicating the terms in the models have significant effect ($P < 0.0001$) on the response.

The cellulose yields on dry weight basis were found to be 48.06% ± 1.02 (BWC) and 44.21% ± 1.14 (ESC). The isolated BWC and ESC have DP of 524.64±0.89 and 701.51±1.16, and molecular weight of 84,990.87 g/mol and 113,644.62 g/mol, respectively. The crystallinity index of BWC and ESC was found to be 74.3% and 79.2%, respectively. Furthermore, Fourier transform infrared (FTIR) spectra's indicated removal of non-cellulosic constituents.

An optimum DS of 1.432 was found for BW-SCMC at the level of 1.47g of MCA, 188 min of etherification process and 48.5^{o}C of etherification temperature with a desirability of 1.000. Whereas optimum DS of 1.141 was found for ES-SCMC at the level of 1.17g of MCA, 166.3 min of etherification process and 53.65^{o}C of etherification temperature with a desirability of 0.967.

Analysis of the triplicates synthesized BW-SCMC and ES-SCMC at the optimum conditions confirmed the effectiveness of optimization. The experimental values were found to be in close agreement with the predicted values confirming the predictability and validity of the model.

The optimized SCMC had a yield of 1.58 g/g (BW-SCMC) and 1.31g/g (ES-SCMC) of BWC and ESC, respectively. The appearance of new bands around 1600 and 1412 cm^{-1} in the FTIR spectra of SCMC samples showed efficient attachment of carboxymethyl groups to the cellulose chains. The XRD analyses of the SCMC samples showed a significant reduction in crystallinity with the main diffraction signal at $2\theta = 20°$. From the TGA, the Tmax of the synthesized SCMC ranged from 285-296 °C. The BW-SCMC (DS: 1.432) exhibited better heat stability than ES-SCMC (1.141) and C-SCMC (DS: 0.87).

The prepared BW-SCMC and ES-SCMC were evaluated as suspending agents in paracetamol suspensions in comparison with commercial SCMC (C-SCMC) at a concentration range of 1–4% (w/v). The resulting suspensions were evaluated for their sedimentation volume (%), degree of flocculation, viscosity, redispersibility and dissolution rate, and real time stability studies were performed for 3 months. The apparent viscosities of the formulations prepared with BW-SCMC and ES-SCMC were higher than those of C-SCMC. The flowability of the suspensions, at all concentration levels of the suspending agents were in the order of C-SCMC > ES-SCMC > BW-SCMC. At 1% and 2 % concentrations, BW-SCMC and ES-SCMC provided higher sedimentation volume than C-SCMC. At 3% and 4%, all exhibited comparable sedimentation volume (100%). Potassium dihydrogen phosphate (KH_2PO_4) employed as a flocculating agent increased the sedimentation volume of all suspension formulations at 1% and 2%. The redispersibility of BW-SCMC and ES-SCMC were better than C-SCMC at lower concentration. All prepared suspensions showed a release of greater than 85% of drug within 1 h. The results of stability studies showed that all suspension formulations were stable. From the findings, it can be concluded that BW-SCMC and ES-SCMC could be used as alternative suspending agents.

Keywords: Bamboo wood, Eucalyptus sawdust, Cellulose, Sodium carboxymethyl cellulose, Suspending agent, Steam explosion

Table of Contents

List of Tables

List of Figures

Acronyms and abbreviations

AGU:	Anhydroglucose units
ANOVA:	Analysis of variance
ASTM:	American standard test methods
BP:	British pharmacopoeia
BW:	Bamboo wood
BWC:	Bamboo wood cellulose
BW-SCMC:	Bamboo wood sodium carboxymethyl cellulose
CCD:	Central composite design
C-SCMC:	Commercial sodium carboxymethyl cellulose
CrI:	Crystallinity index
Cuam:	Cuprammonium hydroxide
DP:	Degree of polymerization
DS:	Degree of substitution
DTA:	Differential thermal analysis
ES:	Eucalyptus sawdust
ESC:	Eucalyptus sawdust cellulose
ES-SCMC:	Eucalyptus sawdust sodium carboxymethyl cellulose
FTIR:	Fourier Transform Infrared Spectroscopy
MCA:	Monochloroacetic acid
NF:	National formulary
NTR:	Number of turns required
RH:	Relative Humidity
Rpm:	Revolution per minute

RSM:	Response surface methodology
SCMC:	Sodium carboxymethyl cellulose
TGA:	Thermogravimetric analysis
USP:	United States Pharmacopoeia
XRD:	X-ray diffraction

1. Introduction

1.1. Cellulose

Cellulose is the most abundant naturally occurring organic substance found on earth, with a total annual biomass production of about 1.5×10^{12} ton (Gupta *et al.,* 2019). Existence of cellulose as the common material of plant cell walls was first recognized by Anselm Payen in 1838 (Marchessault and Sundararajan, 1983). It is one of the main cell wall constituents of all major plants, both nonlignified and lignified. It comprises around 35-50% of the lignocellulosic biomass (Heinze, 2016).

Cellulose occurs almost in pure form in cotton fiber. However, in wood, plant leaves and stalks, it is found in combination with other biomaterials, primarily hemicellulose, lignin and other substances such as pectin, waxes and organic acids, which need to be removed by physical, chemical or biological treatment to gain access to cellulose chains (He *et al.,* 2021). It is also found in the cell walls of green algae and the membranes of most fungi (Bogolitsyn *et al.,* 2020, Kuhn *et al.,* 2012)

Chemically, Cellulose is a long-chain carbohydrate polymer made by the linking of D-glucose units together by β-1, 4-glucosidic bonds (Fig 1.1). In the cellulose chain, the glucose units are in 6-membered rings, called pyranoses. They are joined by acetal linkages between the C-1 of one pyranose ring and the OH of C-4 of the next ring (Gardner and Blackwell, 1974). Since water molecule is lost during acetylation, the glucose units in the cellulose polymer are called anhydroglucose units (AGU). AGU is a single sugar molecule in a polymer consisting of three reactive hydroxyl groups a primary OH on C6 and two Secondary OH on C2 and C3. These hydroxyl groups can undergo a typical reaction known for primary and secondary alcohols (Marchessault and Sundararajan, 1983).

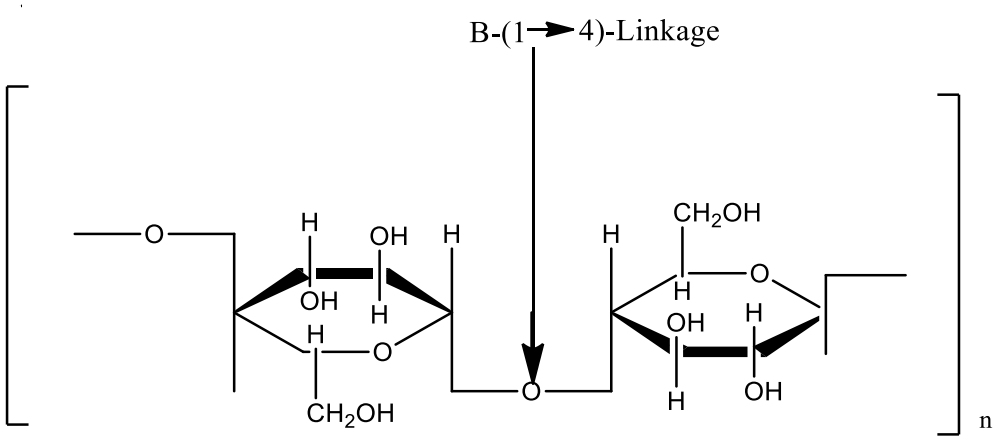

Figure 1-1: Structure of cellulose.

Cellulose is known to be a semi-crystalline polymer having amorphous and crystalline regions which are linked together by intra and inter molecular interactions. Cellulose in crystalline region is formed by hydrogen bonding and van der Waals interactions between glucose chains. It comprises the major proportion of cellulose, whereas amorphous cellulose comprises the small portion and is formed by unorganized cellulose chains surrounded by a non-cellulosic matrix of lignin and hemicellulose (Pizzi and Eaton, 1985). Due to the presence of lignin and hemicellulose, the sources of cellulose are usually known as lignocellulosic materials (Yang *et al.*, 2007, Saha, 2003).

In lignocellulosic material, cellulose is bonded together with hemicelluloses and lignin by covalent bonding, various intermolecular bridges, and van der Waals forces, forming a complex structure. Cellulose in amorphous region is weak and readily hydrolyzed when exposed to excessive amounts of mineral acids. Thus, crystalline cellulose is obtained through hydrolysis of amorphous regions in microfibrils of alpha cellulose, leaving the crystalline phases (Hidayat *et al.*, 2012, Heinze, 2016).

Hemicellulose is a complex, branched and heterogeneous polymeric network of cycled saccharides such as pentoses (xylose and arabinose) and hexoses (glucose, galactose, mannose, rhamnose, and glucuronic and galacturonic acids). It is a water-soluble polysaccharide and mainly amorphous (Saha, 2003, Scheller and Ulvskov, 2010). Lignin is a complex and amorphous organic compound which contains aliphatic and aromatic units that are covalently bound to fibrous polysaccharides within plant cell walls. It consists of aromatic units such as guaiacyl, syringyl and phenylpropanoid

units. The phenylpropane units are crosslinked to each other by various chemical bonds, such as β-O-4-aryl ether linkages, α-O-4-aryl ether, 4-O-5-diaryl ether, β-5- phenylcoumaran, 5-5-biphenyl, β-1-(1,2-diarylpropane) and β-β-(resinol). It has alkali solubility characteristics (Whetten and Sederoff, 1995, Liao *et al.,* 2020).

1.2 Sources of cellulose

Cellulose can be produced from various biomasses ranging from wood to non-wood biomasses. Majorly, commercial sources of cellulose are wood and cotton. Cotton may contain as high as ~98 % of cellulose, and some types of wood may have as much as ~90% (Hsieh, 2007). Agricultural crop residues are an important source for isolation of cellulosic fibers in many countries, especially those that do not have forest. Agricultural wastes, such as banana plant waste (Ibrahim *et al.,* 2013), wheat straw (Liu *et al.,* 2005), sugarcane bagasse (Sun *et al.,* 2004; Saelee *et al.,* 2014), sugarcane straw (Candido and Gonçalves, 2016), corn husk (Reddy and Yang, 2005, Mondal *et al.,* 2015), corn cob (Shogren *et al.,* 2011; Jia *et al.,* 2016), kenaf bast (Zaini *et al.,* 2013), empty fruit bunch (Ngadi and Lani, 2014), rice straw (Reddy and Yang, 2006), rice husk (Rosa *et al.,* 2012), bamboo (Brito *et al.,* 2012; Zhang *et al.,* 2012), cotton linter (Sczostak, 2009) and *Sorghum caudatum* (Ohwoavworhua and Adelakun, 2010) have been studied as a sources of cellulose.

1.3 Eucalyptus sawdust

Eucalyptus is an exotic and most popular tree species that belongs to the family Myrtaceae. Globally, it is the most planted genus of tree species with the genius containing more than 500 species (Castillejo *et al.,* 2023). Although, most Eucalyptus species occur naturally in Australia, it is now widely and successfully grown in many countries (Paine *et al.,* 2011). Currently, more than 100 Eucalyptus species are available in Africa, about 55 of them cultivated in Ethiopia, which spreads in many regions of the country and mostly in the central highlands (Pohjonen and Pukkala, 1990, Forsyth *et al.,* 2004).

According to Alemayehu and Melka, *Eucalyptus globulus* Labill, *E. camaldulensis* Dehnn., *E. saligna* Sm., *E. grandis* W. Hill ex Maid., and *E. tereticornis* Sm. are widely distributed in the country and the first two are the major *Eucalyptus* species planted by smallholder tree growers in many parts of the country. The two eucalyptus species have exhibit altitude-based distribution with eucalyptus camaldulensis being adaptable in lower altitudes (upper *kolla* and *woina dega* zones)

while eucalyptus globulus is mostly found in higher altitudes (*dega* and *wurch* zones) (Alemayehu and Melka, 2022).

Recent studies also showed that eucalyptus is widely planted across the country. Over 500000 ha of the land is covered by Eucalyptus plantation in Ethiopia. *Eucalyptus globulus* is the prominent tree with the highest production in government and community estate plantations, and in the central highlands for around 100 years because of its fast growth through coppicing, resistance to browsing by livestock, and through simple sawing and potted seedling propagation (Dessie *et al.,* 2019). It is commonly used for construction, poles, timber, firewood, charcoal, posts and farm implements wood sources for rural Livelihoods. Moreover, most Ethiopian households planted and produced Eucalyptus trees due to its adaptability, non-palatability for livestock and earn high income from sale of Eucalyptus wood product. Approximately, 68,089.26 m^3 of sawn wood and 526,350 m^3 of roundwood are produced each year in Ethiopia. Due to the high production of these species and their high logging in Ethiopia, a large amount of residual material such as sawdust is produced (Tejada-Tovar *et al.,* 2021).

Sawdust is a by-product of wood, obtained from various woodworking operations, for instance, sawing, planning, sanding, and milling of wood. It is a relatively abundant, cheap lignocellulosic compound, which is found in large quantities and has disposal problems (Rominiyi *et al.,* 2017). Eucalyptus and pine sawdust are important byproducts of the primary processing of wood in Ethiopia which so far have not found a successful exploitation. In some cases, these residues represent a problem and their treatment consumes resources of management, treatment and disposal. Usually, sawdust is used to obtain low value-added products such as pellets and briquettes (bioenergy), charcoal (adsorbent) and wood panels (furniture and construction materials) (Dessie *et al.,* 2019; Pohjonen and Pukkala, 1990).

The main disadvantage of sawdust is the heterogeneity of the material because sawmills process woods from different origins, which generates a mixture of sawdust in which species and age are difficult to know. By chemical extraction processes, the biomass is fractionated to obtain a pulp rich in cellulose, lignin and other chemical components. This general principle can be used to fractionate sawdust, separating all components by sequential processes, thus producing high value cellulose and its derivative products (Huans, 1995; Vassilev *et al.,* 2010).

Eucalyptus Sawdust (ES) is a good raw material for preparation of cellulose due to its high degree of polymerization, crystallinity, purity and its higher content of cellulose (70% of holocellulose with 55% of alpha-cellulose) comparable with other natural resources such as sisal (57–65%) (Morán *et al.,* 2008), bagasse of sugarcane (43–45%) (Sun *et al.,* 2004) and bamboo (45–54%) (Brito *et al.,* 2012). Therefore, collecting such huge quantity of by-product to find out the profitable application by producing valuable products like cellulose and its cellulose derivatives such as sodium carboxymethyl cellulose (SCMC) is quite attractive. This endeavor is also reducing the pollution related issue. In this study, SCMC was synthesized from ES obtained from a timber factory.

1.4 Bamboo wood

Bamboo plants belong to the subfamily Bambusoideae within the grass family of Poaceae. It consists of both herbaceous and woody bamboo and grows mostly in the forest as a grass but not a tree (Calderón and Soderstrom, 1980). According to the report by BPG (2012), there are over 1439 species of woody bamboos in the world. They are native to Africa, the Americas, Asia and some species have been introduced into Europe in recent times. Bamboo is one of the fastest-growing plants on the planet, with high rates of growth in tropical and subtropical climate regions. Africa possesses about 40 species on over 1.5 million ha of land (Bahru and Ding, 2021)

Ethiopia is one of the few countries in the world endowed with a vast bamboo resource base. The country has an estimated one million hectares of natural bamboo forest, 2.7% of the world total and 7% of the African total (Akinlabi *et al.,* 2017). The two indigenous bamboo species in Ethiopia are the African alpine bamboo, *Yushania alpina* (K. Schum), and a monotypic genus of lowland bamboo, *Oxytenanthera abyssinica* (A. Rich.) (Embaye, 2000).

Unlike other countries, bamboo utilization in Ethiopia has been customary and limited to hut construction, fencing and to a lesser extent production of handicrafts, furniture, containers for water transport, and storage, baskets, beehive, firewood, fodder, house utensils, various artifacts, and walking sticks. Its socio-economic and ecological potentials are not yet realized (Kindu and Mulatu, 2010). Despite the recent sporadic initiatives to develop and use bamboo, it has received little emphasis. Cellulose content in bamboo ranges from 40 and 50 percent (Brito *et al.,* 2012, Zhang *et al.,* 2012), which is equivalent to the reported cellulose percentages of softwoods (40 to 52%) and hardwoods (38 to 56%) (Chaouch *et al.,* 2010). Due to its long fiber, bamboo is

unquestionably a viable alternative supply of raw materials for the production of cellulose and its derivatives.

1.5 Modification of cellulose

Modification of cellulose is carried out to overcome shortcomings of native cellulose and increase its usefulness for industrial applications (Morán *et al.,* 2008). The high degree of crystallinity and the presence of large amount of inter and intramolecular hydrogen bonding in the structure make the polymer a poor candidate to be used directly in different pharmaceutical applications. Therefore, the modification of cellulose to its derivatives will expand the application of cellulose as an excipient. Cellulose can be physically modified to microfibrillated cellulose and microcrystalline cellulose, or chemically modified to cellulose ether and ester derivatives (Kamel *et al.,* 2008)

Chemical modification of cellulose involves hydrolysis of the amorphous portions with mineral acids and substitution of hydroxyl groups with different functional groups, resulting in markedly altered physicochemical properties. The chemical and functional properties achieved by modified cellulose is dependent on the source, reaction conditions (reactant concentration, pH, reaction time, and the presence of catalyst), type of substituents, degree of substitution (DS), and the distribution of the substituents in the cellulose molecule. Modification is generally achieved through derivatization such as etherification and esterification, can provide several biodegradable cellulose derivatives, including SCMC, Hydroxypropylmethyl cellulose (HPMC) and cellulose acetate (CA) (Mondal *et al.,* 2015; Shokri and Adibkia, 2013).

1.6 Sodium carboxymethyl cellulose

SCMC is one of the most intensively studied cellulose derivative, first synthesized in 1918 and produced commercially in Germany in the early 1920s. SCMC is an anionic, water-soluble ether derivative of cellulose prepared by treating alkali cellulose swollen in aqueous NaOH and organic liquid (ethanol or isopropanol) with monochloroacetic acid or its sodium salt. At the molecular level, SCMC contains two repeating units: β-D-glucose and β-D-glucopyranose 2-*O*-(carboxymethyl)-monosodium salt, which are connected via β-1,4-glycosidic bonds. the major difference between SCMC and cellulose is the presence of some anionic carboxymethyl groups

(i.e., $–CH_2COOH$) in the SCMC structure that replace the hydrogen atoms from some hydroxyl groups present in the cellulose backbone (Kamrunnahar, 1995).

The preparation of SCMC involves two reaction steps: mercerization and etherification, commonly carried out in water–alcohol mixtures. In the first step, cellulose is treated with NaOH, yielding an activated alkali cellulose. The product is then reacted with sodium monochloroacetate in the following etherification step **(**Fig. 1.2**)**. The DS obtained corresponds to the average number of carboxymethyl groups per anhydroglucose unit, with a theoretical maximum of 3.0, corresponding to the complete substitution of the three reactive hydroxyl groups in the anhydroglucose unit (Cheng *et al.,* 1996).

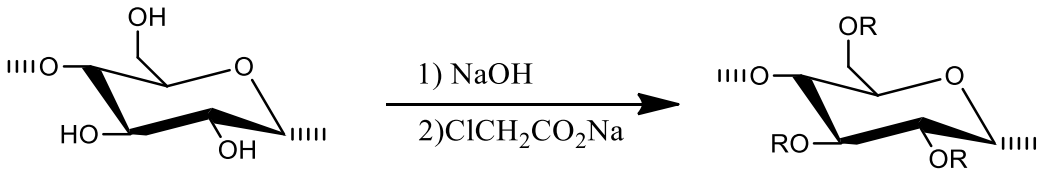

Figure 1-2: Synthesis and structure of sodium carboxymethyl cellulose (SCMC) with different degrees of substitution. R=H or CH_2CO_2Na.

A large number of commercial SCMCs exist, with a variety of DS, purity and rheological properties in aqueous solutions. The DS of commercial SCMC grades for pharmaceutical products is typically between 0.6 and 1.6. DS depends on the accessibility of cellulose fibers, the susceptibility of individual cellulose crystallites and the experimental conditions. The property of SCMC depends on its molecular weight, DS, and the distribution of carboxymethyl substituents along the polymer chains (Lakshmi *et al.*, 2017; Yaşar *et al.,* 2007).

SCMC has been obtained from various (lignocellulosic) materials such as agricultural wastes of spent tea leaves, sugarcane bagasse, coconut fibres, oil palm fibres, dried duckweed and palm kernel cake (Huang *et al.,* 2017), almond shells, almond stems, and fig stems (Moussa *et al.,* 2019) bacterial cellulose (Cheng *et al.,* 1999), bamboo shaving (Chen and Lou, 2014), banana stem and peel and banana pseudo stem (Adinugraha and Marseno, 2005), corn cob waste (Singh and Singh, 2013), cotton linters (Khullar *et al.,* 2005) and cotton stalk (Zhang *et al.,* 2011), grapefruit peel (Karataş and Arslan, 2016, Ngo *et al.,* 2023), Lantana camara (Varshney *et al.,* 2006), mesquite tree (Salama *et al.,* 2018), orange peel (Yaşar *et al.,* 2007), paper waste (Joshi *et al.,* 2015) , pineapple peel (Chumee and Khemmakama, 2014; Putro *et al.,* 2023), pomelo peel (Chumee and

Seeburin, 2014), recycled newspaper (Ünlü, 2013), rice husk (Jarmkom *et al.*, 2021; Yeasmin and Mondal, 2015), rice straw (Abdel-Mohdy *et al.*, 2009), seaweed (Adinugraha and Marseno, 2005), sago biomass (Veeramachineni *et al.*, 2016), pulp (Toğrul and Arslan, 2003), water hyacinth (Saputra *et al.*, 2014), wheat straw, barley straw, and rice hull (Biswas *et al.*, 2014). However, so far, to the best of the researcher's knowledge, no research has described the preparation and physicochemical characterization of SCMC from BW and ES for potential value-added pharmaceutical applications.

1.7 Physicochemical characterization of cellulose and SCMC

The physicochemical properties of cellulose largely depend on the lignocellulosic source, each type of cellulose has its own cell geometry, and the extraction methods used for the isolation of cellulose. On the other hand, the Physicochemical properties of SCMC depend mainly on the DS (Kamrunnahar, 1995, Singh and Singh, 2013). The physicochemical properties of cellulose and SCMC are summarized below.

1.7.1 Degree of polymerization

The molecular size of cellulose is generally expressed in terms of degree of polymerization (DP), which is defined as the average value of the number of monomer (anhydroglucose) units in the cellulose chain. The DP of cellulose varies with the source and treatment of the raw materials. Cellulose in wood pulp have typically a DP value of 300 to 1,700, depending on the method of isolation. Whereas cotton and other lignocellulosic source have a DP in the range of 800–10,000, comparable DP values are also reported in bacterial cellulose (Klemm *et al.*, 2005). The DP of cellulose can be estimated by various physical techniques including the intrinsic viscosity methods. It is usually performed viscosimetrically after dissolving the sample in cuprammonium hydroxide (Cuam) solvent (Liu *et al.*, 2005, Sun *et al.*, 2004, Wüstenberg, 2014).

1.7.2 Degree of substitution

DS is the average number of substitutes of the hydroxyl group by other active molecules in the cellulose chain. During the synthesis of SCMC from cellulose, the DS depends on the number of carboxymethyl substituent groups that are attached to each anhydroglucose unit (Kamrunnahar, 1995; Yeasmin and Mondal, 2015). In addition to cellulose chain length and crystallinity, the DS

value plays a vital role in determining the physicochemical property of SCMC. SCMC polymer with a DS value of less than 0.4 is entirely insoluble in aqueous solvent. In contrast, SCMC is fully soluble beyond a DS of 0.4. The increasing in solubility along with DS is due to increased carboxymethyl substitution along the cellulose chain. SCMC's crystallinity is also related to DS, crystallinity was demonstrated under the DS of 0.82 and significantly reduced beyond 1.0 (Jarmkom *et al.,* 2021; Zhang *et al.,* 2011) Therefore, controlling DS of SCMC is clearly an important factor for practical applications. The DS value is controlled effectively by adjusting the reaction time, temperature and molar ratio of derivatizing agent to cellulose(Yeasmin and Mondal, 2015). The DS value can be determined by using different methods such as titration, FTIR and ^{1}H-NMR (Heinze *et al.,* 2003).

1.7.3 Crystallinity

Naturally, cellulose chains are self-assembled into microfibrils consisting of crystalline and amorphous regions. The crystalline region is more compact than amorphous region, due to the presence of high degree intramolecular and intermolecular hydrogen bonds (Johar *et al.,* 2012). Crystalline cellulose is known to exist in five major polymorphs, which are Iα, Iβ, II, III and IV. Iα and Iβ are the most abundant and naturally produced crystal forms of cellulose (Mittal *et al.,* 2011). Iα allomorph mostly exist in Algae, bacteria and lower plants. While Iβ allomorph is mostly produced by higher plants. Cellulose II is produced by treating cellulose Iα and Iβ with high concentration alkaline followed by neutralizing with ammonia. Moreover, treatment of cellulose I or II with liquid ammonia gives rise to III_I and III_{II} polymorphs, respectively. Cellulose IV can be formed by treatment of cellulose III in glycerol at higher temperature (Klemm *et al.,* 2005; Nishiyama *et al.,* 2003).

The physicochemical behavior of cellulose is strongly related to its degree of crystallinity, the ratio of the mass of crystalline domains to the total mass of cellulose. It affects the swelling, water-binding and the accessibility of the chains for chemical derivatization. The degree of crystallinity of cellulose, varies from 60–80% depending on the source and chemo-mechanical treatment used. The extraction conditions, such as temperature, time and acid concentration also have been found to have an impact on the degree of crystallinity. Therefore, degree of crystallinity should be

considered when considering the manufacturing and applications of cellulose (Flores-Velázquez *et al.,* 2020; Poletto *et al.,* 2013).

Numerous studies demonstrated that crystallinity index of cellulose can be significantly modified by derivatization. SCMC showed the lowest crystal index compared to cellulose when evaluated under XRD. This reduction in crystallinity is due to the substitution of the hydroxyl groups by carboxymethyl groups that have a greater volume. SCMC with a low DS value has more crystalline structure compared to SCMC with high DS. High DS value indicates the presence of more carboxymethyl groups that disrupt the ordered structure of cellulose, leading to SCMC with higher levels of substitution and lower crystallinity (Dai *et al.,* 2019; He *et al.,* 2009).

1.7.4 Thermal analysis

Thermogravimetric analysis (TGA) and Differential Scanning Calorimetry (DSC) are commonly used methods to investigate the thermal degradation properties of cellulose and SCMC. Investigation of the thermal properties of cellulose and SCMC is important in order to determine their ability to withstand elevated processing temperatures. And to qualitatively characterize their stability, compatibility and transition phases based on their respective thermograms (Deepa *et al.,* 2011; Haleem *et al.,* 2014).

TGA provides information about the change in weight of the material as a function of temperature in an inert atmosphere or in the presence of air or oxygen. It indicates the undergoing chemical or physical processes upon heating a sample. The thermal stability of the cellulose fiber is increased with its purity and crystallinity, which decreases after substitution of cellulose hydroxyls with organic acids. Thus, the thermal stability of SCMC is lower than that of the original cellulose (Barud *et al.,* 2008; Jandura *et al.,* 2000).

1.8 Pharmaceutical applications of SCMC

SCMC and its derivatives have found a wide range of applications in food products, cosmetics, pharmaceuticals, composite and packaging industries. Due to the facile, low-cost synthesis process, an abundance of raw materials, biodegradability, mechanical strength, different formability, tune-able hydrophilicity, viscosity, rheological properties, and renewability make SCMC attractive for applications in diverse industrial fields (Rahman *et al.,* 2021). SCMC is used

as various auxiliary agents in the food industry. In food products, such as dietetic foods and ice cream, it acts as a water binder, thickener, suspending agent, or as an emulsion stabilizer (Yildirim-Yalcin *et al.,* 2022). Additionally, SCMC is used to optimize the rheological property, structure, and appearance of food products and their pseudoplastic properties (He *et al.,* 2021).

SCMC and its derivatives (composite/copolymer) have received ample attention for use in pharmaceutical products due to its properties such as biocompatibility, long half-life *in vivo*, high stability and drug binding capacity, pH-sensitivity (for the presence of carboxy group), and best reliable carrier, etc. It is commonly used as binders, stabilizers, emulsifiers, film-forming components and suspending agent in the pharmaceutical industry. It is well known that the properties of SCMC, and hence its applications, depend on the DS, the average value of carboxymethyl groups replacing the hydroxyl groups in AGU of cellulose. For example, in suspending drug applications, SCMC acts as a better suspending agent in the DS range of greater than 0.6 (Mondal *et al.,* 2015; Shokri and Adibkia, 2013). It has also been used in sustained release formulations due to its thickening and diffusion barrier properties (Hu *et al.,* 2021).

1.9 Pharmaceutical suspensions

Pharmaceutical suspensions are thermodynamically unstable liquid dosage forms, were insoluble solid particles dispersed in a liquid continuous phase. Hence, they are included into the group of disperse systems (Patel *et al.,* 1986). To obtain a pharmaceutically acceptable, thermodynamically stable suspension, there is a need to include a suspending agent in a dosage form. By providing a physical barrier to aggregation and enhancing the consistency of the suspending media, it maintains a uniform dispersion of particles that would otherwise settle rapidly to create closely packed sediment and prevents the withdrawal of an accurate dose. Therefore, it is essential to include suspending agents in suspension formulations to reduce the rate of settling and to allow uniform dosing of the drug to the patient (Kulshreshtha *et al.,* 2009).

Certain polymers are used as suspending agents in suspensions owing to their ability to increase the viscosity of the solution. These polymers may be synthetic (carbomers), semi synthetic (NaCMC, HPMC) or natural (alginates, acacia gum, tragacanth, guar gum, bean gum, carrageenan, xanthan gum) (Mogoşanu and Grumezescu, 2015). However, the use of modified natural polymers like SCMC for pharmaceutical applications as a suspending agent is fascinating because they are

cheap, effortlessly available, nontoxic, amenable to chemical modifications, and potentially biocompatible (Nikazar *et al.*, 2023; Zennifer *et al.*, 2021).

1.10 Significance of the study

Commercially available cellulose and its derivatives are mainly derived from wood pulp and cotton linters. This makes the raw materials expensive and increase the cost of cellulose and its derivatives. As an alternative, a wide variety of plants have already been studied for the production of cellulose and its derivatives for use in the development of different dosage forms (Wüstenberg, 2014; Yildirim-Yalcin *et al.*, 2022). Among other sources, ES, by product of timber industry and BW are considered due to their non-toxicity, abundance, availability, renewability, and low cost (Mekonnen *et al.*, 2014; Vallejos *et al.*, 2016). Furthermore, compared with other sources, ES and BW have higher content of cellulose but lower hemicelluloses and lignin content (Karataş and Arslan, 2016; Veeramachineni *et al.*, 2016;).

The high demand and importance of SCMC used in pharmaceutical industries has led to the utilization of locally and naturally occurring materials in the production of SCMC. However, Ethiopian industries have relied on imported SCMC of limited sources for use in various applications. This incurred large amount of foreign currency and this has led to the research for environmentally friendly and locally available sources of cellulose and cellulose derivatives such as SCMC. Therefore, finding alternative cellulose sources, especially from abundantly available and renewable sources is highly valuable (Gupta and Badola, 2022).

Large mass of ES is produced by timber factories in Ethiopia which are considered as waste materials with no value-added application in the country. The absence of a research report on cellulose and SCMC from bamboo and eucalyptus in Ethiopia necessitates the need for preparation and characterization of bamboo wood cellulose (BWC) and bamboo wood sodium carboxymethyl cellulose (BW-SCMC) from bamboo, and eucalyptus sawdust cellulose (ESC) and sodium carboxymethyl cellulose from eucalyptus sawdust (ES-SCMC).

1.11 Research questions

This study attempts to answer the following research questions:

1. What would be the yields of the celluloses and the derivative SCMCs of BW and ES?

2. What are the physico-chemical characteristics of BWC, ESC, BW-SCMC and ES-SCMC?
3. What are the critical factors in the optimization of BW-SCMC and ES-SCMC synthesis as per Response Surface Methodology (RSM) using Central Composite Design (CCD)?
4. What would be the performance of BW-SCMC and ES-SCMC as suspending agents in paracetamol formulations?

1.12 Objectives

1.12.1 General objective

- To prepare and characterize BW-SCMC and ES-SCMC from BW and ES, respectively and evaluate their potential applications as suspending agent in paracetamol suspension formulations.

1.12.2 Specific objectives

- To extract and characterize cellulose from bamboo wood and eucalyptus sawdust.
- To prepare and characterize SCMC from BWC and ESC.
- To optimize the synthesis independent variables of BW-SCMC and ES-SCMC using CCD.
- To evaluate BW-SCMC and ES-SCMC as suspending agent in paracetamol suspension.

2 Material and Methods

2.1 Materials

2.1.1 Plant materials

Eucalyptus sawdust was collected from Debre Zeite, Adama, Ethiopia and the sawdust was generated from the cutting of logs without any type of previous treatment. Whereas Bamboo wood was collected from Bahir Dar, Amhara Region. Both raw materials were then ground in a knife mill and passed through a 1 mm mesh sieve.

2.1.2 Chemicals and solvents

Acetic acid (99.5%) (Sigma-Aldrich, Germany), Toluene (99.5%) (Fisher Chemicals, UK), Ethanol (96%) (UNI-CHEM, India), Methanol (99.9%, Absolute) (Sigma-Aldrich, Germany), Acetone (99.5%) (BDH chemicals, England), Sulphuric acid (98%) (Sorensen, Leuren, Germany Formic Acid (85%), Cupric Sulphate Pentahydrate (98.5%) (Loba Chemie Pvt. Ltd, India), Potassium Iodide, Zinc Chloride (97%), Hydrogen peroxide (30%) (Carlo Erba reagents, France), Sodium Hydroxide (Alphax chemical industry, India), Hydrochloric Acid (37%) (BDH chemicals ltd, Poole, England), Nitric acid (Alphax chemical industry, India), Silica gel, Xylene (98 %,), Ammonium Hydroxide solution (28%) (Carlo Erba reagents, France), Iodine (Hayashi pure chemical industries ltd), Sodium Chloride (Oxford Laboratory, Mumbai, India), Diethyl ether (Central Drug House Ltd, India), monochloroacetic acid (Sigma-Aldrich, Germany), Sodium carboxymethyl cellulose (BDH, England), Methyl paraben (Sigma-Aldrich), Propyl paraben (BDH, England), Glycerin purified (Research-lab fine Chem. Industries, India), Tween® 80 and Potassium dihydrogen phosphate (Atlas Chem. Industrial INC, USA) were used as recieved. Paracetamol powder was kindly donated by Cadila Pharmaceutical Company, Ethiopia.

2.2. Methods

2.2.1 Determination of lignocellulosic components

To determine amounts of the three components of lignocellulosic biomass (cellulose, hemicellulose and lignin) of BW and ES, method proposed by Mansora et al. (2019) were used, which involves solvent extraction method.

2.2.1.1 Determination of the amount of extractive in biomass

Sixty ml of acetone were added to 1 g of BW and ES samples (A), and heated at temperature of 90 °C for 2 h using a hot plate. Then, the samples were dried in oven at 105 – 110 °C until constant weight was obtained (B). By using Eq. (2.1), the amount of extractive was determined (Mansora *et al.,* 2019).

Amount of Extractive (g) = (A-B) (2.1)

2.2.1.2 Determination of the amount of hemicellulose in biomass

NaOH solution (150) was added to 1 g of extractives free BW and ES samples (B), and heated over a hot plate at 80 °C for 3.5 h. Then, the sample was washed with distilled water and dried in oven at 105 – 110 °C until constant weight was obtained (C). The amount of hemicellulose was determined using Eq. (2.2).

Hemicellulose (g)= (B-C) (2.2)

2.2.1.3 Determination of the amount of lignin in biomass

Thirty ml of 98 % sulphuric acid was added to 1 g of extractives free BW and ES fibers (B). The samples were left at ambient temperature for 24 h. Then, it was boiled at 100 °C for 1 h on a hot plate. Finally, it was filtered using nylon cloth and the solid residues were washed with distilled water. The sample was dried in an oven at 105 °C until a constant weight was obtained (D). The final weight of the residues was recorded as lignin content (Mansora *et al.,* 2019).

2.2.2 Cellulose isolation from bamboo wood and eucalyptus sawdust

During the preliminary work, isolation of cellulose from BW and ES were carried out according to the following three methods: (i) Acetic acid-Nitric acid method, (ii) (ii) Formic acid-Acetic acid method and (iii) Steam explosion method.

In all these methods, prior to extraction, the raw fibers were washed with tap water and air dried. The dried fibers were treated with toluene/ethanol (2:1 v/v) for 4 h at 60 ^{o}C with solid to solvent ratio of 1:50 w/v in a Soxhlet apparatus. Finally, it was filtered and washed with ethanol three times at a fiber liquid ratio of 1:10 (w/v) and dried in an oven (Kottermann® 2711, Germany) at 60 ^{o}C (Nagarajan *et al.,* 2018; Trache et al., 2014).

In acetic acid-nitric acid method, 10 g of BW and ES were treated with a 4% (w/w) NaOH solution containing 5 % (v/v) of hydrogen peroxide at 80 °C in water bath for 4 h at a liquid to solid ratio of 20:1. The solution was then filtered and washed repeatedly with distilled water. The crude celluloses were then subjected to a rapid purification treatment with a mixture of 200 ml of 80% acetic acid and 20 ml of 68% nitric acid (v/v=10:1) at 100 °C for 15min. Finally, the residues were washed repeatedly with distilled water, filtered and dried at 60 ^{O}C to constant weight in an oven (Kottermann® 2711, Germany) (Liu et al., 2018).

In peracetic acid method, BW and ES were treated with mixture of glacial acetic acid and 30% hydrogen peroxide in a volume ratio of 70:30 at the liquid to solid ratio 10:1, in water bath at 85^{o}C for 2 h. At the second stage, the alkaline treatment of the samples were carried out with 8% NaOH solution for 60 min at liquid to solid ratio of 12:1. Then, BW and ES pulps were filtered and repeatedly washed with distilled water. Finally, the residues were dried at 60 ^{O}C to constant weight in an oven (Barbash, et al., 2017

In steam explosion method, cellulose was isolated and purified following the method described by Ranganagowda *et al.,* (2019) with slight modification. The dewaxed fibers were each treated with a mixture of 10% NaOH and 10% H_2O_2 in a volume ratio of 1:1 at a fiber to liquor ratio of 1: 20, steamed at 121^{0}C and 1.5 bars in an autoclave for 1h. Then, the residue was filtered through nylon cloth and washed thoroughly with distilled water. The fiber from steam explosion was delignified by soaking in a 1:1 (v:v) mixture of 20% formic acid and 10% H_2O_2 over a water bath at fiber liquor ratio of 1:20 (w/v). The mixture was kept at 85 ^{o}C for 2 h. Following filtration and repeated washing with distilled water, the mixture was treated with 10 % H_2O_2 and 10% NaOH at 65 ^{o}C for 2 h at a fiber to liquor ratio of 1:20. Finally, the residue was washed repeatedly with distilled water, filtered using nylon cloth and dried at 60 ^{o}C to constant weight in an oven.

2.2.3 Preparation of sodium carboxymethyl cellulose

Preparation of SCMC was performed by modifications of the method stated in Pushpamalar *et al.,* (2006). The cellulose fiber (1g) with iso-propanol (100 ml) was first added to a conical flask. Then, 4 ml of 30% NaOH solution was added dropwise and the mixture was stirred using magnetic stirrer for an hour at 30 ˚C. After alkali treatment, etherification reaction was continued by adding 0.5, 1 and 1.5 g of MCA per 1 g of cellulose and the mixture was heated to 30, 50 and 70 ^{o}C with constant

stirring using magnetic stirrer. The reaction was then allowed to proceed under 250rpm for 60-240 min. Then, the reaction mixture was slowly poured into 100ml of methanol with constant stirring for 1 h. Once the precipitation process was completed, the product was filtered and washed repeatedly with distilled water. Finally, it was dried in the oven at 60 °C until a constant weight was obtained.

2.2.4 SCMC synthesis optimization by RSM

2.2.4.1 Experimental design

CCD with three coded values was employed in this study. According to this design, the total number of treatment combinations is $2^k + 2k + n$, where k is the number of independent variables and n is the number of repetitions of experiments at the center point. Duration of etherification (A), monochloroacetic acid concentration (B) and etherification temperature (C) were selected as independent variables (k = 3). All other processing variables were kept invariant throughout the study. The central point (0, 0) was studied in Sextuplicate. For k=3, $2^3 + (2\times3) + 6 = 20$. Hence, a total of 20 experiments were carried out for each cellulose source to find the optimum area, at which the desired response is achieved. A total of 20 experiments were conducted for each cellulose source and the effect of each factor was analyzed by taking minimum, maximum and center values of the operating conditions which has significant influence on SCMC synthesis. All experiments were conducted in a randomized order to minimize the effect of unexpected variability in the observed response due to extraneous factors.

Table 2.1 summarizes the three independent factors studied and the translation of the coded levels to the experimental units employed during the study. The resulting data were fitted into Design Expert Software (Version 10.0.7.0, Stat- Ease Inc, Minneapolis, MN) and analyzed statistically using analysis of variance (ANOVA). The data were also subjected to 3D response surface methodology to determine the influence of the selected factors on the dependent variable.

Table 2-1: Code and Original variables in 2^3 factorials design.

Parameters	Relation of code and original variables		
	-1	0	1
A: Etherification time, t (min)	60	150	240
B: Amount of monochloroacetic acid per gram of cellulose (g)	0.5	1	1.5
C: Etherification temperature (ºC)	30	50	70

2.2.4.2 Validation of the experimental design

To validate the chosen experimental design, the experimental values of preparation responses were quantitatively compared with those of predicted values generated by the software. The percentage relative error was calculated using the following equation (Meka *et al.*, 2016).

$$\text{Relative error } (\%) = \frac{\text{Predicted value} - \text{Experimental Value}}{\text{Predicted value}} * 100 \quad (2.3)$$

DS of the statistically optimized condition were evaluated for verification of the theoretical predictions.

2.2.5 Determination of percent yield

The yield of cellulose extracted from the raw fibers and the SCMC synthesized was measured on the dry weight basis. The cellulose yield, expressed as percentage, was calculated using Eq. (2.4) and SCMC yield was determined by dividing the dry weight of each SCMC to weight of their respective dried cellulose as shown in Eq. (2.5).

$$\text{Yield of Cellulose } \% = \frac{\text{weigt of dry Cellulose residue}}{\text{weight of original fiber sample}} * 100\% \quad (2.4)$$

$$\text{Yield of SCMC } \% = \frac{\text{weigt of dry SCMC residue}}{\text{weight of cellulose sample}} * 100\% \quad (2.5)$$

2.2.6 Characterization of cellulose and sodium carboxymethyl cellulose

2.2.6.1 Organoleptic characteristics

The color, odor, taste and physical appearance of cellulose and SCMC samples were observed.

2.2.6.2 Chemical identification test

Identification tests of the cellulose samples were performed using iodinated zinc chloride solution. Initially, iodinated zinc chloride solution was prepared by dissolving 20 g of zinc chloride and 6.5 g of potassium iodide in 10.5 ml of distilled water. Then, 0.5 g of iodine was added and agitated for 15 min. Then, 10 mg of cellulose fiber was dispersed in 2 ml of iodinated zinc chloride solution. The resulting color was observed (USP 38/NF33, 2015).

2.2.6.3 Moisture content determination

The moisture content of cellulose and SCMC samples were determined according to the USP38/NF33, (2015). A 3 g of each sample (A) was placed on pre-weighed Petri dish and weighed. Then, the Petri dish was kept in an oven at 105 °C for 4 h. After drying, it was cooled in desiccator and weighed accurately until a constant weight (B) was obtained. The moisture content was calculated by using the following formula.

$$\text{Moisture content } (\%) = \frac{A-B}{A} * 100\% \quad (2.6)$$

2.2.6.4 Determination of pH

One gram each of the cellulose and SCMC samples were added to 50 ml distilled water and shaken for 10 min. Then, the pH of the suspension was recorded using a pH meter. All results are the mean of three parallel determinations.

2.2.6.5 Water soluble substances

Two grams sample of ES and BW each was added to 35 ml distilled water, shaken for 10 min and filtered. Then, the filtrate was evaporated to dryness, dried at 100 – 105 ^{o}C for 1 h and weighed. The amount of water-soluble substance was recorded as the difference between the weight of the beaker along with residue and the weight of the empty beaker. The determination was performed in triplicates (USP38/NF33, 2015).

2.2.6.6 Ash value

The ash value of the samples was determined according to the following procedure. The crucible was cleaned and dried at 100 ºC for 30 min. Following cooling for 30 min in a desiccator which contains silica gel, the crucible weight was determined. Then, 3 g of each sample were placed on the crucible and heated until smoking was stopped. The residue was then charred in a furnace at 550 ± 25 °C. After cooling in a desiccator for 45–60 min, the weight of ash was determined.

2.2.6.7 Moisture sorption capacity

One gram of sample powder was evenly distributed over Petri dish and placed in desiccators containing distilled water (100% RH), saturated solution of NaCl (75.6%) and appropriate concentrations of NaOH at 24.66%, 31.58% and 40% of NaOH solutions to provide 60%, 40% and 20% RH, respectively and stored at room temperature. Samples were equilibrated for four weeks and then the moisture uptake of each sample was calculated using Eq. (2.7).

$$\text{Moisture sorption capacity} = \frac{W2-W1}{W1} * 100\% \qquad (2.7)$$

Where, W1 is the weight of the sample before exposure and W2 is the weight of the sample after exposure.

2.2.6.8 Degree of polymerization

The DP of cellulose sample was determined according to the method described by Kambli et al. (2017) using cuprammonium hydroxide (Cuam) solution as solvent. Cuam solution was prepared by dissolving freshly precipitated Cu $(OH)_2$ in aqueous ammonia. Initially, 28 g of CuSO4·5H2O was dissolved in 600 mL distilled water to which 14 mL of NH_4OH (25%) was added and the precipitate, Cu $(OH)_2$, was filtered and repeatedly washed with distilled water to make it sulfate free. The precipitate was then dissolved to 500 mL with NH_4OH (25%) to form Cuam solution. Then, 100 mg of sample was added into 100 ml of the solution. The mixture was vigorously shaken and then placed in a water bath at 25 ºC for 5 min. After the sample was completely dissolved in the solvent, the viscosity of the solution was measured in an Ostwald Capillary viscometer. The viscosity was calculated from the efflux time of cellulose solution and the blank Cuam solution (Eq. 2.8).

$$\eta spe = \frac{\eta}{\eta 0} - 1 \quad (2.8)$$

Where, ηspec = specific viscosity, η/η0 = relative viscosity and η & η0 are the time (seconds) required for the sample and blank solutions, respectively, to travel from upper to lower mark.

The DP value was then calculated from the specific viscosity according to Eq. (2.9). Average value of three independent determinations was taken.

$$DP = \frac{2000\eta sp}{c*(1+0.29\eta spec)} \quad (2.9)$$

Where, c is concentration (in g/L) of cellulose and 0.29 is viscometer constant.

The molecular weight of cellulose sample was determined from DP by using Eq. (2.10).

M. Wt. of cellulose = DP x 162 (2.10)

2.2.6.9 Degree of substitution of SCMC

The DS of SCMC samples was determined by standard ASTM D1439 method. Accordingly, 1 g of dried SCMC powder was added to 20 mL of 90% ethanol and stirred for 5 min. After that, 1 mL of nitric acid (2M) was added and the solution was boiled on hot plate followed by 10 min of stirring. Then, the resultant solution was filtered and the solid residue was washed five times with 10 mL of 80% ethanol. Finally, the product was washed with methanol, dried at 100 ºC for 3 h and kept in a desiccator.

For titration, 100 mg of dried SCMC powder was suspended in 20 mL of distilled water in 100 mL Erlenmeyer flask and stirred continuously. Thereafter, 5 mL of 0.3 M NaOH was added and heated till boiling for 15 min to dissolve the SCMC. After cooling at room temperature, the resulting solution was titrated with 0.3 M HCl, using phenolphthalein as an indicator. This procedure was done in triplicate and the average volume of HCl was recorded. The SCMC content and the DS were calculated based on the Eqs. (2.11) and (2.12), respectively.

$$\text{Carboxymethyl content (\%CM)} = \frac{(Vo-Vn)M \times 0.059 \times 100}{m} \quad (2.11)$$

$$\text{Degree of Substitution(DS)} = \frac{162 \times \%\ CM}{5900-(58 \times \%\ CM)} \quad (2.12)$$

Where; Vo = mL of HCl used to titrate blank, Vn = mL of HCl used to titrate sample, M = molar concentration of HCl used and m = sample amount (g).

2.2.6.10 Fourier transform infrared spectroscopy (FTIR)

Perkin Elmer Fourier Transform Infrared Spectrophotometer (L1600400 Spectrum TWO DTGS, SN: 108152, Llantrisant, UK) was used to study the functional groups and chemical structure of extracted cellulose and SCMC samples. Pellets were made separately from SCMC and cellulose samples using KBr and FTIR spectra were recorded between 400 and 4000 cm^{-1}.

2.2.6.11 X-ray diffraction

X-ray diffraction patterns were acquired for all samples at room temperature. To determine the crystal structure and crystallinity, all samples were first dried in a dry oven at 100 °C for 30 min and then measured with automated powder X-ray diffractometer (XRD-7000S SHIMADZU, Japan). In this, the samples were placed in the cavity of a disc sample holder of the diffractometer. The XRD data were generated with Cu-Ka radiation (λ = 1.542° A) at 40 kV voltage and 30 mA current, 2θ angle range of 10°–40°, angle step of 0.02°, a time step of 0.4 seconds and scan speed of 3°/min. The crystalline indexes (CrI) of the samples were calculated from the X-ray diffraction patterns based on the peak height method developed by Segal et al. (1959) as shown in Eq. (2.12).

$$\text{CrI}\ (\%)\ = \frac{\text{I}(002)-\text{I}(\text{am})}{\text{I}(002)} * 100 \qquad (2.12)$$

Where: CrI is crystallinity index (%); I (002) is maximum diffraction peak intensity which represents the crystalline material; and I (am) is minimum intensity of the diffraction peak that represents the amorphous material.

2.2.7 Drug-excipient interaction study

FT-IR spectra for pure paracetamol and paracetamol with SCMC samples were acquired at room temperature using FT-IR spectrophotometer (FTIR-8400S, Shimadzu, Japan) in transmittance mode. The samples were first ground in a mortar to reduce the average particle size. About 8 mg of finely ground samples were mixed with liquid paraffin in a mortar and pestle. The sample mixture was then placed onto the face of a potassium bromide (KBr) plate and the second window was placed on top of the first salt plate to form a thin film of the mull by compression between the two plates. The sandwiched plates were placed in the IR spectrometer and the spectra were

obtained. Each IR spectrum was collected with 20 scans and spectral resolution of 4 cm^{-1}. Scanning was performed between wave numbers 4000- 400 cm^{-1}. Background spectrum was collected before running each sample. IR Solution Software was used for data treatment.

2.2.8 Preparation of paracetamol suspensions

Twelve formulations of paracetamol suspension were prepared using different concentrations (1%, 2%, 3% and 4% w/v) of BW-SCMC, ES-SCMC and C-SCMC as suspending agent. The composition and quantities of the suspension formulations are shown in Table 2.2. C-SCMC was used as standard suspending agent for comparison purpose. All the suspensions were prepared based on the method described elsewhere (Saeedi, *et al.,* 2003). The suspending agent and Tween 80 were initially dispersed in distilled water containing the preservatives. Then, the Paracetamol which was wetted with sorbitol was added to the vehicle and stirred continuously till uniform dispersion was obtained. It was then transferred to a 25 mL measuring cylinder. The cylinder was filled up to volume with distilled water and then shaken vigorously for 2 min. The same procedure was used for each suspending agent and a total of twelve formulations were prepared.

2.2.9 Evaluation of prepared suspensions

Compendial and non-compendial tests were undertaken on the suspension formulations to assess the quality, stability and performance of BW-SCMC and ES-SCMC in comparison with the C-SCMC.

2.2.9.1 Rheology of the suspensions

2.2.9.1.1 Effect of suspending agent concentration

The effect of suspending agent concentration on viscosity was studied using a vibrational viscometer (VIBRO Viscometer, SV-10, Japan). The viscosities of the suspensions were measured in mPas within 24 hs after preparation. The measurement was made at a constant shear rate and room temperature (20 ^{o}C). Apparent viscosities recorded are an average of three determinations.

2.2.9.1.2 Effect of shear rates on apparent viscosity

To determine the effect of shear rate on viscosity, viscosity measurements of each suspension were made at 30, 60, 100 and 200 rpm using a rotational viscometer (Viscostare plus L, Kinematica AG,

Switzerland, spindle 4). All the measurements were conducted at room temperature and measured in kPas within 48 h. of preparation. Values recorded are an average of three determinations.

2.2.9.2 Sedimentation volume

The sedimentation volume is the ratio of the ultimate volume of the sediment to the initial volume of the total suspension as the suspension settles in a cylinder under standard conditions. Fifty mililiters of each formulation was transferred to a 100 ml graduated cylinder and kept at room temperature. The sedimentation volumes (%) of the formulations were recorded every day for seven days and then every week for 3 consecutive weeks based on the Eq (2.13). The readings of sedimentation volume were taken when the cloudy supernatant started to become clear up on the top surface of the suspension. Results recorded are averages of three determinations.

$$F = \frac{Vu}{Vo} \qquad (2.13)$$

Where, Vu is the ultimate volume of the sediment and Vo is the original volume of the suspension.

2.2.9.3 Flow rate

The flow rates of suspensions were measured as the time required for 10 ml of each sample to flow through 10 ml pipette and were calculated using eq. 2.14. Determinations were made in triplicate and the result obtained are expressed as the mean value.

$$\text{Flow rate} = \frac{Vs}{T} \qquad (2.14)$$

Where, Vs volume of sample in the pipette (in ml) and T is time (in sec) required for the 10 ml suspension to totally elute out of the pipette.

2.2.9.4 Effect of electrolyte concentration on sedimentation volume

To 50 ml of suspension containing 1% of each suspending agent, different concentrations of NaCl (10^{-4} M, 10^{-3} M, 10^{-2} and $5*10^{-2}$ M) were added and the sedimentation volume of each respective formulations were noted every day for seven consecutive days and compared with a control group.

2.2.9.5 Redispersibility of suspensions

The redispersibility of suspensions was measured based on the method described elsewhere (Saeedi *et al.,* 2003). Fifty ml of each suspension formulations were allowed to settle for one week

and four weeks. Then, the measuring cylinders were manually rotated upside down and, the number of turns (one complete cycle) required to uniformly redisperse the sedimented paracetamol particles throughout the suspension was determined and recorded.

2.2.9.6 Degree of flocculation

The degree of flocculation of 1% and 2% suspension formulations were evaluated according to the method described by Kumar *et al.,* (2009) using the following Eq. 2.15. To determine the degree of flocculation, flocculated suspensions were prepared using 0.004 M KH_2PO_4 as a flocculating agent.

$$\beta = \frac{Vu}{V\infty} \qquad (2.15)$$

Where, β is the degree of flocculation, Vu is the total volume of flocculated suspension and V∞ is the ultimate volume of the deflocculated suspension.

2.2.9.7 Construction of UV calibration curve

Seven different concentrations (5 µg/ml to 15 µg/ml) of paracetamol, the model drug used in the study, were prepared from stock solutions containing 200 µg/ml of paracetamol in phosphate buffer of pH 5.8. Then, the absorbance of each of these concentrations were measured at λ_{max} 243 nm in UV-Visible Spectrophotometer (T92+, UK) using the phosphate buffer solutions as blank. The absorbance readings were plotted against concentration of the solutions, and a linear regression equation and correlation coefficient were obtained.

2.2.9.8 Dissolution study of suspensions

Dissolution test was conducted according to the USP specification (USP38/NF33, 2015) using dissolution apparatus Type II (Paddle Method) (ERWEKA, DT600, Germany). Phosphate buffer (pH 5.8, 900 ml) was used as the dissolution medium at 37 ± 0.5 °C and stirring rate of 50 rpm. From each suspension 5 ml was introduced carefully into the bottom of the vessel. Five milliliters of aliquots of the dissolution medium were removed at 5, 10, 15, 20, 30, 45 and 60 min and filtered using filter paper. At each sampling point, an equal amount of fresh medium kept at similar temperature was transferred into the dissolution vessel to keep the sink condition. One milliliter of

the filtered sample was diluted to 25 mL with fresh dissolution medium and absorbance was read with UV/Visible spectrophotometer (UV Spectrometer, T92+) at 243 nm. Phosphate buffer (pH = 5.8) was used as a blank. Drug content and cumulative drug released were calculated from the absorbance data after all the necessary corrections for dilution were taken.

Table 2-2: Formulae for the preparation of paracetamol suspension using BW-SCMC, ES-SCMC and C-SCMC as suspending agent.

Ingredient	**Formulation code and composition**											
	FC-1	FC-2	FC-3	FC-4	FB-1	FB-2	FB-3	FB-4	FE-1	FE-2	FE-3	FE-4
Paracetamol (g)	6	6	6	6	6	6	6	6	6	6	6	6
C-SCMC (w/v)	1%	2%	3%	4%								
BW-SCMC (w/v)					1%	2%	3%	4%				
ES-SCMC (w/v)									1%	2%	3%	4%
Methyl paraben (w/v)	0.18	0.18	0.18	0.18	0.18	0.18	0.18	0.18	0.18	0.18	0.18	0.18
Propyl paraben (w/v)	0.02	0.02	0.02	0.02	0.02	0.02	0.02	0.02	0.02	0.02	0.02	0.02
Tween 80 (% w/v)	0.05	0.05	0.05	0.05	0.05	0.05	0.05	0.05	0.05	0.05	0.05	0.05
Sorbitol (% v/v)	30	30	30	30	30	30	30	30	30	30	30	30
Sucrose (% w/v)	15	15	15	15	15	15	15	15	15	15	15	15
Distilled water, (qs)**	100	100	100	100	100	100	100	100	100	100	100	100

** quantity sufficient to make to 100ml of suspension.

2.2.9.9 Stability study

Paracetamol suspensions were placed in the stability chamber and maintained at the real-time condition of 30˚C/65% Relative humidity (RH), and accelerated condition of 40˚C/75% RH and in a refrigerator at 4˚C for 3 months. Samples were collected at 0, 30, 60 and 90 days. The analysis comprised of testing certain parameters, which could change during storage, such as pH, drug content, physical appearance and odor. The appearance of each sample was evaluated by visual inspection of the suspension. Furthermore, analysis of particle size was performed initially and after 90 days using laser diffraction particle-size analyzer (Mastersizer 2000, Malvern Instruments Ltd, and Worcestershire, WR14 1XZ, UK). The suspensions were assayed for total paracetamol concentration using the UV-spectrometric method. Results recorded are averages of triplicate determinations.

2.2.9.10 Statistical analysis

Origin 8 Software (OriginLab Corporation, MA, and USA) was used to statistically analyze the results and one way analysis of variance (ANOVA) was applied for comparison of all results. To demonstrate graphically the influence of each factor on responses and to indicate the optimum level of factors, the contour and response surface plots were generated using Design-Expert 10.0.7.0 software (Stat-ease, Corp. Australia). At 95% confidence interval, p-values of < 0.05 were considered statistically significant. All the data measured and reported were averages of a minimum of triplicate measurements and the values are expressed as mean ± standard deviation.

3. Results and Discussion

3.1 Components of Bamboo wood and Eucalyptus sawdust

It is well-known that lignocellulosic biomass consists mainly three major components (hemicellulose, cellulose, and lignin) together with trace amounts of extractives and minerals. Mostly, cellulose, hemicellulose and lignin cover 40-70%, 20-30%, and 10-25% of lignocellulosic biomass on dry basis, respectively (Hidayat *et al.,* 2012; Klemm *et al.,* 2005). The chemical compositions of BW and ES are shown in Table 3.1.

The result of this study is not in good congruence with the result reported by Rehman *et al.,* (2018) on ES, which reported the presence of 27.60% of hemicellulose, 20.60% of lignin, and 5.26% of extractives. This difference may be due to environmental factors, method used for extraction and type of eucalyptus species used. In contrary, comparable lignin and hemicellulose amounts were reported by Carrillo et al., (2018), 13.75 ± 0.3 and 28 ± 0.6, respectively. The study result on BW is in good agreement with literature values (Lin *et al.,* 2021). As shown in Table 3.1, BW contains higher amount of lignin and lower amount of hemicellulose compared to ES.

Table 3-1: The biomass components of bamboo wood and eucalyptus sawdust.

Biomass	**Components (% w/w)**		
	Total extractives	hemicellulose	lignin
Eucalyptus sawdust	6.5 ± 0.83	30 ± 1.21	12 ± 0.51
Bamboo Wood	8.4 ± 1.1	17.1 ± 0.62	21 ± 1.24

Data are presented as mean ± SD (n = 3).

3.2 Yield of cellulose

Before applying the current cellulose extraction method for characterization and modification of BWC and ESC, preliminary studies were conducted in order to select a method which gives a better characteristic of cellulose. During the preliminary study, isolation of cellulose was carried out using the following three solvent extraction methods: (i) Acetic acid-Nitric acid method (Sun

and Tomkinson, 2005). (ii) sodium hydroxide-steam explosion method (Ranganagowda *et al.*, 2019) and (iii) Formic Acid-Acetic acid methods (Schneider *et al.*, 2016). These extraction methods resulted in different yields and color of cellulose fibers. The sodium hydroxide-steam explosion extraction gave BWC and ESC with a better organoleptic property compared to the other methods. The obtained cellulose samples were white, fluffy, odorless and tasteless fibrous materials (Figure. 3.1).

Figure 3-1: Photographs of A) Extracted bamboo wood cellulose (BWC) and B) eucalyptus sawdust cellulose (ESC) (from left to right), respectively.

The high energy steam produced in an autoclave during the sodium hydroxide-steam explosion pretreatment process makes the cellulose more susceptible to oxidation through the diffusion of sodium hydroxide and hydrogen peroxide resulting in removal of hemicellulose and lignin components from the lignocellulosic biomass (Ranganagowda *et al.*, 2019).

The cellulose yield primarily depends on the source and the method of extraction used. The different extraction methods used during preliminary study resulted in different yields. The percentage yields were found to be 50.24% ±1.36 and 47.1%±1.4 (Acetic acid -Nitric acid method), 48.06%±1.02 and 44.21%± 1.14 (alkali-steam explosion method) and 46.14%± 1.3 and 44.01%± 1.06 (formic-acetic acid method) from BW and ES, respectively.

The observed differences in yield may be due to degradation of cellulose to different extent in those pretreatments (Lu *et al.,* 2020). Though, both steam-alkali method and formic-acetic acid method of extraction gave white fiber from both sources, the former gives a higher yield. The Acetic acid-Nitric acid-based method gave higher yield than the other methods but the obtained fiber was off white. The alkali-steam explosion based method gives a reasonably high yield and a better quality of cellulose. Consequently, selected for extraction and characterization of BWC and ESC.

The yield of cellulose following treatment of BW with alkali-steam explosion-based treatment was in agreement with a previously conducted study which reported the yield of cellulose to be 50.2% ± 1.2) (Lu *et al.,* 2020). The slightly decreased yield of cellulose in the present study might be associated with the chemicals used, temperature and treatment duration applied in the isolation process. In addition to formic acid, steams are likely to be involved in cellulose degradation (Wang *et al.,* 2009; Boonterm *et al.,* 2016). Study by Rehman et al. (2018) also revealed that yield from eucalyptus wood was 42.7%, which is in good harmony with the current study.

Compared to the yield of cellulose isolated from *Luffa cylindrica* fiber (37.3 %), jute (33.5%) and corn cob (36%), the result of this study were greater (Jahan *et al.,* 2010). In contrast, the yield of BW and EC were lower than cellulose from Sorghum straw (45.4%) (Ohwoavworhua and Adelakun, 2010), cotton (86.7%) (Zhang *et al.,* 2011), cotton linter (78.3%) (Sczostak, 2009), and Flax fibres (72.4%) (Azhar *et al.*, 2021). These differences are mainly due to the type of samples and method employed for cellulose extraction.

3.3 Optimization of SCMC synthesis

3.3.1 Degree of substitution

The various properties of SCMC depend on its DS, average number of carboxyl content per AGU. Below a DS of 0.4 SCMC exhibit less solubility in water. However, polymer solubility will increase with increasing DS. In this respect, DS is a key factor to produce SCMC because the industrial utility of the SCMC exclusively depends on its DS. Thus, DS was chosen as dependent variable for SCMC's quality. All the optimization experiments were done with respect to the DS (Zhang *et al.,* 2011.

The DS of all the 20 experiments done for BW-SCMC and ES-SCMC as per CCD are presented in Table 3.2 and 3.3, respectively. The DS of prepared BW-SCMC and ES-SCMC were aranged from 1.12 to 1.43 and 0.73 to 1.16, respectively. SCMC obtained from BW cellulose exhibited the highest DS (1.43) when 1:1.5 ratio of Cellulose: MCA (g/g) was used at 50^{o}C for 150 min of etherification period (Table 3.2). But, the least DS (0.73) were observed in ES-SCMC at 1:1 ratio of Cellulose: MCA (g/g) at 50 ^{o}C and etherification duration of 150min (Table 3.3). Moreover, different DS was obtained for each SCMC prepared from the byproducts at similar carboxymethylation conditions. This indicates DS of SCMC products were dependent on the source of cellulose at similar carboxymethylation condition. The DS value of BW-SCMC (1.43) in current study is comparable with the result reported by Moussa et al., (2019). However, higher than the DS of SCMC from cotton linter (1.08) reported by Haleem *et al.*, (2014) and from corn stalk (0.83) reported by Zhang et al., (2011). This might have been due to the difference in etherification condition used during the carboxymethylation process and also, the types of cellulosic sources used in the preparation of SCMC.

3.3.2 Selection of mathematical models

The relationship between the three independent variables (reaction duration, amount of MCA and Temperature) and the response variable (DS) were analyzed using response surface methodology. Polynomial models including linear, interaction and quadratic terms were generated for DS using Design Expert software. The best fitting mathematical model was selected based on the comparisons of several statistical parameters including the coefficient of variation (CV), the multiple correlation coefficient (R^2), adjusted multiple correlation coefficient (adjusted R^2) and the predicted residual sum of square (PRESS) provided by the Design Expert software (Tables 3.4 and 3.5).

The fit of the model was evaluated through R^2-values. As observed from Tables 3.4 and 3.5, R^2 were high (> 0.90) for the response, which indicates a high degree of correlation between the experimental and predicted responses. In addition, the 'Predicted $R^{2'}$ value was in good agreement with the 'Adjusted $R^{2'}$ value (the difference is less than 0.2), indicating dependable models. Tables 3.4 and 3.5 also show that the selected models have smaller PRESS values compared to other models; again, indicating the models fit the data. Based on the fit summary, quadratic model was selected as best fit for DS as suggested by the software. In this study, the fit summary output was

analyzed without performing any transformation (logarithmic, power, inverse, etc.) on the response data. Table 3.6 and 3.7 of Sequential Model Sum of Squares [Type I] was performed for the selected models for DS. It can be observed that a Quadratic vs 2FI model was chosen based on the probability value (p-value) of the various models under consideration (<0.0001).

Table 3-2. The central composite design of BW-SCMC with independent variables and the corresponding response variable.

S.N	A	B	C	t (min)	MCA (g)	T (°C)	DS
1	0	1	0	150	1.5	50	1.43
2	0	0	1	150	1	70	1.33
3	0	0	-1	150	1	50	1.42
4	1	0	0	240	1	50	1.36
5	1	1	-1	240	1.5	30	1.28
6	1	-1	-1	240	0.5	30	1.12
7	0	-1	0	150	0.5	50	1.39
8	1	1	1	240	1.5	70	1.31
9	-1	-1	-1	60	0.5	30	1.18
10	-1	1	1	60	1.5	70	1.18
11	-1	0	0	60	1	50	1.31
12	-1	1	-1	60	1.5	30	1.21
13	0	0	0	150	1	50	1.4
14	0	0	-1	150	1	30	1.27
15	0	0	0	150	1	50	1.42
16	0	0	0	150	1	50	1.41
17	0	0	0	150	1	50	1.4
18	0	0	0	150	1	50	1.4
19	-1	-1	1	60	0.5	70	1.25
20	1	0	1	240	0.5	70	1.27

Table 3-3. The central composite design of ES-SCMC with independent variables and the corresponding response variable.

S. N	A	B	C	T (min)	MCA (g)	T (ºC)	DS
1	0	1	0	150	1.5	50	1.11
2	1	0	0	240	1	50	1.06
3	0	0	0	150	1	50	1.13
4	0	0	1	150	1	70	1.02
5	-1	1	1	60	1.5	70	0.89
6	-1	-1	1	60	0.5	70	0.74
7	0	-1	0	150	0.5	50	1.03
8	1	1	1	240	1.5	70	0.95
9	-1	-1	-1	60	0.5	30	0.73
10	-1	1	-1	240	1.5	30	0.80
11	0	0	-1	150	1	30	0.93
12	-1	1	-1	60	1.5	30	0.71
13	0	0	0	150	1	50	1.16
14	-1	0	0	60	1	50	0.96
15	0	0	0	150	1	50	1.14
16	0	0	0	150	1	50	1.13
17	0	0	0	150	1	50	1.13
18	0	0	0	150	1	50	1.12
19	1	-1	-1	240	0.5	30	0.83
20	1	-1	1	240	0.5	70	0.85

Table 3-4: Fit summary statistics for DS of the 20 experiments of synthesized BW-SCMC as per CCD.

Response	Source	SD	R-Squared	Adjusted R-Squared	Predicted R-Squared	PRESS	
DS	Linear	0.0997	0.0962	-0.0732	-0.6489	0.2903	
	2FI	0.1047	0.1913	-0.1820	-4.7266	1.01	
	Quadratic	**0.0060**	**0.9979**	**0.9961**	**0.9928**	**0.0013**	**Suggested**
	Cubic	0.0073	0.9982	0.9942	0.8539	0.0257	Aliased

Table 3-5: Fit summary statistics for DS of the 20 experiments of synthesized ES-SCMC as per CCD.

Response	Source	SD	R-Squared	Adjusted R-Squared	Predicted R-Squared	PRESS	
DS	Linear	0.1600	0.1040	-0.0640	-0.6115	0.7366	
	2FI	0.1743	0.1356	-0.2633	-5.4108	2.93	
	Quadratic	**0.0122**	**0.9967**	**0.9938**	**0.9870**	**0.0059**	**Suggested**
	Cubic	0.0148	0.9971	0.9908	-0.1942	0.5459	Aliased

3.3.3 Model adequacy checking

The model reliability was verified by using ANOVA. ANOVA was used to analyze the data to obtain the interaction between process of independent variables and response. This was conducted by Fisher's statistical test for sum of square due to regression to the mean sum of square due to error and indicated the significance of each controlled factor on the tested model.

The results of ANOVA (Table 3.8 and 3.9) indicated that A, B, C, AB, AC, BC, A^2, C^2 and A, B, C, BC, A^2, C^2 are significant ($p<0.05$) model terms for BW-SCMC and ES-SCMC, respectively. Values greater than 0.05 indicate the model terms are not significant. As can be seen from Table 3.8 and 3.9, the p-values of lack of fit (LOF) were greater than 0.05 for the response variable, which further strengthened the reliability of the model (for a model to be successfully used for prediction, the LOF, which is a special diagnostic test for adequacy of a model that compares the pure error and describes the variation of data around the fitted model, should be insignificant).

Adequate precision (signal to noise ratio) values higher than 4 for the response (Table 3.10 and 3.11) confirmed that the proposed models can be used to navigate the design space. For the models % CV were not greater than 10%; indicating the reproducibility of the models.

Table 3-6: Sequential Model Sum of Squares of BW-SCMC.

Response	Source	Sum of Squares	df	Mean Square	F-value	p-value	
DS	Mean vs Total	34.60	1	34.60			
	Linear vs Mean	0.0169	3	0.0056	0.5678	0.6441	
	2FI vs Linear	0.0167	3	0.0056	0.5093	0.6828	
	Quadratic vs 2FI	**0.1420**	**3**	**0.0473**	**1294.87**	**< 0.0001**	**Suggested**
	Cubic vs Quadratic	0.0000	4	0.0000	0.2105	0.9233	Aliased
	Residual	0.0003	6	0.0001			
	Total	34.77	20	1.74			

Table 3-7: Sequential model sum of squares of ES-SCMC

Response	Source	Sum of Squares	df	Mean Square	F-value	p-value	
DS	Mean vs Total	18.82	1	18.82			
	Linear vs Mean	0.0475	3	0.0158	0.6191	0.6127	
	2FI vs Linear	0.0145	3	0.0048	0.1586	0.9223	
	Quadratic vs 2FI	**0.3936**	**3**	**0.1312**	**878.44**	**< 0.0001**	**Suggested**
	Cubic vs Quadratic	0.0002	4	0.0000	0.1937	0.9330	Aliased
	Residual	0.0013	6	0.0002			
	Total	19.28	20	0.9638			

The adequacy of the models was also confirmed with residual plot tests of regression models. Two plots related to residuals, namely, the normal probability plot of residuals and the plot of internally studentized residuals versus predicted values were considered as additional tests of model adequacy checking tools. The normal probability plot is a graphical technique for assessing whether or not a data set is normally distributed. The residual is the difference between the observed and the predicted value (or the fitted value) from the regression. If the points on the plot fall fairly close to straight line, then the data are normally distributed.

Table 3-8: Summary of ANOVA results for dependent variable (DS) of the 20 experiments of synthesized BW-SCMC as per CCD.

Source	Sum of Squares	df	Mean Square	F-value	p-value	
Model	0.1757	9	0.0195	533.97	< 0.0001	significant
A-t	0.0044	1	0.0044	120.62	< 0.0001	
B-MCA	0.0044	1	0.0044	120.62	< 0.0001	
C-T	0.0081	1	0.0081	222.15	< 0.0001	
AB	0.0081	1	0.0081	222.31	< 0.0001	
AC	0.0023	1	0.0023	62.31	< 0.0001	
BC	0.0063	1	0.0063	173.08	< 0.0001	
A^2	0.0155	1	0.0155	423.08	< 0.0001	
B^2	0.0000	1	0.0000	0.0000	1.0000	
C^2	0.0348	1	0.0348	951.92	< 0.0001	
Residual	0.0004	10	0.0000			
Lack of Fit	0.0001	5	0.0000	0.2187	0.9396	not significant
Pure Error	0.0003	5	0.0001			
Cor Total	0.1761	19				

The normal probability plot of residuals and the plot of residuals versus predicted values of the responses for DS are shown in the preceding figures. The results in Figure 3.2a and Fig. 3.3a, show that point clusters are placed closely to the diagonal line implying that the errors are distributed normally for the responses. Furthermore, the residuals in Figure 3.2b and Fig. 3.3b, appear to be randomly scattered about zero. These results again indicate that the model satisfies the assumptions of the ANOVA.

Table 3-9: Summary of ANOVA results for dependent variable (DS) of the 20 experiments of synthesized ES-SCMC as per CCD.

Source	Sum of Squares	df	Mean Square	F-value	p-value	
Model	0.4556	9	0.0506	338.94	< 0.0001	significant
A-t	0.0196	1	0.0196	131.39	< 0.0001	
B-MCA	0.0101	1	0.0101	67.70	< 0.0001	
C-T	0.0178	1	0.0178	119.23	< 0.0001	
AB	0.0003	1	0.0003	1.85	0.2038	
AC	0.0002	1	0.0002	1.03	0.3352	
BC	0.0140	1	0.0140	93.92	< 0.0001	
A^2	0.0363	1	0.0363	243.10	< 0.0001	
B^2	0.0088	1	0.0088	58.58	< 0.0001	
C^2	0.0639	1	0.0639	427.67	< 0.0001	
Residual	0.0015	10	0.0001			
Lack of Fit	0.0006	5	0.0001	0.6983	0.6484	not significant
Pure Error	0.0009	5	0.0002			
Cor Total	0.4571	19				

Table 3-10: Numerical test results of model adequacy checking for BW-SCMC as per CCD.

Response	Source	R- Squared	Adjusted R-Squared	Predicted R-Squared	Adequate precision	% CV
DS	Quadratic	0.9979	0.9961	0.9928	73.4098	0.4597

Table 3-11: Numerical test results of model adequacy checking for ES-SCMC as per CCD.

Response	Source	R- Squared	Adjusted R-Squared	Predicted R-Squared	Adequate precision	% CV
DS	Quadratic	0.9967	0.9938	0.9870	48.4618	1.26

.

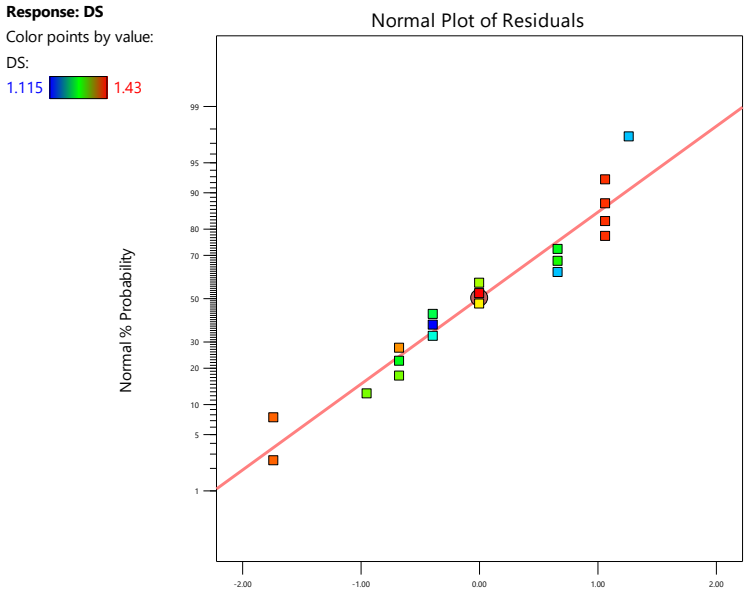

a.

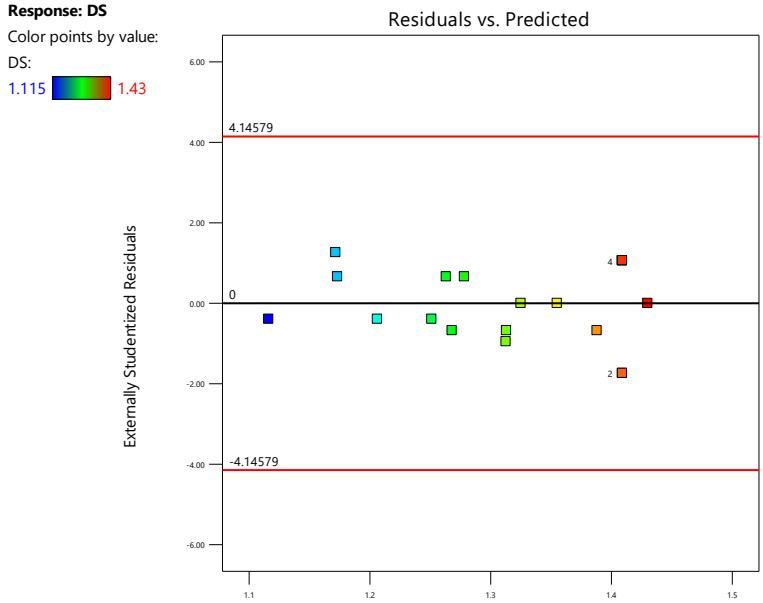

b.

Figure 3-2: a) Normal probability plot of residuals b) plots of the residuals against predicted response for DS results of BW-SCMC as per CCD.

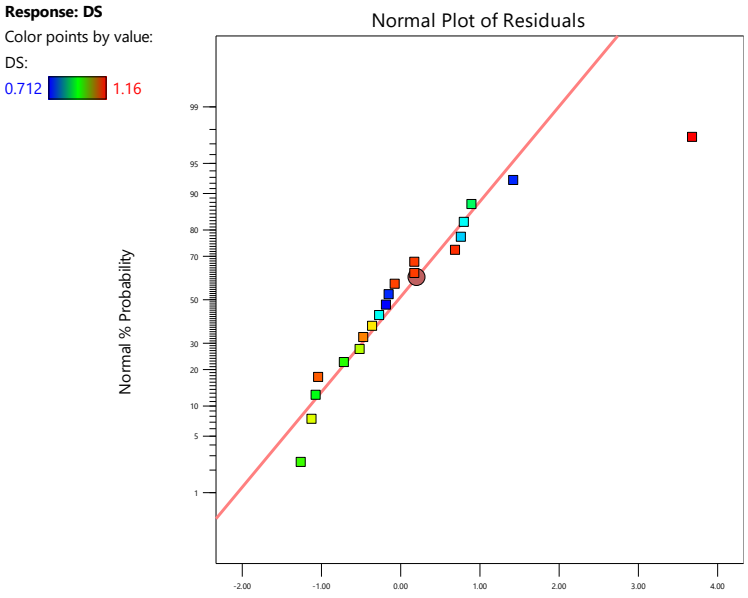

a.

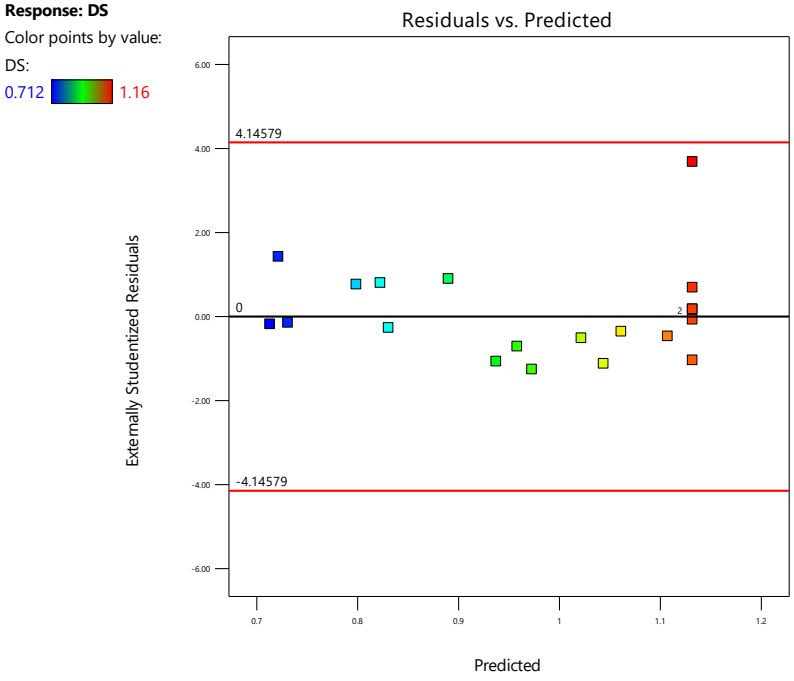

b.

Figure 3-3: a) Normal probability plot of residuals b) plots of the residuals against predicted response for DS results of ES-SCMC as per CCD

In order to determine the levels of factors which yield optimum response, mathematical relationships were generated between the dependent (DS) and independent variables. The final equations in terms of coded factors (Eq. 3.1 and Eq. 3.2) were developed for BW-SCMC and ES-SCMC, respectively using model term coefficients shown in Tables 3.8 and 3.9.

$$DS = +1.41+0.02A+0.02B+0.03C+0.032AB+0.017AC-0.03BC-0.08A^2-0.11C^2 \quad (3.1)$$

$$DS = +1.13+0.04A+0.032B+0.04C+0.042BC-0.11A^2-0.06B^2-0.15C^2 \quad (3.2)$$

The p-values were used as a tool to check the significance of each coefficient, which was necessary to understand the pattern of the mutual interactions between the best factors (Chen *et al.,* 2009). The smaller the p-value, the bigger the significance of the corresponding coefficient (Li *et al.,* 2007). A coefficient is the amount the response changes when that term is changed by one unit, while holding the other terms constant. Coefficients of developed models have physical meanings on response variable. Both the magnitude and sign of coefficients are important. The magnitude implies the strength while the sign indicates the direction of that factor variable on the corresponding response variable. A positive sign indicates a positive effect whereas a negative sign indicates a negative effect on the response (Singh *et al.,* 2010).

As seen in Eq. 3.1 and 3.2, and Table 3.12, DS of both SCMC's was affected positively by the duration of etherification, amount of MCA and Temperature of etherification. The second order interactions (AB and AC) affect the DS of BW-SCMC positively, whereas (BC) negatively. Only the second order interaction BC significantly affects the DS of ES-SCMC positively. Quadratic effects (A^2 and C^2) were found to have significant negative relationship with DS for both SCMC.

Table 3-12: Estimated model term regression coefficients for the DS of BW-SCMC and ES-SCMC as per CCD.

Response		**Intercept**	**A**	**B**	**C**	**AB**	**AC**	**BC**	**A^2**	**B^2**	**C^2**
DS	BW-SCMC	1.41	0.02	0.02	0.03	0.032	0.017	-0.03	-0.08	-	-0.11
	ES-SCMC	1.13	0.04	0.032	0.04	-	-	0.042	-0.11	-0.06	-0.15

3.3.4 Contour plot and surface response analysis

The 2D contour and 3D response surface plots are the graphical representations of the fitted regression models. These plots, presented on the basis of the model equations, display the interaction between the independent variables and assist in determining the optimum values of the variables within the ranges considered (Chen*et al.,* 2009). Contour plots (Figures 3.4a, 3.5a, 3.6a,

3.7a, 3.8a and 3.9a,) and response surface plots (Figures 3.4b, 3.5b, 3.6b, 3.7b, 3.8b and 3.9b) for the obtained response (DS) were drawn based on the model polynomial functions to assess the change of the response surface. These plots explain the relationship between the dependent (DS) and independent variables.

As can be seen from the plots, the results are in agreement with the ANOVA results indicated in Tables 3.8 and 3.9. The contour and response surface plots shown in Figure 3.4 and 3.5, indicate the combined effect of A (duration of etherification) and B (amount of MCA) on the response DS of the BW-SCMC and ES-SCMC, respectively. As can be seen from these plots, the factors have non-linear relationship on DS. Both the factors appeared to have pronounced effect on the response. This was in agreement with the ANOVA results (Table 3.8 and 3.9), where A and B showed more significant effect ($p < 0.0001$) on DS. The contribution of the second order terms from Eq. 3.1 and 3.2, and Tables 3.8 and 3.9 were interpreted as the presence of curvature in the plots.

The contour and response surface plots shown in Figures 3.6 and 3.7, indicate the combined effect of the two factors A (duration of etherification) and C (Temperature) on the response variable, DS of BW-SCMC and ES- SCMC, respectively. The series of circular lines of the contour plot and the non-twisted response surface of Figure 3.6, indicates that there was no significant interaction effect of the two parameters on DS of ES-SCMC. The plots show that the quadratic model components individually affect DS, with significant effect. The same is indicated in the ANOVA results (Table 3.9), where A and C showed more significant effect ($p < 0.0001$) on DS. On the contrary, Figure 3.7, shows the two factors A (duration of etherification) and C (Temperature) have significant interaction effect ($p < 0.0001$) on the response variable, DS of BW-SCMC. In the same way, the contour and response plots shown in Figure 3.8 to Figure 3.9 for the combined effect of the two factors B (Amount of MCA) and C (Temperature) on the response variable (DS) of BW-SCMC and ES-SCMC were consistent with their ANOVA results indicated in Tables 3.8 and 3.9.

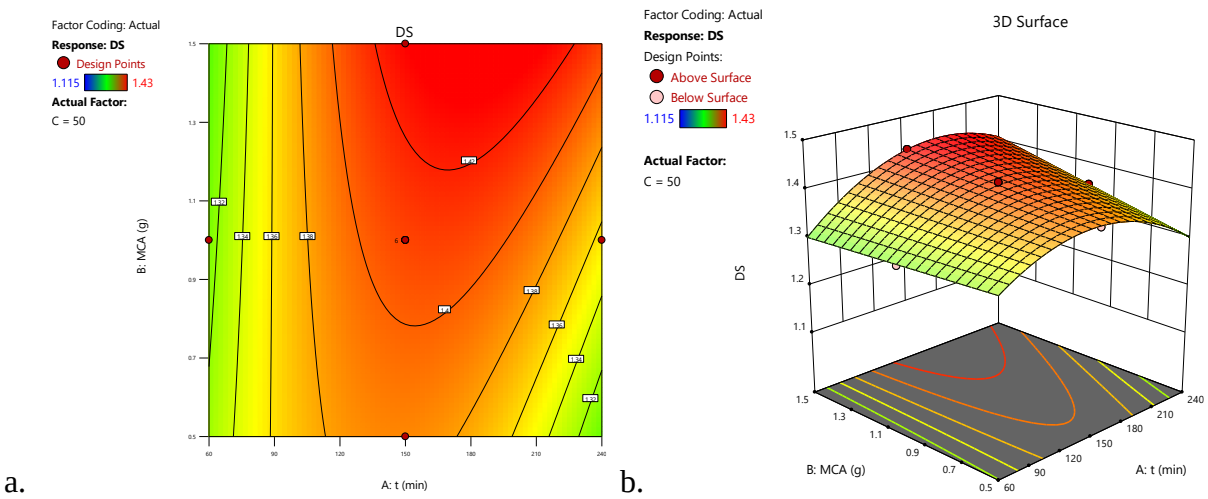

Figure 3-4: a) Contour plot and b) response surface plot showing the effect of A (duration of etherification)) and B (amount of MCA) on the response DS of BW-SCMC as per CCD.

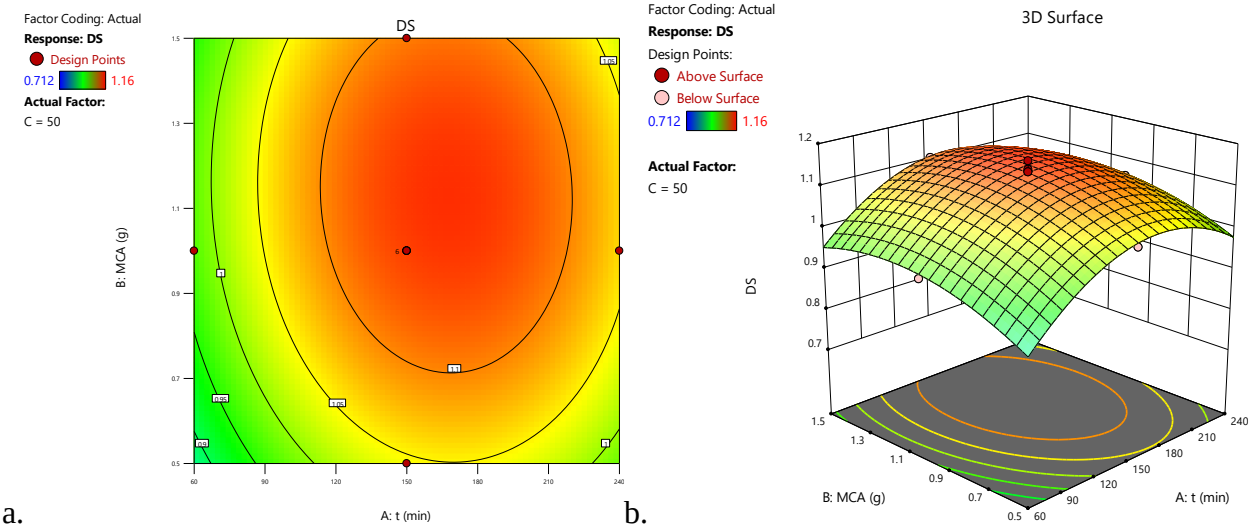

Figure 3-5: a) Contour plot and b) response surface plot showing the effect of A (duration of etherification) and B (amount of MCA) on the response DS of ES-SCMC as per CCD.

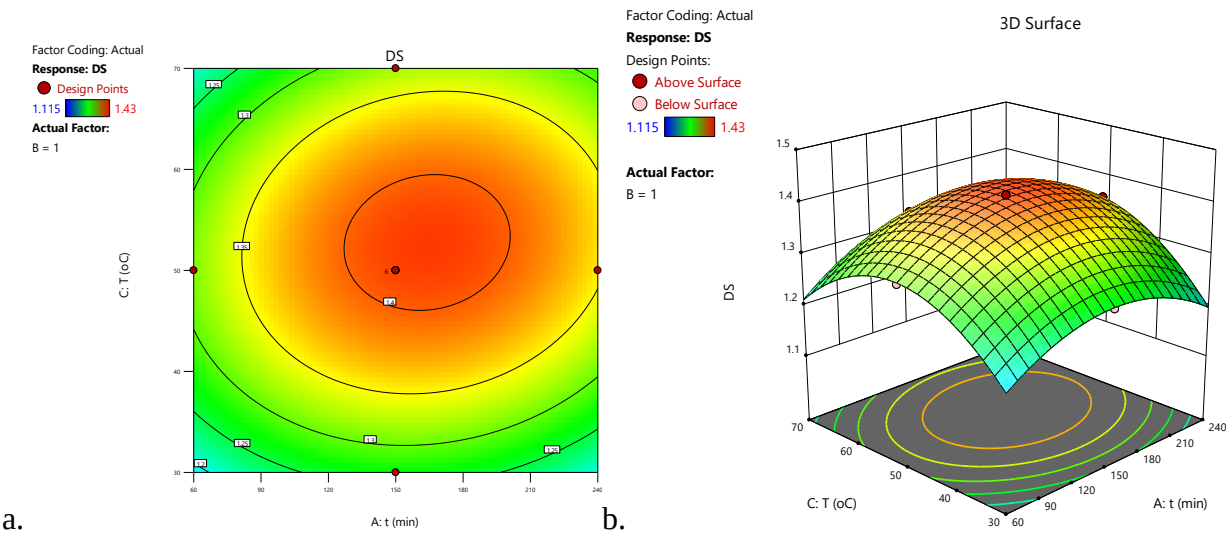

a. b.

Figure 3-6: a) Contour plot and b) response surface plot showing the effect of A (duration of etherification)) and C (Temperature of etherification) on the response DS of BW-SCMC as per CCD.

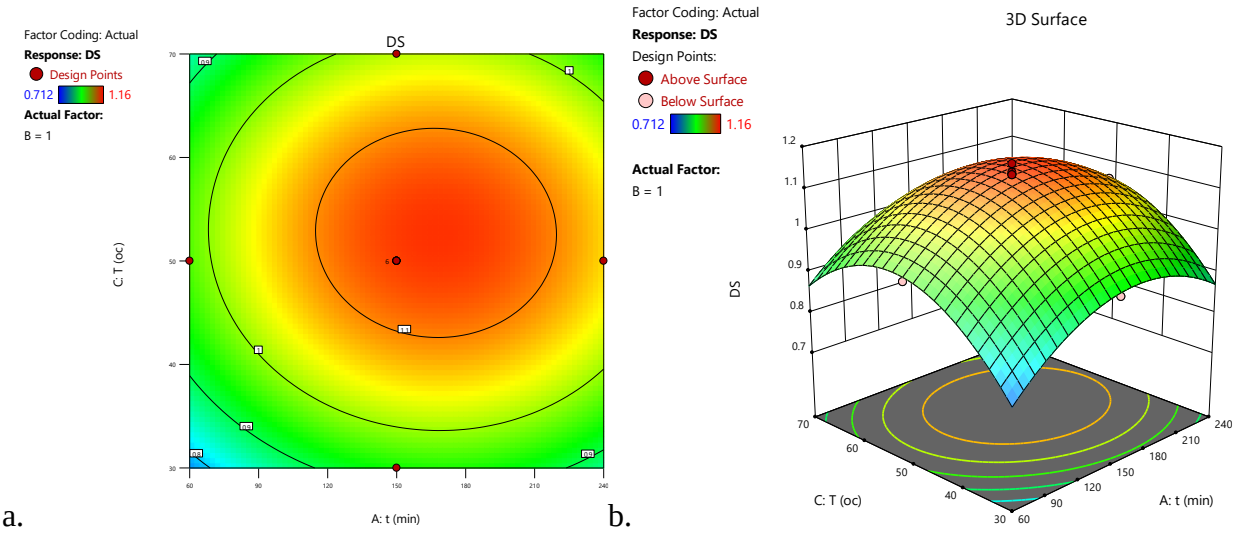

a. b.

Figure 3-7: a) Contour plot and b) response surface plot showing the effect of A (duration of etherification) and C (Temperature of etherification) on the response DS of ES-SCMC as per CCD.

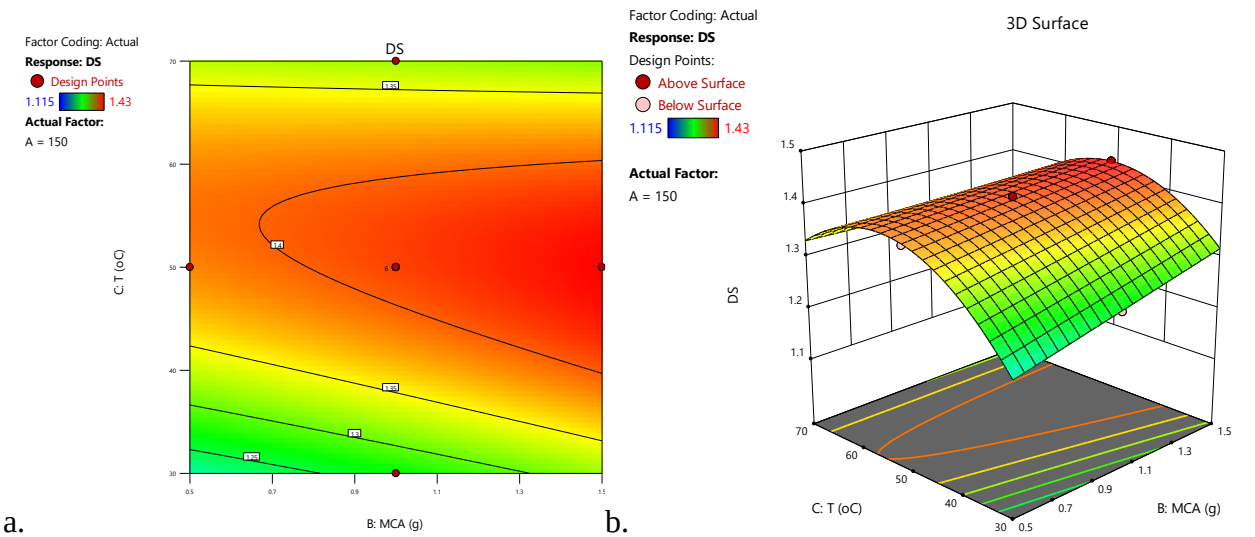

a. b.

Figure 3-8: a) Contour plot and b) response surface plot showing the effect of B (Amount of MCA) and C (Temperature of etherification) on the response DS of BW-SCMC as per CCD.

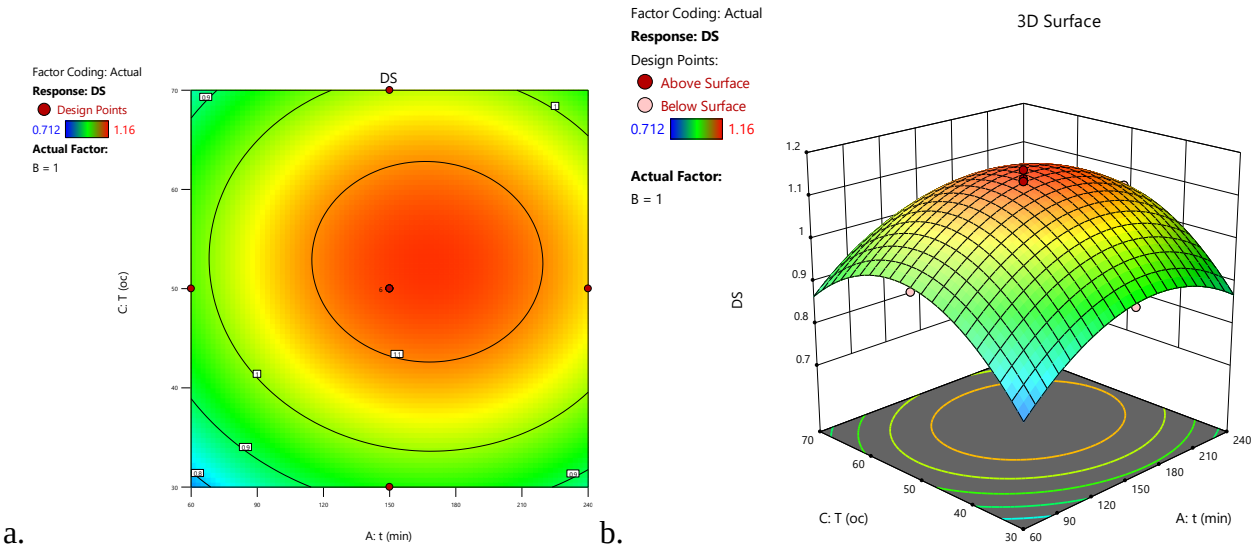

a. b.

Figure 3-9: a) Contour plot and b) response surface plot showing the effect of B (Amount of MCA) and C (Temperature of etherification) on the response DS of ES-SCMC as per CCD.

3.3.5 Optimization of DS

After generating the model polynomial equation to relate the dependent (DS) and independent variables, the synthesis was optimized for DS response. The final optimal experimental parameters were obtained using numerical optimization techniques of Design-Expert 10.0.7.0 software, which allows compromise among various factors and searches for a combination of factor levels that jointly optimize the response by satisfying the requirement set. In optimizing of the carboxymethylation process the duration of etherification, amount of MCA and temperature were set “in range” and the DS was set as “maximize”. Table 3.13, presents the criteria defined for factors and response during optimization with numerical technique.

The desirability function approach is one of the most widely used methods for optimization of several factors. Overall desirability function is a measure of how well the combined goals for independent and response factor are satisfied. Desirability function ranges from 0 to 1, with value closer to one indicating a higher satisfaction of response goal(s). Table 3.14, shows some of the predicted optimum values according to the set goal for BW-SCMC and ES-SCMC. In this study, a total of five result were obtained for BW-SCMC and among these the one with the overall desirability of 1.00 was selected by the software, which exhibits the desired combinations of process parameters that would provide the highest response to DS. Whereas a total of 100 results were obtained for ES-SCMC and among these the one with the overall desirability of 0.967 was selected by the software.

Table 3-13: Constraints for factors and response used during numerical optimization for synthesized BW-SCMC and ES-SCMC as per CCD.

Factor constraints					
Factor		**Goal**	**Lower Limit**	**Upper Limit**	**Importance**
A: t (min)		is in range	60	240	3
B: MCA (g)		is in range	0.5	1.5	3
C: T (ºC)		is in range	30	70	3
Response constraints					
DS	BW-SCMC	Maximize	1.11	1.43	3
	ES-SCMC	Maximize	0.71	1.16	3

Table 3-14: Numerical optimization results of predicted optimum values for BW-SCMC and ES-SCMC as per CCD.

S.N	**SCMC type**	**t (min)**	**MCA (g)**	**T (ºC)**	**DS**	**Desirability**	
1.	BW-SCMC	187.76	1.47	48.15	1.435	1.000	Selected
2.	ES-SCMC	166.31	1.17	53.66	1.145	0.967	Selected

3.3.6 Validation of the optimized synthesis

To experimentally confirm the validity of the obtained optimal conditions, confirmation experiments were carried out in triplicate at the optimal combinations of the factors (t = 187.76 and 166.3min, MCA= 1.465 and 1.17g, and T = 48.15 and 53.65ºC for BW-SCMC and ES-SCMC, respectively). Table 3.15, provides the predicted values, experimental results and the percentage error values obtained at optimal levels of the factors. As seen in the table, the values of percentage errors had fallen within 5% and this confirmed that the experimental values of the optimized conditions agreed well with the predicted values.

Table 3-15: Response values of predicted, experimental and percentage error obtained at optimal levels of the factors of BW-SCMC and ES-SCMC.

Response	Type	Predicted value	Experimental value	% Error
DS	BW-SCMC	1.435	1.432	0.29
	ES-SCMC	1.145	1.141	0.35

3.4 Identification tests and properties of cellulose and SCMC

The obtained BWC and ESC were white in color and fibrous in nature. Identification tests were performed for all cellulose samples and all samples turned violet-blue in iodinated zinc chloride solution, confirming the presence of cellulose (Ibrahim *et al.,* 2010; Gumuskaya *et al.,* 2003). Both BW-SCMC and ES-SCMC samples physically appeared white color and fine powder. The organoleptic properties of the prepared cellulose and SCMC samples fulfilled the parameters specified in pharmacopoeias (USP 30/NF 25, 2007; BP, 2016).

Table 3-16: Some physicochemical properties of cellulose and SCMC samples. Data are presented as the mean ± SD (n = 3).

Test	**Samples**					**Standard per USP/NF**
	BWC	ESC	BW-SCMC	ES-SCMC	C-SCMC	
Water soluble substances	0.08±0.2	0.05±0.19	0.04±0.12	0.09±0.2	0.13±0.19	≤ 0.25%
Moisture content	5.5±0.81	5.2±1.12	5±0.67	4±1.35	4.8±1.63	≤ 7%
pH	5.5±0.2	5.67±0.21	6.3±0.27	6.2±0.3	6.5±0.15	5-7
Total ash (%)	0.06	0.058	0.02	0.02	0.03	≤ 0.1%
DP	524.64±0.89	701.51±1.16	-	-	-	
M. Wt.	84,990.87	113,644.62	-	-	-	

Percentage of water-soluble fraction, moisture content, pH and ash value of all samples of cellulose and SCMC were within the acceptable range stated in USP 30/NF 25, 2007, as presented in table 3.16. Moisture content is the most important parameter that affects flow properties and viscoelastic property of SCMC. The moisture content of all samples is within the range of USP specification (Table 3.16). The ash value is indicative of the inorganic content of the sample, is important to assess purity. As shown in the table, the ash value of the celluloses sample were less than 0.04. Moreover, the SCMC samples have exceptionally low value than the cellulose samples. This indicates that the SCMC samples are almost free of inorganic compounds (Chumee and Seeburin, 2014, Dai *et al.*, 2019; Yaşar *et al.*, 2007).

3.5 Sodium carboxymethylcellulose yield

In the present study, the yield of optimized BW-SCMC and ES-SCMC were 158.2±1.01% and 131.4±1.17%, respectively. These values are higher than the yield of SCMC from bamboo wood (112.7%) reported by Chen and Lou, (2014) and from ES (104.3%) reported by Amaral et al., (2019). This difference might be due to difference in carboxymethylation conditions used during the etherification process. Furthermore, the yield and DS of SCMC products were dependent on the source of cellulose at similar carboxymethylation condition.

3.6 Degree of polymerization

The DP of cellulose samples is usually determined from intrinsic viscosities of the cellulose solution in cupr-ammonium hydroxide solution. The DP and molecular weight of BWC and ESC are presented in Table 3.16. The isolated BWC and ESC have DP of 524.64±0.89 and 701.51±1.16, and molecular weight of 84,990.87 g/mol and 113,644.62 g/mol, respectively. The result is comparable with literature value of cellulose isolated from various sources. According to various publications, the DP of cellulose ranges from 500-2,249 and the molecular weight also ranges from 81,000-364,340 g/mol (Hallac and Ragauskas, 2011; Khalil *et al.,* 2018). These values depend on the sources of cellulose and method of isolation implemented i.e. type and concentration of chemicals used, temperature, and duration of treatment.

3.7 Fourier transform infrared spectroscopy analysis

FTIR spectroscopy is widely used as a powerful technique for the characterization of cellulose and its derivatives in order to obtain direct information on chemical changes that occur during various chemical treatments. The FTIR spectra of BWC and ESC are shown in Figure 3.10. It is evident from the graph that the two spectra observed shows very close similarity, which indicates the samples have similar chemical composition. Strong peaks of O-H stretching vibrations are reflected with broad band in the region 3150–3400 cm^{-1}. So, the observed broad absorption bands at 3425 cm^{-1} (BWC) and 3428 cm^{-1} (ESC) are due to the stretching vibration of the OH group (Tarchoun *et al.,* 2019).

A band at 2903 cm^{-1} (BWC) and 2908 cm^{-1} (ESC) is attributable to asymmetric C–H stretching vibration in methyl and methylene groups. The absorption bands at 1638 cm^{-1} (BWC) and 1646 cm^{-1} (ESC) spectrum are due to the bending mode of the absorbed water. The peaks at 1416 cm^{-1}

(BWC) and 1422 cm^{-1}(ESC) are attributed to C-H scissoring bending, the peaks at 1050 cm^{-1} (BWC) and 1055 cm^{-1} (ESC) are due to C-O ether stretching vibration from the antisymmetric C–O–C pyranose ring, the small peaks at 894 cm^{-1} (BWC) and 912 cm^{-1} (ESC) originate from C-O stretching of 2^{o} alcohol from β-glycosidic linkages between glucose units in cellulose (Veeramachineni *et al.*, 2016; Yang *et al.*, 2007).

The presence of lignin in the extracted cellulose can be noticed by the presence of peaks at 1500-1600 cm^{-1} and 1220-1245cm^{-1} due to aromatic C=C and C-O phenolic bonds, absence of these peaks in both BC and EC FTIR, shows the applied method is able to extract lignin effectively, which leads to purer cellulose. The purity of isolated cellulose is further confirmed by absence of peaks around 1715-1735 cm^{-1} which is attributed to C=O stretch bond of either the acetyl and uronic ester groups of the hemicelluloses or the ester linkage of carboxylic group of the ferulic and p-coumeric acids of lignin and/or hemicelluloses (Jahan *et al.*, 2011; Rosa *et al.*, 2010).

The FT-IR spectra of BW-SCMC, ES-SCMC and C-SCMC samples are shown in Figure 3.11, and the patterns of spectra between prepared BW-SCMC and ES-SCMC, and C-SCMC were similar. The broad band peak at 3428 cm^{-1} (C-SCMC), 3421 cm^{-1} (ES-SCMC), and 3421 cm^{-1} (BW-SCMC) is due to the stretching frequency of the O-H group. A band at 2920 cm^{-1} (C-SCMC), 2928 cm^{-1} (ES-SCMC) and 2920 cm^{-1} (BW-SCMC) are attributable to C-H stretching vibration (Ventura-Cruz and Tecante, 2019; Wang *et al.*, 2019).

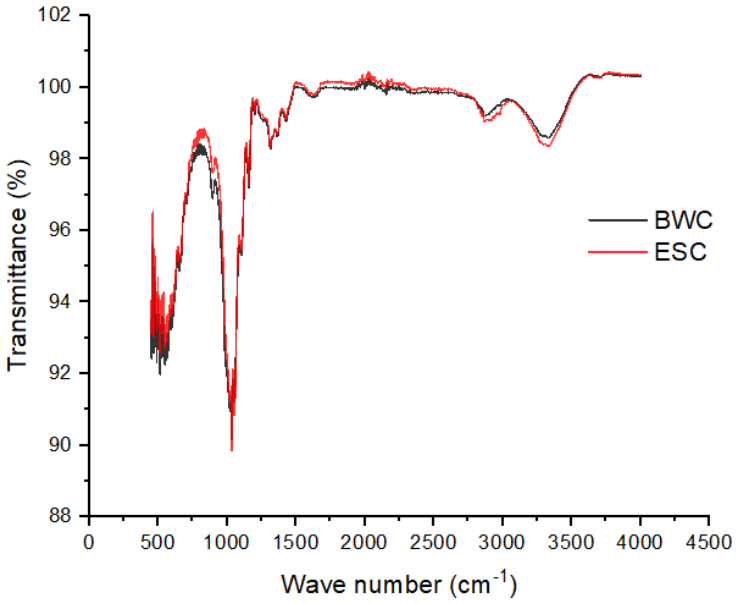

Figure 3-10: FTIR spectra of the celluloses extracted from BW and ES.

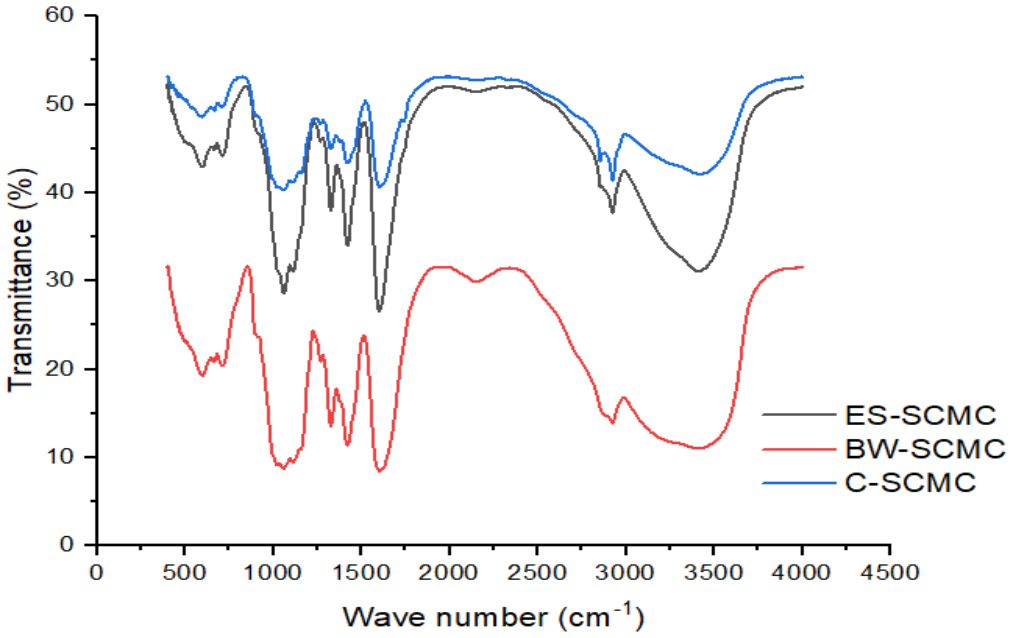

Figure 3-11: FTIR spectra of C-SCMC, BW-SCMC and ES-SCMC.

The presence of a new and strong absorption band at 1609 cm^{-1} (C-SCMC), 1601 cm^{-1} (BW-SCMC) and 1616 cm^{-1} (ES-SCMC) confirms the stretching vibration of the carboxyl group (COO^{-}), 1419 cm^{-1} (C-SCMC), 1420 cm^{-1} (BW-SCMC) and 1419 cm^{-1} (ES-SCMC) is assigned

to carboxyl groups as the sample salts. The bands around 1328 cm^{-1} (C-SCMC), 1328 cm^{-1} (BW-SCMC) and 1335 cm^{-1} (ES-SCMC), and 1108 cm^{-1} (C-SCMC), 1116 cm^{-1} (BW-SCMC) and 1123cm^{-1} (ES-SCMC) are assigned to O-H bending vibration and C-O-C stretching, respectively. Wavelength 736 cm^{-1} (C-SCMC), 722 cm^{-1} (BW-SCMC) and 714 cm^{-1} (ES-SCMC) are detected for 1, 4-glycoside of cellulose (Adinugraha *et al.,* 2005; Candido and Gonçalves, 2016).

Appearance of peaks at 1730 cm^{-1} (C-SCMC), 1732 cm^{-1} (BW-SCMC), 1725 cm^{-1} (ES-SCMC) (C=O stretch carboxylic acid) and 1260 cm^{-1} (C-SCMC), 1268 cm^{-1} (BW-SCMC) and 1254 cm^{-1} (ES-SCMC), C-O stretch carboxylic acid in the prepared SCMC spectrum are the indication of successful completion of etherification reaction and confirms the formation of sodium carboxymethyl cellulose (Rachtanapun *et al.,* 2012). A significant increase in the intensity of C=O band was observed after carboxymethylation as more carboxylic groups were introduced. Similar functional groups of SCMC from higher plants have already been reported in previous studies (Veeramachineni *et al.,* 2016; Yaşar *et al.,* 2007). The strong C=O peak for BW-SCMC product implies considerable extent of etherification in the synthesis, suggesting a relatively high content of the carboxymethyl groups in the SCMC product (Ahuja *et al.,* 2018).

3.8 Crystallinity analyses

X-ray diffraction analysis is a special technique for estimating the degree of crystallinity in polymer. Cellulose is semi-crystalline in nature, the crystalline portion gives a strong signal with sharp peaks while amorphous portion is represented by weak and broader signals in the diffraction pattern (Garvey *et al.,* 2005). The X-ray diffraction patterns of BWC, ESC, BW-SCMC, ES-SCMC and C-SCMC are shown in Figure 3.12. The XRD profiles of BWC and ESC exhibits a typical diffraction peak at 18.7 ^{o} and 22.7 ^{o}, and 19.4 ^{o} and 22.6 ^{o}, respectively. These peaks are attributed to the crystalline structure of cellulose I, which is known to be native and predominant crystalline structure of bamboo and eucalyptus cellulose. Different literatures reported that the typical peaks of cellulose-I are usually found at 2θ values of around 13^{o} and 25^{o} (Rasheed *et al.,* 2020). Moreover, the absence of doublet peak at the 002 plane of the samples indicates that both samples are comprised of cellulose-I polymorph without cellulose-II. This finding is also supported by the IR spectrum of both samples (Figure 3.12). Where, absorbance at 1315 cm^{-1} and 1312^{-1} is seen on IR spectrum of BWC and ESC respectively, which corresponds to CH-2 wagging

of cellulose-I (Klemm *et al.*, 2005). Differences observed in peak height and width between the samples is due to difference in their degree of crystallinity and crystal size (Wang *et al.*, 2009).

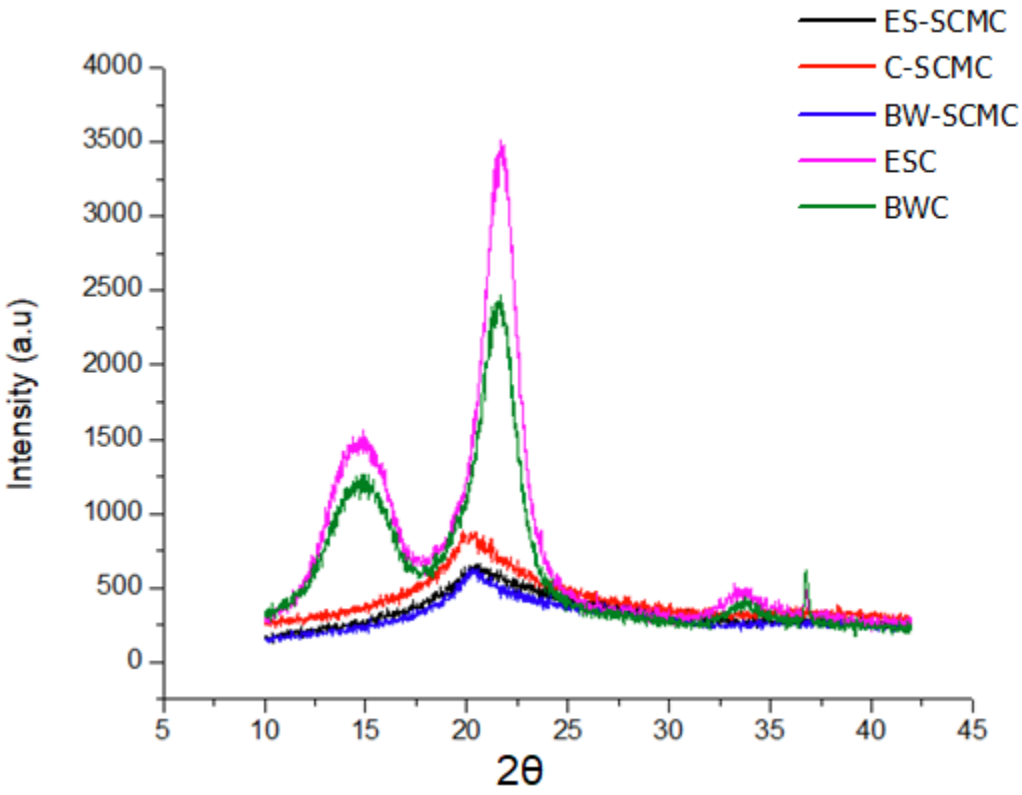

Figure 3-12; X-ray diffractograms of BWC, ESC, C-SCMC, BW-SCMC and ES-SCMC.

The crystallinity index (CrI) is calculated following the amorphous subtraction method proposed by Park *et al.*, (2010). The CrI of BWC and ESC was found to be 74.3% and 79.2%, respectively. The cellulose obtained from eucalyptus showed the greatest crystallinity index (79.2%). This might be due to the removal of most of the amorphous non-cellulosic compounds, such as lignin and hemicellulose from eucalyptus than bamboo. The CrI of BWC and ESC in this study were higher than those reported elsewhere for other biomasses such as *Posidonia oceanica* brown algae (60.50%) (Tarchoun *et al.*, 2019), potato pulp (62.54%) (Cheng *et al.*, 2019), corn stalk (77.45%) (Reddy and Yang, 2005), and *Ulva lactuca* cellulose (59%), which indicate the removal of non-cellulosic materials from the extracted celluloses, as confirmed by a higher value in the respective CrI.

The X-ray diffraction patterns (Figure. 3.12) of BW-SCMC and ES-SCMC show the SCMC samples had peaks of lower intensity than the cellulose precursor samples, due to destruction of the crystalline structure of the original cellulose with etherification. Carboxymethylation of cellulose caused significant changes in the arrangement of the polymer chains of cellulose. During the carboxymethylation process, the cellulose molecules are placed in an alkaline solution to result in cleavage of hydrogen bonds. The presence of the carboxymethyl moieties which substitute the hydrogen atoms of the hydroxyl groups of cellulose result in swelling of cellulose. This swelling of the cellulose granules exerts a tension on neighboring crystal cellulose molecules and tends to distort them. Further swelling leads to uncoiling or dissociation of their double-helical region and the breakup of their crystalline structure, affecting the establishment of hydrogen bonds involving these groups that are responsible for the adoption of a more ordered arrangement by the cellulose (Adinugraha *et al.,* 2005).

The calculated data also indicates that the optimized methods were able to change the crystal type and portion of the celluloses. Based on respective diffraction peaks, all characteristic peaks for native cellulose have almost disappeared and transformed into an amorphous phase. The optimized BW-SCMC and ES-SCMC method were able to decrease crystallinity from 74% to 42% and 79% to 48%, respectively. The BW-SCMC (DS: 1.432) resulted from this work had lower crystallinity (42%) than ES-SCMC (DS: 1.141) and the commercial sample C-SCMC (DS: 0.871), this was shown in Figure 3.12. According to Lin et al. (1990), the crystallinity of SCMC decreases with the increase of the degree of substitution, whereas in SCMC with DS higher than 1, the crystallinity peak was very small.

3.9 Thermal stability

Thermogravimetric analysis is one of the most widely used techniques to investigate the thermal decomposition of macromolecules such as cellulose and its derivatives. DTA was used to measure the exothermal or endothermal changes with increase in temperature (Zhang *et al.,* 2012). Supermolecular structures of cellulose and SCMC behave differently when undergoing thermal degradation thus the degradation profile of these polymers should be examined. Figures 3.13 and 3.14 show the TGA and DTA behavior of cellulose and SCMC samples, respectively.

As observed from the thermograms, thermal properties of BWC and ESC displayed three typical decomposition stages with different rates and extents. On the TGA curve, Initial weight loss stage

of the samples, BWC (27–115 °C), ESC (34-127 °C), ES-SCMC (29.3-129.5), BW-SCMC (30.2-129.2) and C-SCMC (27.4-129.50) known as drying stage occurred at temperature ranging from 27-130°C with endothermic peaks on DTA curves (Figures 3.13b and 3.14b). Their corresponding weight losses were 7.63%, 6.85%, 14.48%, 12.35% and 10.39%, respectively. Many studies reported this initial stage weight loss is due to evaporation of loosely bound moisture on the surface of the samples and evolution of absorbed water. The extent of temperature range for water evaporation depends on the original moisture content of the sample (Johar *et al.,* 2012; Trache *et al.,* 2014).

The major and second decomposition peaks of BWC, ESC, C-SCMC, ES-SCMC and BW-SCMC appeared at about 231-325°C, 237-331°C, 209-301°C, 211-325° and 228-337°C, respectively. These peaks are attributed to the degradation of the samples due to decarboxylation, depolymerization and decomposition of glycosyl units. A sudden reduction in weight loss in BWS and ESC thermograms occurred between 180-290 °C, due to the loss of hemicellulose. The low thermal stability of hemicellulose is due to the presence of acetyl groups. A second and more pronounced weight loss was observed between 315-420 °C due to the main degradation of cellulose (Poletto *et al.,* 2013), Cellulosic materials degrade at low to moderate temperatures, followed by pyrolysis of lignin, the main contributors to the evolution of the volatile compounds. Lignin has aromatic rings with various branches. Thus, the activity of the chemical bonds in lignin covered an extremely wide range which lead to the degradation of lignin to occur slowly at temperature ranging from ambient to 900 °C, thus the decomposition is overlapped in between hemicellulose and cellulose. A similar profile was reported for fibers from wood (Park *et al.,* 2010).

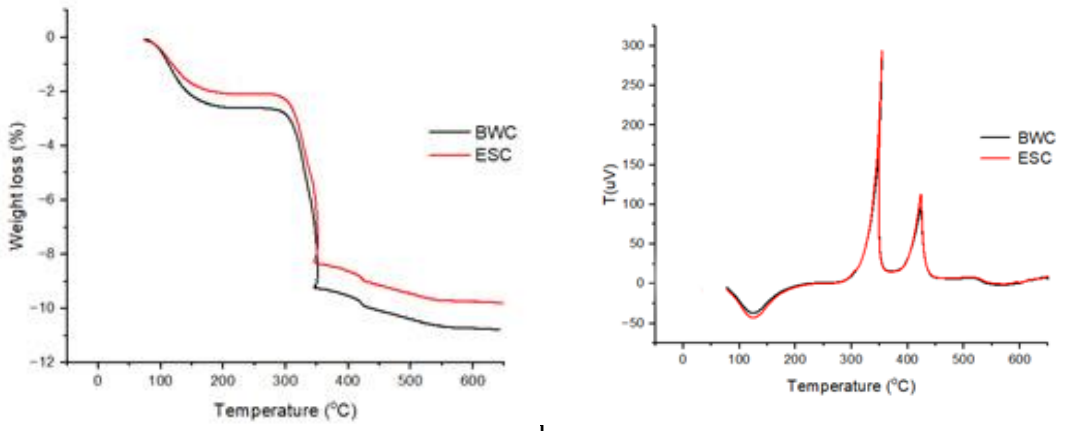

a. b.

Figure 3-13: Thermal degradation behaviors: a. TGA of BWC and ESC and b. DTA of BWC and ESC.

In the second degradation peak, C-SCMC, ES-SCMC and BW-SCMC started to decompose at 209°C, 215°C and 228 °C, respectively, which were at lower temperatures compared to the degradation temperature of BWC (231°C) and ESC (237°C), which may be due to the decarboxylation of COO groups in SCMC and the loss of CO_2 at lower temperature (Veeramachineni *et al.*, 2016). This result would suggest that cellulose with higher crystallinity exhibited higher thermal stability than its corresponding SCMC derivative, presence of carboxymethyl group reduces the crystallinity due to the presence of sodium and random irregularities produced by the relatively bulky side groups of carboxymethyl substituted on the cellulose backbone (Chen *et al.*, 2014). Moreover, a 50% weight loss happened in a relatively lower temperature range of 295-307 °C for SCMC samples when compared to 320-360 °C for cellulose precursors. Similar results were reported by salama *et al.*, (2018).

The decomposition peaks where the maximum mass loss occurred for BWC and ESC are at 327 and 335°C respectively. Degradation peak of BWC (CrI-74%) is lower than ESC (CrI-79%), this might be due to a difference in degree of crystallinity. The decomposition temperature of cellulose depends on their molecular weight and purity. In addition, the decomposition temperature is affected by polymer morphology and degree of crystallinity, high crystallinity of a polymer means high decomposition temperature (Princi *et al.*, 2005).

As shown in the thermogram, the thermal properties of SCMC are sensitive to DS changes. It has been reported that the thermal stability of SCMC increases with DS and molecular weight (Barud *et al.*, 2008; Casaburi *et al.*, 2018). This can be explained by the fact that, as DS increases, more carboxymethyl groups are introduced onto the C (2) and C (3) carbons of the AGU, which require more energy when compared to the least sterically hindered group C_6COOCH_3, and increase the apparent activation energy for thermal decomposition, leading to an increase in thermal stability (Araujo *et al.*, 2020). The increase in thermal stability at high DS can be also attributed to the possible inhibition of inter and intra-molecular hydrogen bond formation when the OH groups are substituted with carboxymethyl groups and low amount of remaining hydroxyl groups after etherification (Agustin *et al.*, 2015; Zhang *et al.*, 2011). These results also confirm that the thermal stability of BW-SCMC (DS of 1.432) is greater than ES-SCMC (DS of 1.141) and SCMC (DS of 0.871).

The third stage on the TGA curves started in the intervals of 395-450 °C (BWC) and 410-450 °C (ESC). At this stage only a small amount of weight losses, 9.95% (BWC) and 12.95% (ESC) were observed. Oxidative degradation of the charred residues of lignin is responsible for the observed effect.

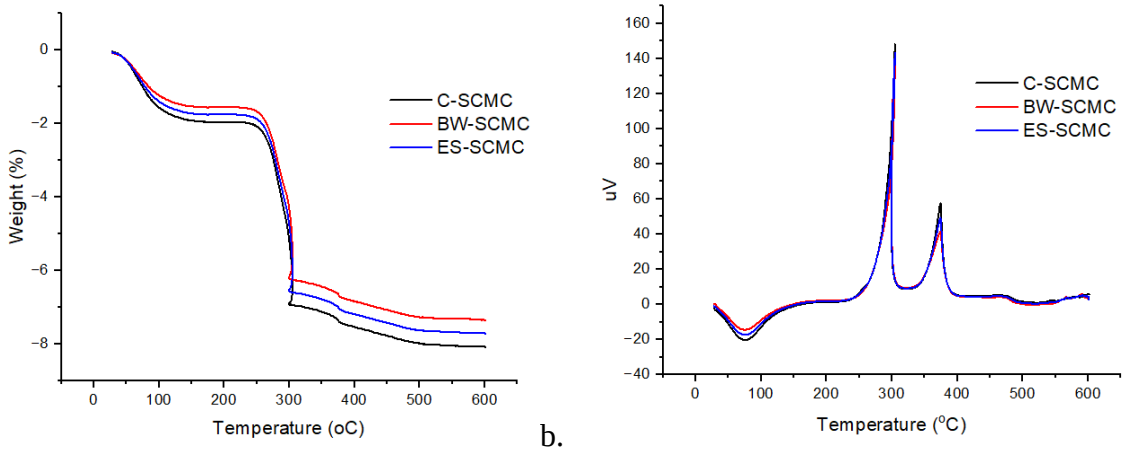

a. b.

Figure 3-14: Thermal degradation behaviors: a. TGA of C-SCMC, BW-SCMC and ES-SCMC; b. DTA of C-SCMC, BW-SCMC and ES-SCMC.

3.10 Moisture sorption pattern

The moisture sorption capacity is a measure of the moisture sensitivity of the powder material. A water sorption isotherm reflects the interaction between a powder material and water by relating the humidity of air in equilibrium with the water content of the solid material at a constant temperature (Puncochová *et al.,* 2011). The evaluation of moisture sorption profiles of pharmaceutical excipients is of utmost importance for a suitable formulation of liquids dosage forms. Chemical stability and physical properties of the formulation can be changed if too much water is bound due to water sorption ability of the powders (Roskar and Kmetec, 2005). The moisture sorption profiles of BW-SCMC, ES-SCMC and C-SCMC are depicted in Figure 3.15.

As can be seen in figure below, the moisture uptake of SCMC powders slightly increased with RH at lower values but increased significantly above 75% relative humidity. The BW-SCMC (DS: 1.432) had the highest moisture uptake when compared with ES-SCMC (DS: 1.141) and C-SCMC (DS: 0.871). This might have resulted from their high DS due to higher surface area and more accessible hydroxyl groups. In contrast, the increase in the surface area and hydroxyl groups at higher DS powder, hydrophilicity is developed. At higher DS, when more hydroxyl groups are substituted by carboxymethyl groups, moisture sorption is increased (Chen *et al.*, 2014; Zhang *et al.,* 2011).

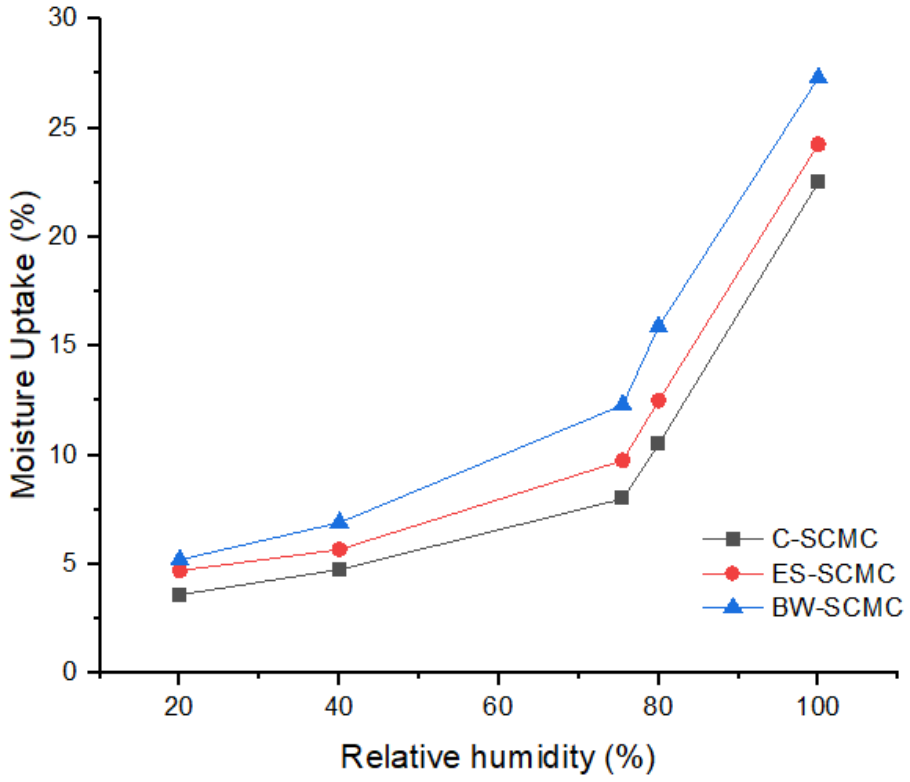

Figure 3-15: Moisture sorption pattern of C-SCMC, ES-SCMC and BW-SCMC at various RH and room temperature.

3.11 Drug-excipient compatibility studies

Figure 3.16 depicts the FTIR spectra of pure paracetamol and physical mixture (1:1) of paracetamol and BW-SCMC, ES-SCMC and C-SCMC, respectively. The characteristic peaks of paracetamol are observed at the same wavenumber in both the pure paracetamol sample and the mixture, indicating that there was no interaction between the drug and excipients. The band at 3321 cm^{-1} represents N-H stretching while the broad peak at similar position shows presence of O-H stretching. Stronger bands above 2800 cm^{-1} are attributed to the stretching vibrations of the methyl groups of both paracetamol and SCMC. On the other hand, C=O stretching of the carboxyl ion of paracetamol was reflected by a peak at 1651 cm^{-1} in both pure drug and the powder mixture. The band at 1562 cm^{-1}, which is characteristic of C=C stretching of paracetamol, 1615 – 1450 cm^{-1} (the aromatic ring C=C-C stretching bands), 1377 – 1040 cm^{-1} (C−N−H group), and 810 cm^{-1} (=C-H bending) are also seen the mixture figure (Burgina *et al.*, 2004; Zaki, 2011). Since,

characteristic peaks of both paracetamol and SCMC are reflected on the spectrum of the powder mixture, it suggest no incompatibility issue.

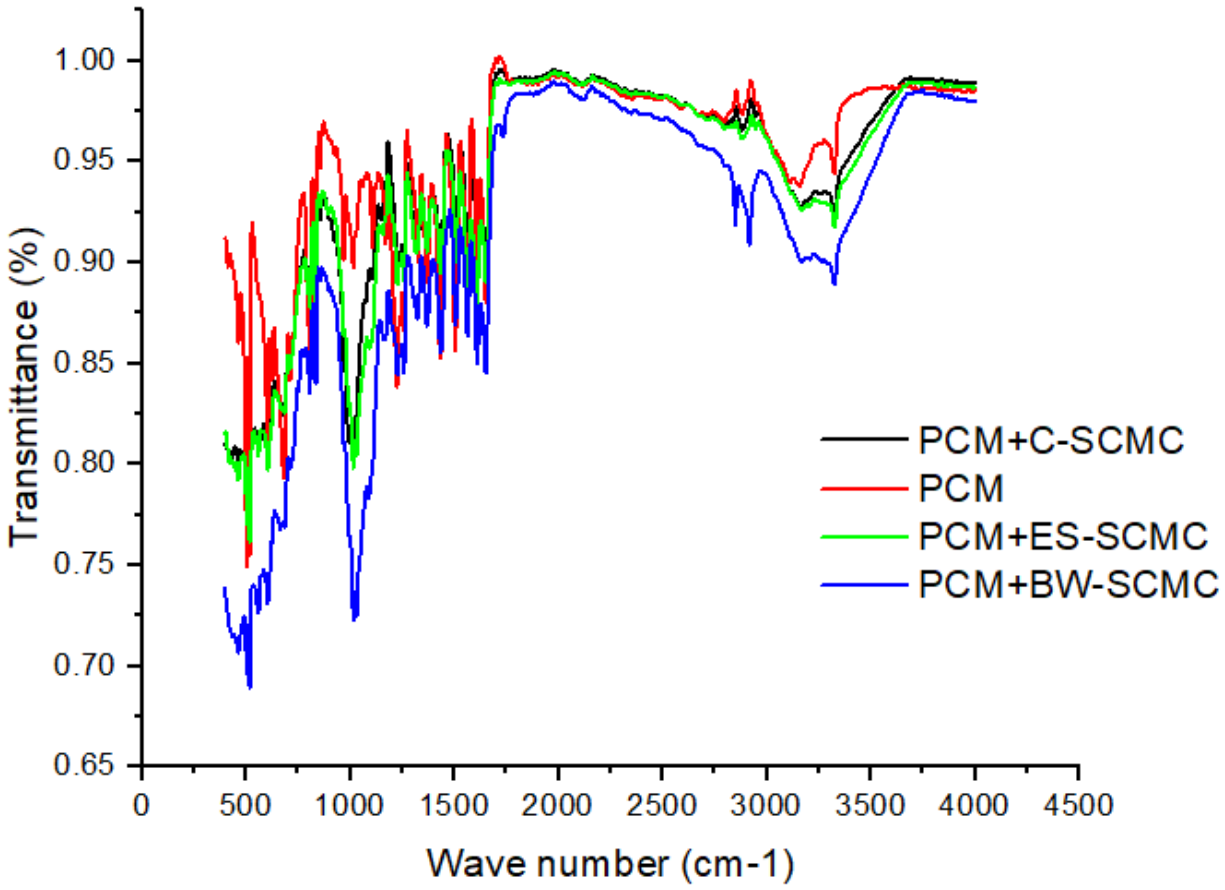

Figure 3-16: FTIR spectra of pure paracetamol powder, and physical mixture of paracetamol and C-SCMC, BW-SCMC, ES-SCMC.

3.12 Evaluation of suspension properties

3.12.1 Rheology of the suspensions

3.12.1.1 Effect of SCMC concentration on apparent viscosity

Viscosity is a critical factor which affects the stability and pourability of pharmaceutical suspensions. At a fixed shear rate of 20 rpm, the apparent viscosities of all paracetamol suspensions as a function of different concentrations of suspending agent were measured and the results are presented in Figure 3.17. As shown in the figure, the viscosity of the paracetamol dispersions was

increased with an increase in SCMC concentration. Suspensions containing BW-SCMC exhibit significantly ($p < 0.05$) higher viscosity than ES-SCMC and C-SCMC based suspensions. This suggests that paracetamol suspensions formulated with BW-SCMC might have a low terminal settling velocity. Thus, the dispersed phase settles at a slower rate and remains dispersed for a longer time, yielding higher stability to the formulated suspension than ES-SCMC and C-SCMC. The difference in suspending ability between SCMC samples is probably due to the difference in their DS, particle size distribution and molecular weight. Hon *et al.*, (2001), showed that increasing DS value of SCMC results in an increase in viscosity of suspensions.

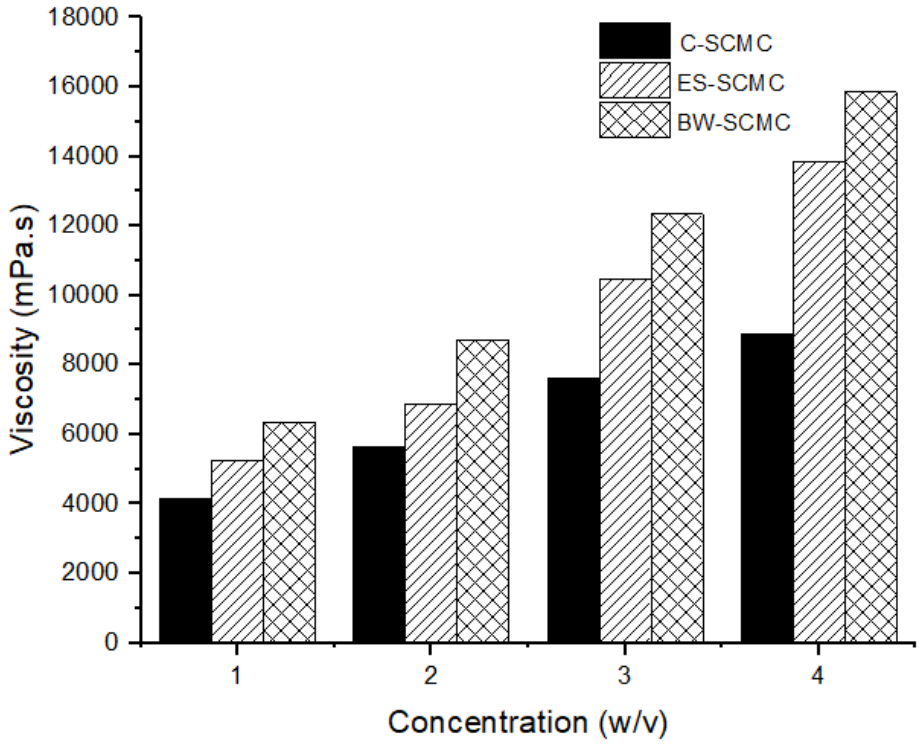

Figure 3-17: Apparent viscosities of suspensions at various concentrations of suspending agents.

3.12.1.2 Effect of shear rate on viscosity of the suspensions

The viscosity of all paracetamol suspensions was measured at different shear rate (50, 100, 150 and 200rpm), and plot of viscosity (mPa.s) vs shear rate (rpm) is depicted in Figure 3.18. It can be observed from the figure that increase in shear rate resulted in reduction of the viscosity of the dispersions. This behavior was observed on all formulations and shearing at 200rpm leading to a greater reduction in the viscosity, rendering them pseudoplastic flow, which is one of the ideal

characteristics of suspending agent (Azam and Haider, 2008). The decrease in the viscosity can be attributed to the breakdown of their large molecular structures into smaller shapes due to the cavitation effect. The result is in agreement with other studies (Brhane, 2020; Gaikar *et al.*, 2011).

3.12.2 Flowability of the suspensions

The flowability of a suspension is an important quality measurement as it determines ease of withdrawal of the drug from the container and ensures the uniformity of dose during administration. The drug remains dispersed for a longer time yielding a better distribution of the drug throughout the formulated suspension. Based on the rate and extent of flow out from a pipette, suspensions are classified as less viscous, intermediate viscosity and highly viscous. If the suspension is able to come out totally from the pipette, it is considered as less viscous for which flow rates can be calculated. If it partly comes out but not totally, it is considered as having intermediate viscosity. However, suspensions which are not able to come out totally from the pipette are considered as high viscous (Hon *et al.*, 200; Mollet and Grubenmann, 2001).

Flow rate properties of the formulated suspensions are shown in Table 3.17. All formulations exhibited an inverse flow rate characteristic to the concentration of the suspending agents. At all concentration levels of the suspending agents, flow rates were in the order of C-SCMC>ES-SCMC>BW-SCMC. The flow rates of BW-SCMC and ES-SCMC were comparable at their corresponding concentrations. High concentrations of SCMC showed a low flow rate due to its highly viscous nature. Comparable results were reported by Gebresamuel and Gebre-Mariam, (2013) where suspensions containing 4%, 5% and 6% SCMC were too viscous to exit the pipette. Another study also showed suspension with SCMC concentration of 3% and 4% (w/v) were too viscous (Brhane, 2020). The difference in flow rates of the formulations might be due to the variation in viscosity of the suspending agents (Gaikar *et al.*, 2011).

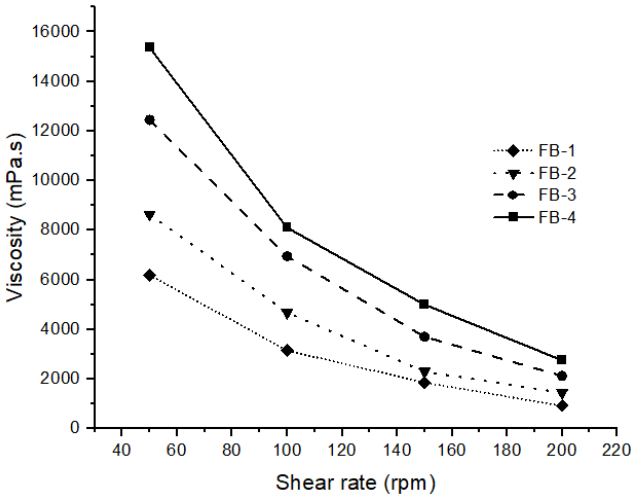

a.

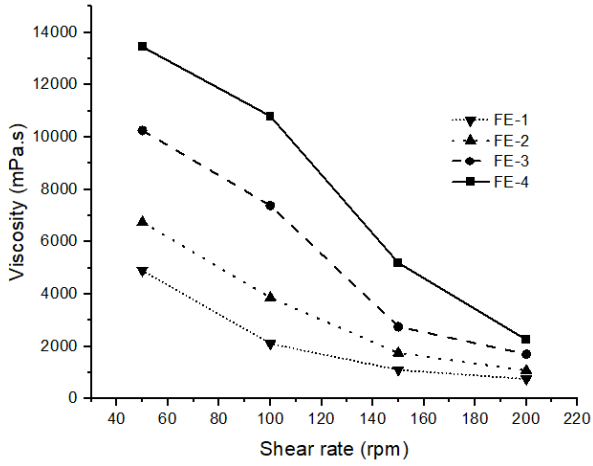

b.

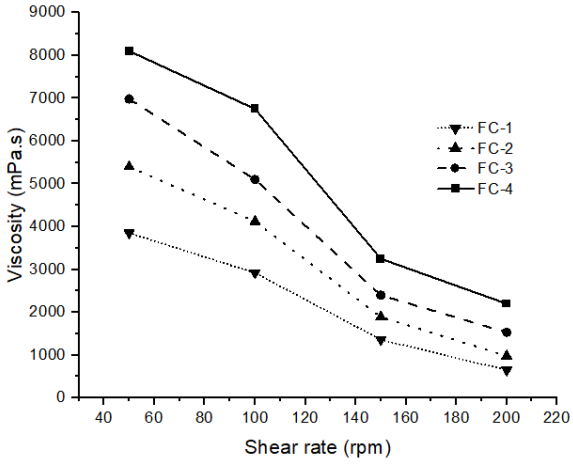

c.

Figure 3-18: Apparent viscosities of suspensions at various concentrations of suspending agent and shear rate. a) BW-SCMC, b) ES-SCMC and c) C-SCMC.

Table 3-17: The flow rate of the suspension formulations. (Key: - IV; intermediately viscous and HV; highly viscous. Data are presented as the mean ± SD (n = 3).

Suspending agent concentration (% w/v)	**Flow rate (ml/sec)**		
	C-SCMC	BW-SCMC	ES-SCMC
1	0.65±0.95	0.27±0.91	0.36±0.85
2	0.4±0.7	0.05±0.35	0.17±0.6
3	0.1±0.65	IV	IV
4	IV	HV	HV

3.12.3 Sedimentation volume

Sedimentation volume is the ratio of the height of the sediment after settling to the initial height of the suspension in the cylinder. The larger the ratio, the better is the suspending ability of the suspending agent. The value of sedimentation value is preferred to have a value of 1 or approaching 1. The sedimentation volume (%) of the suspension formulations after a week and a month are presented in Figures 3.19 and 3.20, respectively. As it can be seen from the Figure 3.19b, the sedimentation volume of BW- SCMC based formulations FB-3 and FB-4 have stabilized throughout the week while FB-1 and FB-2 has continued to decrease until the fifth day. FE-3 and FE-2 show a stable sedimentation after fifth day while FE-1 was stable after sixth day (Figure 3.19c). All C-SCMC based formulations showed a decrease in sedimentation value up to day sixth (Figure 3.19a).

In all suspension formulations, sedimentation volume were increased with increasing SCMC concentration. BW-SCMC and ES-SCMC exhibited higher sedimentation volume than C-SCMC in all concentration ranges, which indicates better suspending characteristics of the polymers owing to their high viscosity. This finding is consistent with the results reported in the literature (Nattapulwat *et al.,* 2009; Gebresamuel and Gebre-Mariam, 2013). Furthermore, at lower concentration of the suspending agents (1% and 2%), FB-1 and FB-2, provided higher

sedimentation volume than FC-1 and FC-2 at day seven, but at 3% and 4% concentration both give comparable sedimentation volume. BW-SCMC and ES-SCMC show comparable sedimentation value at all concentration ranges, as depicted in Figure 3.19b and c.

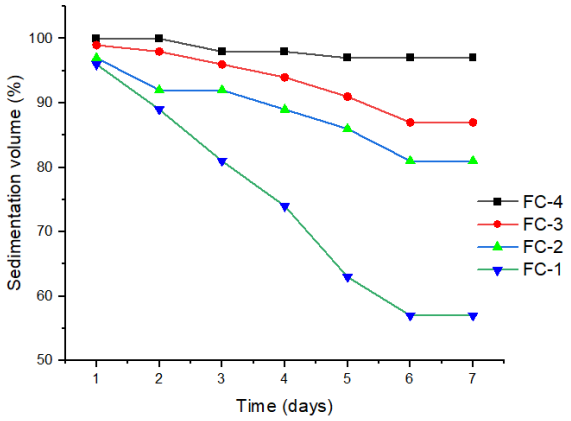

a.

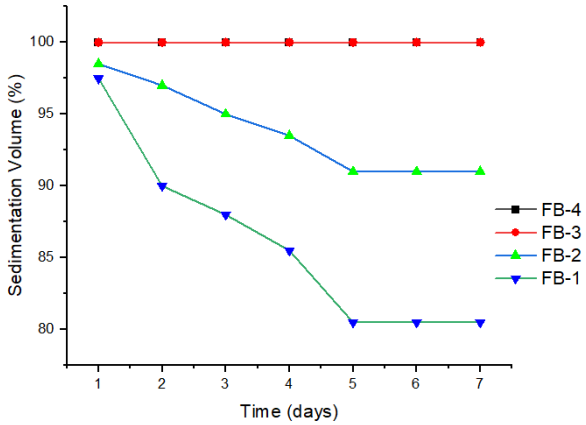

b.

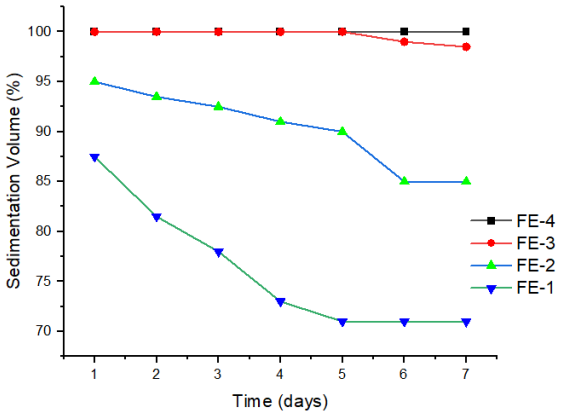

c.

Figure 3-19: One week sedimentation volume (%) profiles of suspensions at different concentrations of the suspending agents, (a) C-SCMC (FC-4 – FC-1), (b) BW-SCMC (FB-4 – FB-1), and (c) ES-SCMC (FE-4 – FE-1).

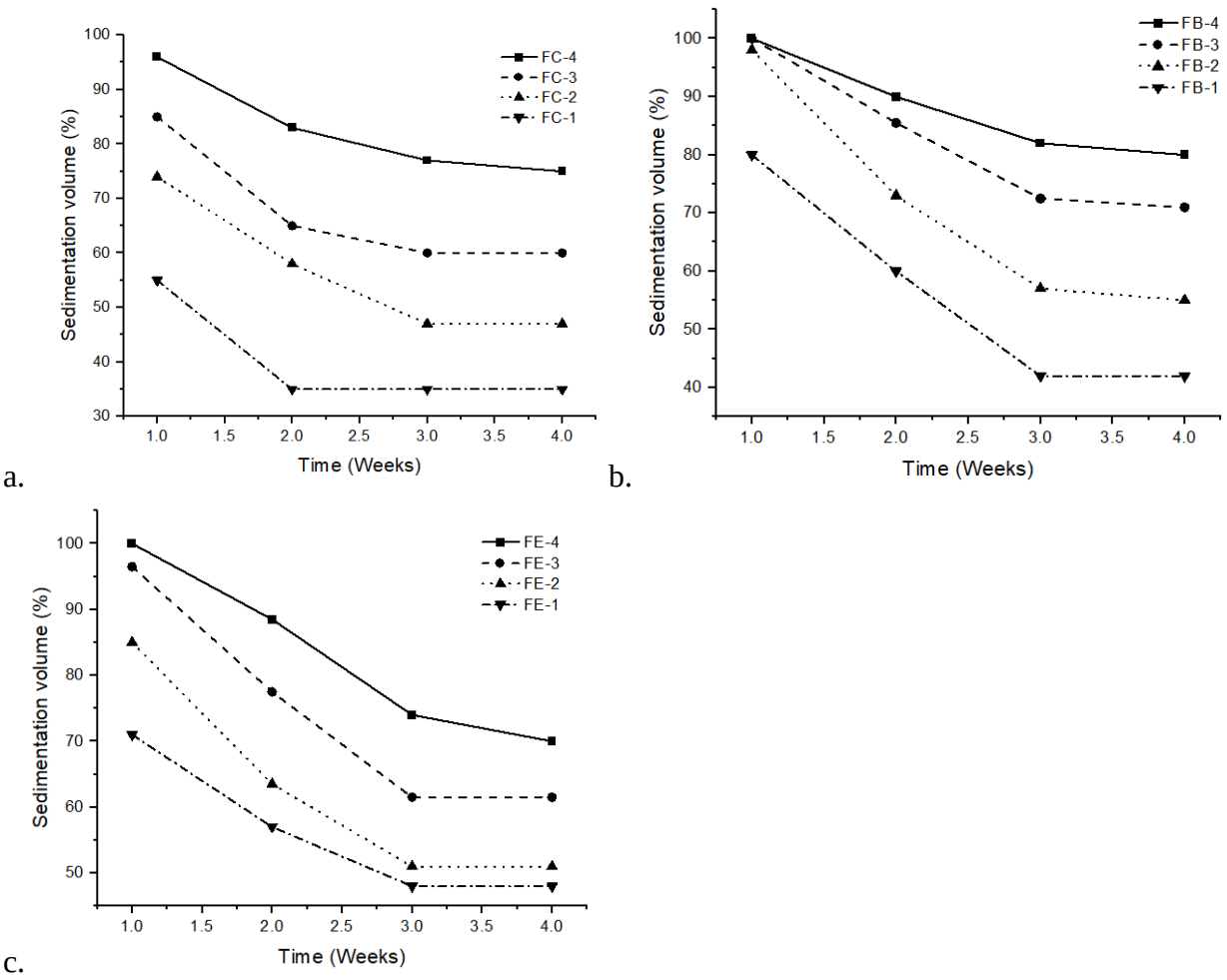

Figure 3-20: Four-weeks sedimentation volume (%) profiles of suspensions at different concentrations of the suspending agents, (a) C-SCMC (FC-4 – FC-1), (b) BW-SCMC (FB-4 – FB-1) and (c) ES-SCMC (FE-4 – FE-1)).

3.12.4 Effect of electrolyte concentration on sedimentation volume

One of the most commonly used groups of flocculating agents are electrolytes. Electrolytes act by reducing the zeta potential of the suspension. Upon persistent addition of electrolytes, the zeta potential lowers to a level where the attraction force of dispersed particles outweigh the repulsive force and loose floccules will be formed, resulting in an increase in sedimentation volume. The effect of electrolyte (NaCl) at different concentrations on the sedimentation volumes of

paracetamol suspensions containing C-SCMC, BW-SCMC and ES-SCMC at 1% (W/V) concentration are presented in Figure 3.21.

As shown in the figure, there was a low sedimentation volume in the formulations devoid of electrolytes and followed by formulations that had low NaCl concentration. On the other hand, the sedimentation volumes of all suspensions have increased with the concentration of electrolyte. This might be attributed to the alteration in zeta potential of the dispersed particles, the easy adsorption of added electrolytes on the surface of the drug particles to induce flocculation due to the low natural electrolyte concentration the polymer itself (Kittipongpatana *et al.,* 2009; Nwokocha and Ogunmola, 2008).

The sedimentation volumes of the suspension formulations of C-SCMC containing NaCl decreased at faster rate in the first three days followed by a steady decrease at slow rate. At the end of the week, the sedimentation volume of the suspensions containing 10^{-4} M, 10^{-3} M, 10^{-2} M, $5*10^{-2}$ M of NaCl and the control were 58.5%, 60.15%, 61.25%, 63.25% and 55.75%, respectively (Figure 3.21a). The difference was not statically significant ($p>0.05$) among the formulations. Figure 3.21b shows that, unlike the formulation with C-SCMC, the sedimentation volume of suspension formulations with BW-SCMC containing NaCl decrease at a slower rate over the first three days and become start to be stabilized after the fifth day. At the seventh day, the sedimentation volumes were 81.25%, 82.75%, 83.25%, 87.5% and 80.5% for suspension formulations containing 10^{-4} M, 10^{-3} M, 10^{-2} M, $5*10^{-2}$ M of NaCl and the control, respectively. The sedimentation volume of the control (80.5) is significantly lower ($p<0.05$) than formulation containing $5*10^{-2}$ M NaCl (87.5). On contrary, the observed difference in sedimentation volume between the control and the remaining formulation is not statistically significant ($p>0.05$). As depicted in Figure 3.21c, a similar trend was observed with suspensions containing ES-SCMC. The difference in sedimentation volume between the control and the other formulations were not statically significant ($p>0.05$).

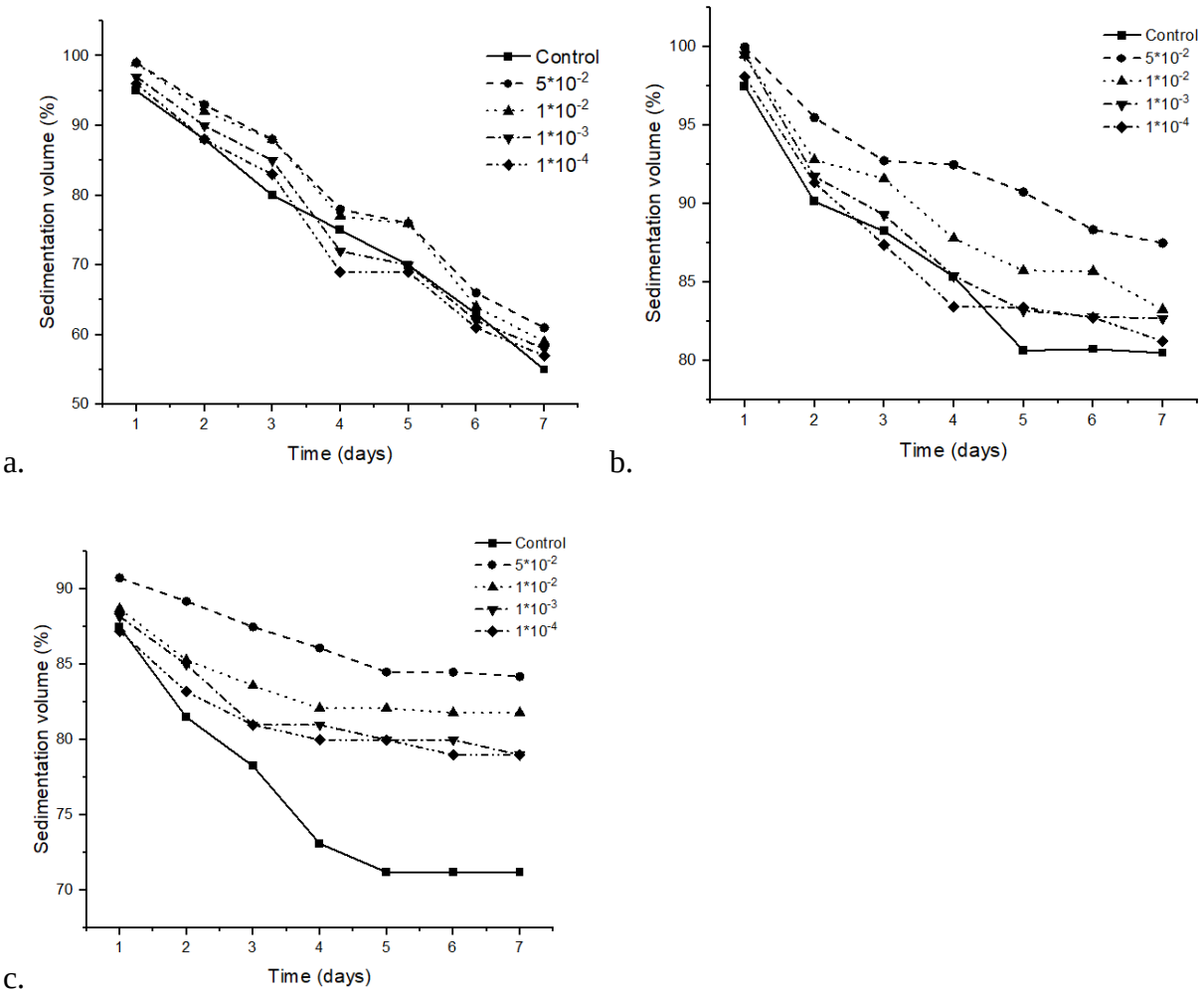

Figure 3-21: Effect of different electrolyte concentrations on sedimentation volumes (%) of suspensions prepared using 1% suspending agent. (a) C-SCMC, (b) BW-SCMC and (c) ES-SCMC.

3.12.5 Redispersibility of suspensions

Any pharmaceutical suspensions must be readily dispersible to ensure uniform dosage administration and precision. This depends on suspension homogeneity at the time of administration after shaking. Easily redispersed sediments in a suspension allow for withdrawal of uniform doses. If the sediment remains even after shaking vigorously for a specified time, the system is described as caked. Redispersibility is described by the number of turns (complete cycles) required to uniformly redisperse the sedimented particles throughout the suspension (Mann

et al., 2007; Mollet and Grubenmann, 2001). The number of inversions required to redisperse the suspension formulations after a week and a month is presented in Table 3.18.

After a week, the number of turns required to redisperse the suspension formulations prepared with 1% (13 cycles) C-SCMC was significantly ($p < 0.05$) higher than those prepared with ES-SCMC (5 cycles) and BW-SCMC (1 cycle) formulations of the same concentration. Similarly, at the concentration of 2%, the number of inversions required for the formulation prepared with C-SCMC after a week (6 cycles) was higher than that of ES-SCMC (2 cycles) and BW-SCMC (No Turn Required). At a concentration of 3% and 4%, all formulations required no inversion after a week.

All these suspensions were found to be easily redispersible after maximum turns required to rotate 180˚after storage for 30 days (Table 3.18). The number of turns required to redisperse the suspension formulations prepared with 1% (19 cycles) C-SCMC was significantly ($p < 0.05$) higher than those prepared with 1% (7 cycles) ES-SCMC and BW-SCMC (3 cycles). At the concentration of 2%, there was no significant difference ($p > 0.05$) in the number of turns required for redispersion for C-SCMC (6 cycles) and ES-SCMC (2 cycles), but there is significant difference with BW-SCMC (NTR). At a concentration of 4%, all formulations required no inversion after a month as the formulations were completely suspended. Thus, suspensions containing BW-SCMC as a suspending agent were easily redispersed than C-SCMC (DS: 0.871) containing preparations at the same concentration level and time. This could be due to the higher viscosity of the formulations with BW-SCMC attributed to its higher DS value (1.432). The redispersibility rate of all suspensions was decreased with an increase in the concentration of the suspending agents. This is because the increment in viscosity was contributed to retarding the settling velocity of the particles thereby reducing the interparticle interactions and favored ease of redispersibility (Gebresamuel and Gebre-Mariam, 2013; Moreton, 2009).

Table 3-18: Redispersibility of the suspension formulations after a week and a month. (Key:- NTR: Number of Turn Required; Data are presented as the mean ± SD (n = 3)).

Suspending agent concentration (% w/v)	**Rate of redispersibility (cycles)**					
	After a week			After a month		
	C-SCMC	BW-SCMC	ES-SCMC	C-SCMC	BW-SCMC	ES-SCMC
1	13 ± 1.00	1 ±1.00	5 ± 1.00	19 ±1.00	37 ± 1.00	7 ± 1.00
2	6 ± 1.00	NTR	2 ± 1.00	11 ±1.00	1+ ± 1.00	4 ± 1.00
3	NTR	NTR	NTR	4 ±1.00	1 ± 1.00	2 ± 1.00
4	NTR	NTR	NTR	NTR	NTR	NTR

3.12.6 Degree of flocculation

The flocculation characteristics of the suspension formulations at 1% and 2% w/v of the suspending agents were studied using KH_2PO_4 as a flocculating agent for a month and the results are presented in Figure 3.22. At 1% w/v concentration of C-SCMC, BW-SCMC and ES-SCMC, the degree of flocculation was 1.2, 1.43 and 1.35, respectively. At 2% w/v, the values were 1.03 (C-SCMC), 1.185 (BW-SCMC) and 1.15 (ES-SCMC). Suspension formulations containing C-SCMC didn't show a significant difference ($p < 0.05$) in the degree of flocculation in comparison with ES-SCMC and BW-SCMC at both concentrations.

SCMC is a linear polymer and it has a good tendency to form flocs. Reports indicated that flocculation by polymer could be attributed to the simultaneous interaction of a polymer molecule with more than one particle. The good flocculating properties of BW-SCMC are also supported by literature that reported that anionic cellulose derivatives with a higher DS have good flocculating properties (Suthar and Patel, 2011; Wang *et al.*, 2010).

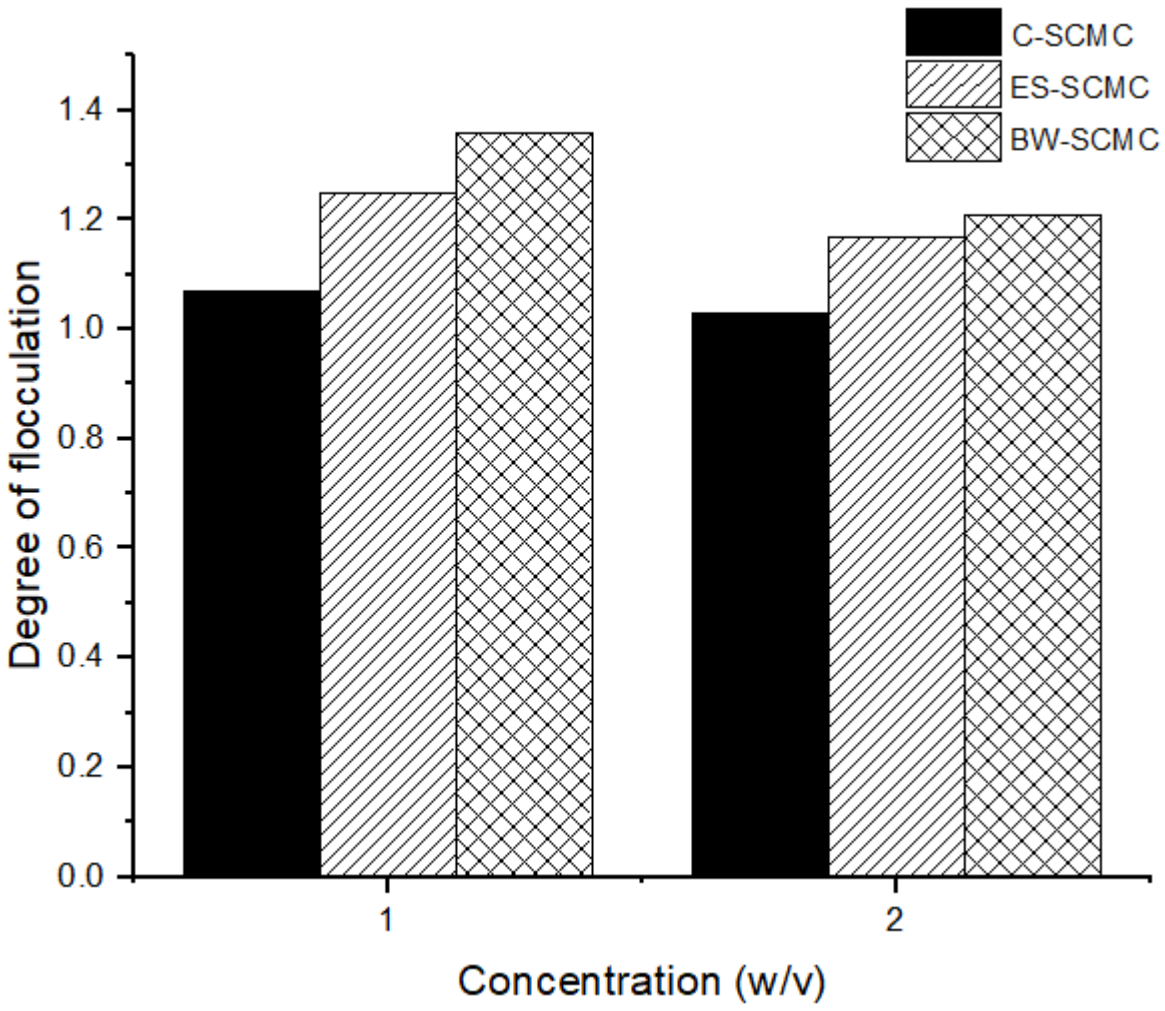

Figure 3-22: The degree of flocculation for paracetamol suspension formulations containing 1% and 2% w/v of suspending agents: C-SCMC, BW-SCMC and ES-SCMC.

3.12.7 UV calibration curve of paracetamol

From stock solution of 200 µg/ml of paracetamol in phosphate buffer (pH 5.8), standard calibration curve was plotted at seven different concentrations (µg/ml). The absorbance (at 243 nm) versus concentration of the solutions was plotted and a calibration curve with a linear regression equation of Y = 0.0579X-0.00731 (where Y is the absorbance and X is the concentration in µg/ml) and a correlation coefficient, R^2 = 0.9997 was obtained (Figure 3.23).

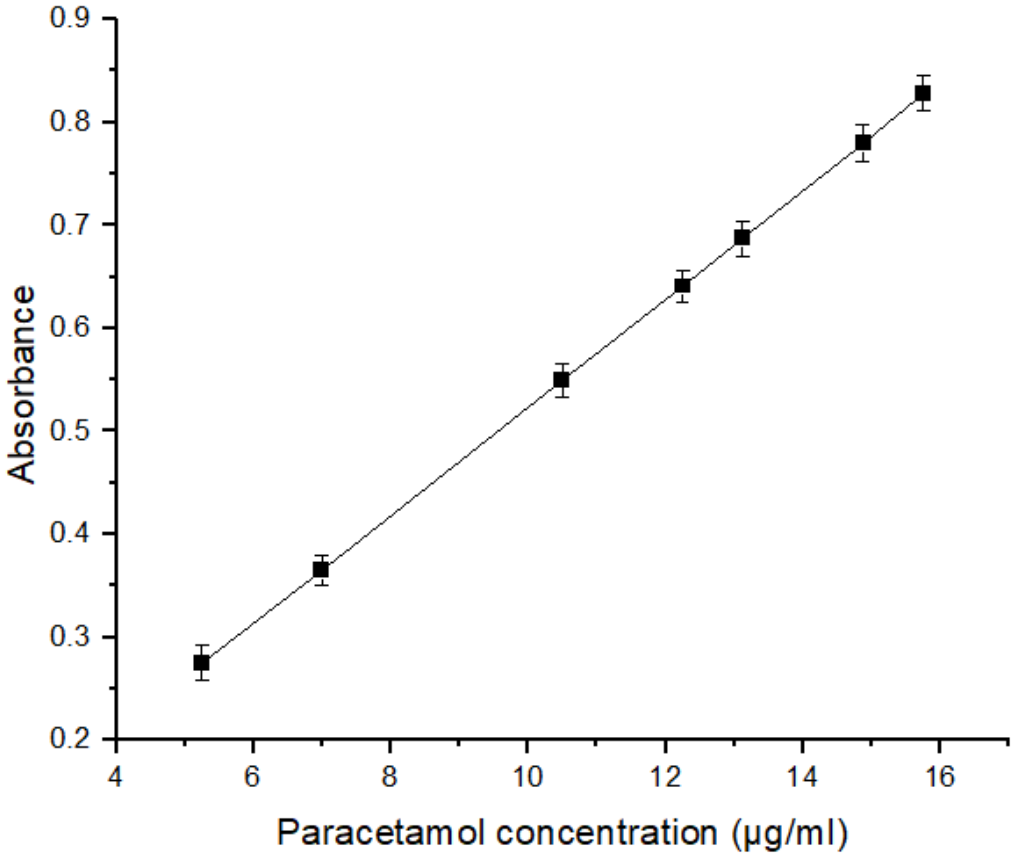

Figure 3-23: UV Calibration curve of paracetamol standard in pH 5.8 phosphate buffer at 243 nm with 95% confidence interval (R^2 = 0.999).

3.12.8 Dissolution profiles of the suspensions

Dissolution of drugs is a necessary criterion for determination of drug bioavailability. It is also used as the single most important quality control test for assuring batch-to batch bioequivalence, once the bioavailability of the dosage form is determined. The dissolution of heterogenous systems including suspensions may exhibit inconsistent dissolution profile. Thus, their dissolution profile should be determined. There is no official specification for the acceptable range of dissolution of Paracetamol suspensions within a specified period of time. However, the USP38/NF33, (2015) specifies drug release acceptable range of not less than 85% within 60 min for Paracetamol tablets.

The dissolution profiles of the paracetamol suspensions prepared with different concentration of suspending agent are shown in Figure 3.24. All formulations that contain different concentrations of C-SCMC, BW-SCMC and ES-SCMC release the drug within the USP acceptance range (USP

30/NF 25, 2007). The result showed that FC-1 and FC-2 released more than 85% of the paracetamol within 30 min whereas FE-4, FB-3 and FB-4 attained the limit within 50 min. The quick release from C-SCMC formulations could be attributed to the relatively low viscosity of the suspensions as compared to ES-SCMC and BW-SCMC. The observed decrease in dissolution rate as the concentration of suspending agent increase is due to the effect of viscosity, this is in agreement with reports by Azam and Haider (2008) whereby viscosity increased with increase in concentration of suspending agent, which in turn, decreases the dissolution rate.

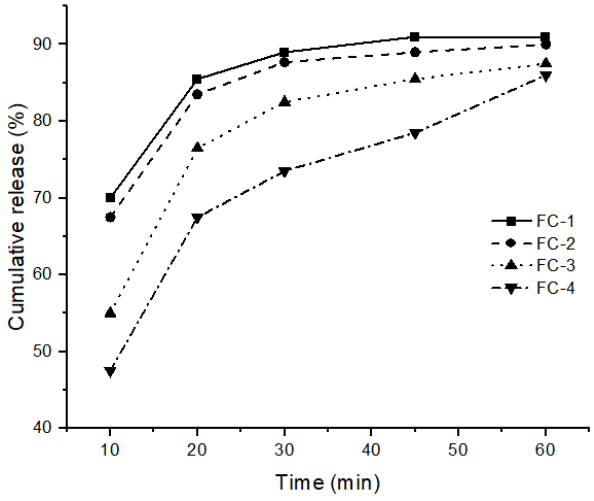

a.

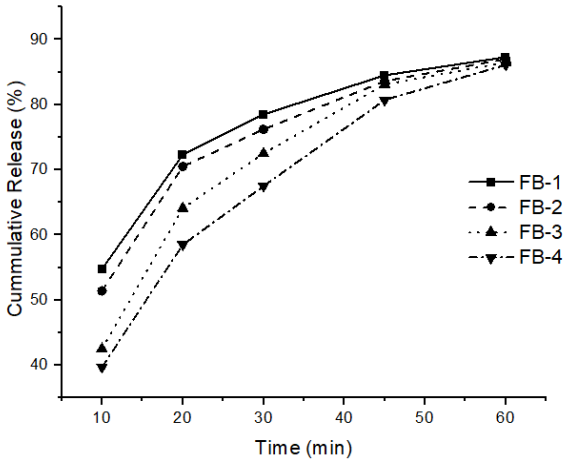

b.

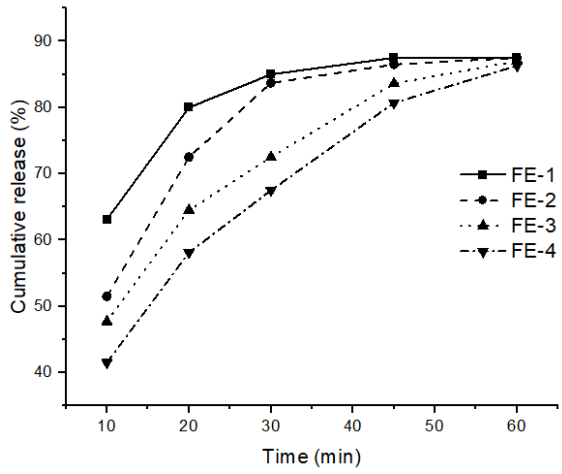

c.

Figure 3-24: Cumulative *in vitro* release profiles of paracetamol suspensions containing different concentrations of (a) C-SCMC, (b) BW-SCMC and (c) ES-SCMC as the suspending agent. Data are presented as the mean ± SD (n = 3).

3.12.9 Stability studies

Instabilities in formulation are often detectable only after considerable storage periods under normal conditions. To assess the stability of a formulated product it is common to expose it to high stress condition, i.e., elevated temperature and humidity that are known likely to cause product deterioration. High stress conditions enhance the deterioration of the product and therefore reduce the time required for testing. This enables more data to be gathered in shorter time, which will allow unsatisfactory formulations to be eliminated early in a study. Oral liquids such as suspensions, syrups, emulsion and colloidal dispersions are more complex than solid dosage forms because of interactions that occur in liquid state, and hence need adequate stability evaluation (Mollet and Grubenmann, 2001; Nash, 1996).

The bulk visual appearance (creamy-white), as well as the odor of all suspension formulations, remained the same throughout the three-month stability study. None of the paracetamol suspensions indicated any sign of color change during the storage period. The changes in pH of all paracetamol suspension formulations were within the acceptable range, the pH range stated in BP for paracetamol suspension formulation is in the range of 5.0–6.5. Similarly, at all storage conditions, no significant change ($p>0.05$) was seen in the content of paracetamol as the loss in assay value was less than 5% in all formulations, the assay recovery of the formulations was within the acceptable range (90.0 to 110.0%) as shown in Table 3.19. The suspension formulations showed negligible ($p>0.05$) increment in particle size throughout the study period (Table 3.20). From the stability results, all paracetamol suspensions were stable at all storage conditions during the study period.

Table 3-19: pH and assay values paracetamol formulations stored at 4˚C, 30˚C / 65% relative humidity and 40˚C / 75% relative humidity for 3 months.

Formulations	**Storage time**	**pH**			**% Assay**		
		Storage conditions			Storage conditions		
		30˚C/65% RH	40˚C/75% RH	4˚C	30˚C/65% RH	40˚C/75% RH	4˚C
FC-1	First day	6.21 ± 0.03	6.21 ± 0.05	6.21 ± 0.05	100.15 ± 0.03	100.15 ± 0.03	100.15 ± 0.03
	3-months	6.28 ± 0.05	6.29± 0.02	6.31 ± 0.02	100.05 ± 0.05	98.5 ± 0.05	98.73 ± 0.02
FB-1	First day	6.03 ± 0.01	6.03 ± 0.07	6.09 ± 0.03	101.35 ± 0.27	101.35 ± 0.27	101.35 ± 0.27
	3-months	6.11 ± 0.01	6.11 ± 0.01	6.17 ± 0.02	99.95 ± 0.14	97.95 ± 0.14	97.15 ± 0.14
FE-1	First day	6.09 ± 0.01	6.09± 0.01	6.03 ± 0.01	101.5 ± 0.03	101.5 ± 0.01	101.5 ± 0.03
	3-months	6.13 ± 0.02	6.17 ± 0.02	6.17 ± 0.02	99.65 ± 0.21	98.65 ± 0.15	97.65 ± 0.11

Table 3-20: Stability profiles, in terms of particle size of paracetamol suspensions stored at 4˚C, 30˚C / 65% relative humidity and 40˚C / 75% relative humidity for 3 months.

Formulations	**Storage time**	**Particle size (µm)**		
		Storage conditions		
		30˚C/65% RH	40˚C/75% RH	4˚C
FC-1	First day	62.99±0.74	62.99±0.74	62.99±0.74
	3-months	63.75±0.65	64.13±0.25	64.07±0.22
FB-1	First day	69.99±0.71	69.99±0.71	69.99±0.71
	3-months	70.25±0.31	70.86±0.23	71.23±0.39
FE-1	First day	72.11±0.71	72.11±0.71	72.11±0.71
	3-months	72.83±0.43	73.85±0.19	73.87±0.57

4. Conclusion

Cellulose fiber was extracted from BW and ES using steam explosion method. The BWC and ESC yields were 48.1% ± 1.02 and 44.2% ± 1.14, respectively. The XRD spectra of the celluloses at 2θ exhibited the characteristic peaks of cellulose at 18.7 º and 22.7 º (ESC), and 19.4 º and 22.6º (BWC). The experimental DS values of the synthesized BW-SCMC (1.432) and ES-SCMC (1.141) under the optimum conditions were close to the predicted values.

BW-SCMC, ES-SCMC and C-SCMC showed pseudoplastic flow and their viscosity were in the order of BW-SCMC > ES-SCMC > C-SCMC. The flow rates of the suspensions followed the order: C-SCMC > ES-SCMC > BW-SCMC. Suspensions from BW-SCMC and ES-SCMC showed higher sedimentation volume than those of C-SCMC. Furthermore, BW-SCMC and ES-SCMC showed better redispersiblity than C-SCMC at lower concentrations.

Dissolution studies of the suspension formulations showed that all formulated suspensions with SCMC as suspending agent achieved > 85% drug release within a 1 h period. Stability studies showed that the suspension formulations were stable at all storage conditions. Hence, it can be concluded that BW-SCMC and ES-SCMC can be used as alternative suspending agents in suspension formulations.

5. Suggestions for further work

Based on these results the followings are suggested:

- Characterize the morphology of BW-SCMC and ES-SCMC
- Conduct real time stability studies for both BW-SCMC and ES-SCMC based suspensions.

6. References

ABDEL-MOHDY, F., ABDEL-HALIM, E., ABU-AYANA, Y. & EL-SAWY, S. 2009. Rice straw as a new resource for some beneficial uses. *Carbohydrate Polymers*, 75, 44-51.

ADINUGRAHA, M. P. & MARSENO, D. W. 2005. Synthesis and characterization of sodium carboxymethylcellulose from cavendish banana pseudo stem (Musa cavendishii LAMBERT). *Carbohydrate Polymers*, 62, 164-169.

AKINLABI, E. T., ANANE-FENIN, K., AKWADA, D. R., AKINLABI, E. T., ANANE-FENIN, K. & AKWADA, D. R. 2017. Bamboo taxonomy and distribution across the globe. *Bamboo: the multipurpose plant*, 1-37.

ALEMAYEHU, A. & MELKA, Y. 2022. Small scale eucalyptus cultivation and its socioeconomic impacts in Ethiopia: A review of practices and conditions. *Trees, Forests and People,* 8, 100269.

ASTM D1439 – 03, 2010. Standard Test Methods of Testing Sodium carboxymethyl cellulose. West Conshohocken, PA United States 19439-2959.

AZAM MG, AND HAIDER SS. Evaluation of the dissolution behavior of paracetamol suspensions. Dhaka Univ J PharmSci.2008; 7:53–58. Wang L, Pan S, HuH, Miao W, and Xu X. Synthesis and properties of carboxymethyl kudzu root starch. *Carbohydrate Polymers*. 2010; 80: 174–179.

AZHAR, S. W., XU, F. & QIU, Y. 2021. Evaluation and characterization of cellulose nanofibers from flaxseed fiber bundles. *AATCC Journal of Research*, 8, 8-14.

BAHRU, T. & DING, Y. 2021. A review on bamboo resource in the African region: a call for special focus and action. *International Journal of Forestry Research,* 2021, 1-23.

BARUD, H. S., DE ARAÚJO JÚNIOR, A. M., SANTOS, D. B., DE ASSUNÇÃO, R. M., MEIRELES, C. S., CERQUEIRA, D. A., RODRIGUES FILHO, G., RIBEIRO, C. A., MESSADDEQ, Y. & RIBEIRO, S. J. 2008. Thermal behavior of cellulose acetate produced from homogeneous acetylation of bacterial cellulose. *Thermochimica acta,* 471, 61-69.

BISWAS, A., KIM, S., SELLING, G. W. & CHENG, H. 2014. Conversion of agricultural residues to carboxymethylcellulose and carboxymethylcellulose acetate. *Industrial Crops and Products,* 60, 259-265.

BOGOLITSYN, K., PARSHINA, A. & ALESHINA, L. 2020. Structural features of brown algae cellulose. *Cellulose,* 27, 9787-9800.

BOONTERM, M., SUNYADETH, S., DEDPAKDEE, S., ATHICHALINTHORN, P., PATCHARAPHUN, S., MUNGKUNG, R. & TECHAPIESANCHAROENKIJ, R. 2016. Characterization and comparison of cellulose fiber extraction from rice straw by chemical treatment and thermal steam explosion. *Journal of Cleaner Production,* 134, 592-599.

BP, 2016a. *In vitro* drug evaluation, in: British Pharmacopoeia Commission - British Pharmacopoeia-The Stationery Office. Crown Copyright 2008.

BP, 2016b. Carmellose (Sodium), in: British Pharmacopoeia Commission - British Pharmacopoeia-The Stationery Office. Crown Copyright 2015, London, pp. 2015–2016.

BRITO, B. S., PEREIRA, F. V., PUTAUX, J.-L. & JEAN, B. 2012. Preparation, morphology and structure of cellulose nanocrystals from bamboo fibers. *Cellulose,* 19, 1527-1536.

CALDERÓN, C. E. & SODERSTROM, T. R. 1980. The genera of Bambusoideae (Poaceae) of the American Continent: Keys. *Smithsonian Contributions to Botany*.

CANDIDO, R. & GONÇALVES, A. 2016. Synthesis of cellulose acetate and carboxymethylcellulose from sugarcane straw. *Carbohydrate polymers,* 152, 679-686.

CASTILLEJO, M. A., PASCUAL, J., JORRÍN-NOVO, J. V. & BALBUENA, T. S. 2023. Proteomics research in forest trees: A 2012-2022 update. *Frontiers in Plant Science,* 14, 1130665.

CHAOUCH, M., PÉTRISSANS, M., PÉTRISSANS, A. & GÉRARDIN, P. 2010. Use of wood elemental composition to predict heat treatment intensity and decay resistance of different softwood and hardwood species. *Polymer Degradation and Stability,* 95, 2255-2259.

CHEN, W. Q. & LOU, D. P. 2014. Synthesis of sodium carboxymethyl cellulose based on pretreated bamboo shaving. *Advanced Materials Research,* 997, 169-172.

CHENG, F., LI, G., FENG, J. & ZHANG, J. 1996. Characteristics of carboxymethyl cellulose synthesized in two-phase medium C6H6□ C2H5OH. I. Distribution of substituent groups in the anhydroglucose unit. *Journal of applied polymer science,* 61, 1831-1838.

CHENG, H., TAKAI, M. & EKONG, E. A., 1999. Rheology of carboxymethylcellulose made from bacterial cellulose. Macromolecular Symposia. *Wiley Online Library,* 145-153.

CHUMEE, J. & KHEMMAKAMA, P. 2014. Carboxymethyl cellulose from pineapple peel: Useful green bioplastic. *Advanced Materials Research,* 979, 366-369.

CHUMEE, J. & SEEBURIN, D. 2014. Cellulose extraction from Pomelo peel: synthesis of carboxymethyl cellulose. *International Journal of Materials and Metallurgical Engineering,* 8, 435-437.

CHUMEE, J., SEEBURIN, D., 2014. Cellulose Extraction from Pomelo Peel: Synthesis of Carboxymethyl Cellulose. *International Journal of Material England*. 8, 435–437.

COSTA, S. M., MAZZOLA, P. G., SILVA, J. C., PAHL, R., PESSOA JR, A. & COSTA, S. A. 2013. Use of sugar cane straw as a source of cellulose for textile fiber production. *Industrial Crops and Products,* 42, 189-194.

DAI, H., ZHANG, Y., MA, L., ZHANG, H. & HUANG, H. 2019. Synthesis and response of pineapple peel carboxymethyl cellulose-g-poly (acrylic acid-co-acrylamide)/graphene oxide hydrogels. *Carbohydrate polymers,* 215, 366-376.

DEEPA, B., ABRAHAM, E., CHERIAN, B. M., BISMARCK, A., BLAKER, J. J., POTHAN, L. A., LEAO, A. L., DE SOUZA, S. F. & KOTTAISAMY, M. 2011. Structure, morphology and thermal characteristics of banana nano fibers obtained by steam explosion. *Bioresource technology,* 102, 1988-1997.

DESSIE, A. B., ABATE, T. & MEKIE, T. M. 2019. Eucalyptus: the popular exotic tree crop in Ethiopia. *Acta Scientific Agriculture,* 3, 50-56.

EMBAYE, K. 2000. The indigenous bamboo forests of Ethiopia: an overview. *AMBIO: A Journal of the Human Environment,* 29, 518-521.

FLORES-VELÁZQUEZ, V., CÓRDOVA-PÉREZ, G. E., SILAHUA-PAVÓN, A. A., TORRES-TORRES, J. G., SIERRA, U., FERNÁNDEZ, S., GODAVARTHI, S., ORTIZ-CHI, F. & ESPINOSA-GONZÁLEZ, C. G. 2020. Cellulose obtained from banana plant waste for catalytic production of 5-HMF: Effect of grinding on the cellulose properties. *Fuel,* 265, 116857.

FORSYTH, G., RICHARDSON, D., BROWN, P. & VAN WILGEN, B. 2004. A rapid assessment of the invasive status of Eucalyptus species in two South African provinces: working for water. *South African Journal of Science,* 100, 75-77.

GAIKAR NV, SANDHYA P, AND CHAUDHARI CA. 2011. Evaluation of Curculigoorchioides mucilage as suspending Agent. *International Journal of Pharmaceuticals Technology Research*. 3:831–835

GARDNER, K. & BLACKWELL, J. 1974. The structure of native cellulose. *Biopolymers: Original Research on Biomolecules,* 13, 1975-2001.

GARVEY, C. J., PARKER, I. H. & SIMON, G. P. 2005. On the interpretation of X-ray diffraction powder patterns in terms of the nanostructure of cellulose I fibres. *Macromolecular Chemistry and Physics,* 206, 1568-1575.

GEBRESAMUEL, N. AND GEBRE-MARIAM, T., 2013. Evaluation of the suspending properties of two local Opuntia spp. mucilages on paracetamol suspension. *Pakistan Journal Pharmaceutical Science*, *26*(1), 23-9.

GUPTA, A. & BADOLA, A. 2022. Pharmaceutical Suspension: A review. *World Journal of Pharmaceutical Research,* 11, 1011-1025.

HALEEM, N., ARSHAD, M., SHAHID, M. & TAHIR, M. A. 2014. Synthesis of carboxymethyl cellulose from waste of cotton ginning industry. *Carbohydrate polymers,* 113, 249-255.

HALEEM, N., ARSHAD, M., SHAHID, M., TAHIR, M.A., 2014. Synthesis of carboxymethyl cellulose from waste of cotton ginning industry. *Carbohydrate. Polymers*. 113, 249–255.

HALLAC, B.B. AND RAGAUSKAS, A.J., (2011). Analyzing cellulose degree of polymerization and its relevancy to cellulosic ethanol. *Biofuel Bio production Bio refining*. 5:215-225.

HE, X., LU, W., SUN, C., KHALESI, H., MATA, A., ANDALEEB, R. & FANG, Y. 2021. Cellulose and cellulose derivatives: Different colloidal states and food-related applications. *Carbohydrate Polymers,* 255, 117334.

HE, X., WU, S., FU, D. & NI, J. 2009. Preparation of sodium carboxymethyl cellulose from paper sludge. *Journal of Chemical Technology & Biotechnology: International Research in Process, Environmental & Clean Technology,* 84, 427-434

HEINZE, T. 2016. Cellulose: structure and properties. *Cellulose chemistry and properties: fibers, nanocelluloses and advanced materials*, 1-52.

HEINZE, T., LIEBERT, T. F., PFEIFFER, K. S. & HUSSAIN, M. A. 2003. Unconventional cellulose esters: synthesis, characterization and structure–property relations. *Cellulose*, 10, 283-296.

HIDAYAT, B. J., FELBY, C., JOHANSEN, K. S. & THYGESEN, L. G. 2012. Cellulose is not just cellulose: a review of dislocations as reactive sites in the enzymatic hydrolysis of cellulose microfibrils. *Cellulose,* 19, 1481-1493

HSIEH, Y.-L. 2007. Chemical structure and properties of cotton. *Cotton: Science and technology*, 3-34.

HU, Y., HU, S., ZHANG, S., DONG, S., HU, J., KANG, L. & YANG, X. 2021. A double-layer hydrogel based on alginate-carboxymethyl cellulose and synthetic polymer as sustained drug delivery system. *Scientific reports,* 11, 9142.

HUANG, C. M., CHIA, P. X., LIM, C. S., NAI, J. Q., DING, D. Y., SEOW, P. B., WONG, C. W. & CHAN, E. W. 2017. Synthesis and characterisation of carboxymethyl cellulose from various agricultural wastes. *Cellulose. Chemistry and Technology,* 51, 665-672.

HUMANS, I. W. G. O. T. E. O. C. R. T. 1995. Wood Dust. *Wood Dust and Formaldehyde.* International Agency for Research on Cancer.

IBRAHIM, M. M., EL-ZAWAWY, W.K., JUTTKE, Y., KOSCHELLA, K. AND HEINZE T. (2013). Cellulose and microcrystalline cellulose from rice straw and banana plant waste: preparation and characterization. *Cellulose* 20: 2403-2416

JAHAN, M.S., SAEED, A., HE, Z., NI, Y., 2011. Jute as raw material for the preparation of microcrystalline cellulose. *Cellulose* 18, 451–459.

JANDURA, P., RIEDL, B. & KOKTA, B. V. 2000. Thermal degradation behavior of cellulose fibers partially esterified with some long chain organic acids. *Polymer Degradation and Stability,* 70, 387-394.

JARMKOM, K., KHOBJAI, W., TEACHAOEI, S. & SHUWISITKUL, D. 2021. Synthesis of carboxymethyl cellulose from rice husk. *International Journal of Applied Pharmaceutics*, 50-54.

JIA, F., LIU, H.-J. & ZHANG, G.-G. 2016. Preparation of carboxymethyl cellulose from corncob. *Procedia Environmental Sciences,* 31, 98-102.

JOHAR, N., AHMAD, I. & DUFRESNE, A. 2012. Extraction, preparation and characterization of cellulose fibres and nanocrystals from rice husk. *Industrial Crops and Products,* 37, 93-99.

JOSHI, G., NAITHANI, S., VARSHNEY, V., BISHT, S. S., RANA, V. & GUPTA, P. 2015. Synthesis and characterization of carboxymethyl cellulose from office waste paper: a greener approach towards waste management. *Waste Management,* 38, 33-40.

KAMEL, S., ALI, N., JAHANGIR, K., SHAH, S. & EL-GENDY, A. 2008. Pharmaceutical significance of cellulose: A review. *Express Polymer Letter,* 2, 758-778.

KAMRUNNAHAR, M. 1995. Optimization of the process parameters for the production of sodium carboxymethyl cellulose.

KARATAŞ, M. & ARSLAN, N. 2016. Flow behaviours of cellulose and carboxymethyl cellulose from grapefruit peel. *Food Hydrocolloids*, 58, 235-245.

KHULLAR, R., VARSHNEY, V., NAITHANI, S., HEINZE, T. & SONI, P. 2005. Carboxymethylation of cellulosic material isolated from cotton (Gossypium) linters with respect to degree of substitution and rheological behavior. *Journal of applied polymer science*, 96, 1477-1482.

KINDU, M. & MULATU, Y. 2010. Status of bamboo resource development, utilization, and research in Ethiopia: A review. *Ethiopian Journal of Natural Resources,* 1, 79-98.

KLEMM, D., HEUBLEIN, B., FINK, H. P. & BOHN, A. 2005. Cellulose: fascinating biopolymer and sustainable raw material. *Angewandte chemie international edition,* 44, 3358-3393.

KUHN, P. J., TRINCI, A. P., JUNG, M. J., GOOSEY, M. W. & COPPING, L. G. 2012. *Biochemistry of cell walls and membranes in fungi*, Springer Science & Business Media

KULSHRESHTHA, A. K., SINGH, O. N. & WALL, G. M. 2009. *Pharmaceutical suspensions: from formulation development to manufacturing*, Springer.

LAKSHMI, D. S., TRIVEDI, N. & REDDY, C. 2017. Synthesis and characterization of seaweed cellulose derived carboxymethyl cellulose. *Carbohydrate Polymers,* 157, 1604-1610.

LIAO, J. J., ABD LATIF, N. H., TRACHE, D., BROSSE, N. & HUSSIN, M. H. 2020. Current advancement on the isolation, characterization and application of lignin. *International journal of biological macromolecules,* 162, 985-1024.LIN, Q., HUANG, Y. & YU, W. 2021. Effects of extraction methods on morphology, structure and properties of bamboo cellulose. *Industrial Crops and Products,* 169, 113640.

LIU, R., YU, H. & HUANG, Y. 2005. Structure and morphology of cellulose in wheat straw. *Cellulose,* 12, 25-34.

LU, H., LIN, X., HE, B. & ZHAO, L. 2020. Enhanced separation of cellulose from bamboo with a combined process of steam explosion pretreatment and alkaline-oxidative cooking. *Nordic Pulp & Paper Research Journal,* 35, 386-399.

MANN, A.S., JAIN, N.K., KHARYA, M.D. (2007). Evaluation of the suspending properties of Cassia tora Mucilage on Sulphadimidine suspension. *Asian Journal of Experimental Science*. 21: 63-67.

MANSORA, A. M., LIMA, J. S., ANIB, F. N., HASHIMA, H. & HOA, W. S. 2019. Characteristics of cellulose, hemicellulose and lignin of MD2 pineapple biomass. *Cellulose,* 72, 79-84.

MARCHESSAULT, R. & SUNDARARAJAN, P. 1983. Cellulose. *The polysaccharides.* Elsevier. 5:215-225

MASRULLITA, M., NURLAILA, R., ZULMIARDI, Z., SAFRIWARDY, F., AULIANI, A. & MERIATNA, M. 2022. Synthesis carboxyl methyl cellulose (CMC) from rice straw (Oryza Sativa L.) waste. *International Journal of Engineering,* 2, 24-29.

MEKA, V. S., LI, C. E. & SHESHALA, R. 2016. Design and statistical optimization of effervescent floating drug delivery system of theophylline using response surface methodology. *Acta Pharmaceutica,* 66, 35-51.

MEKONNEN, Z., WORKU, A., YOHANNES, T., ALEBACHEW, M. & KASSA, H. 2014. Bamboo Resources in Ethiopia: Their value chain and contribution to livelihoods. *Ethnobotany Research and Applications,* 12, 511-524.

MOGOŞANU, G. D. & GRUMEZESCU, A. M. 2015. Pharmaceutical natural polymers: structure and chemistry. *Handbook of Polymers for Pharmaceutical Technologies: Structure and Chemistry,* 1, 477-519.

MONDAL, M. I. H., YEASMIN, M. S. & RAHMAN, M. S. 2015. Preparation of food grade carboxymethyl cellulose from corn husk agrowaste. *International Journal of Biological Macromolecules,* 79, 144-150.

MOLLET, H., GRUBENMANN, A. (2001). Formulation technology: emulsions, suspensions, solid forms. WILEY-VCH, Germany, 131-172.

MORÁN, J. I., ALVAREZ, V. A., CYRAS, V. P. & VÁZQUEZ, A. 2008. Extraction of cellulose and preparation of nanocellulose from sisal fibers. *Cellulose*, 15, 149-159.

MORETON, R.C. (2009). Commonly used excipients in pharmaceutical suspensions. In: pharmaceutical suspension from formulation development to manufacturing, Kulshreshtha, A.K., Singh, O.N., Wall, M.G. (eds), 1st edn, *Springer, New York*, pp 67 102.

MOUSSA, I., KHIARI, R., MOUSSA, A., BELGACEM, M. N. & MHENNI, M. F. 2019. Preparation and characterization of carboxymethyl cellulose with a high degree of substitution from agricultural waste. *Acta Pharmaceutica*, 20, 933-943.

NATTAPULWAT N, PURKKAO N, AND SUWITHAYAPAN O. Preparation and application of carboxymethyl yam (Dioscorea esculenta) starch. *Journal of the American Chemical Society,* 2009; 10: 193–198

NAGARAJAN, K., BALAJI, A. & RAMANUJAM, N. 2018. Isolation and characterization of cellulose nanocrystals from Saharan aloe vera cactus fibers. *International Journal of Polymer Analysis and Characterization,* 15, 149-159.

NGADI, N. & LANI, N. S. 2014. Extraction and characterization of cellulose from empty fruit bunch (EFB) fiber. *Journal of Technologies,* 68, 35-39.

NGO, V. A., NGUYEN, T. K. C., TRAN, Q. K., DUONG, X. Q., PHAM, Q. T. & NGO, H. A. T. 2023. Extraction of Pectin and Cellulose from Grapefruit Peels and Production of Carboxymethyl Cellulose. *Journal of Science: Natural Sciences and Technology,* 39, 105-121.

NIKAZAR, S., PEZESHKPOUR, S. & BAHROLOLOUMI, S. 2023. Plant polysaccharides as suspending agents in pharmaceutical suspensions. *Plant Polysaccharides as Pharmaceutical Excipients, 23, 49-81*.

NISHIYAMA, Y., SUGIYAMA, J., CHANZY, H. & LANGAN, P. 2003. Crystal structure and hydrogen bonding system in cellulose Iα from synchrotron X-ray and neutron fiber diffraction. *Journal of the American Chemical Society,* 125, 14300-14306.

NWOKOCHA LM, AND OGUNMOLA GB. Carboxymethylation of cassava starch indifferent solvents and solvent-water mixtures: Optimization of reaction conditions. *J Applied Sci*. 2008; 8: 1581–1585.

OHWOAVWORHUA, F. & ADELAKUN, T. 2010. Non-wood fibre production of microcrystalline cellulose from Sorghum caudatum: Characterisation and tableting properties. *Indian Journal of Pharmaceutical Sciences,* 72, 295.

PAINE, T. D., STEINBAUER, M. J. & LAWSON, S. A. 2011. Native and exotic pests of Eucalyptus: a worldwide perspective. *Annual review of entomology,* 56, 181-201.

PATEL, N., KENNON, L. & LEVINSON, R. 1986. Pharmaceutical suspensions. *The Theory and Practice of Industrial Pharmacy,* 3, 479-501.

PIZZI, A. & EATON, N. 1985. The structure of cellulose by conformational analysis. 2. The cellulose polymer chain. *Journal of Macromolecular Science—Chemistry,* 22, 105-137.

POHJONEN, V. & PUKKALA, T. 1990. Eucalyptus globulus in Ethiopian forestry. *Forest ecology and Management,* 36, 19-31.

POLETTO, M., PISTOR, V. & ZATTERA, A. J. 2013. Structural characteristics and thermal properties of native cellulose. *Cellulose-fundamental aspects,* 2, 45-68.

PUSHPAMALAR, V., LANGFORD, S., AHMAD, M. & LIM, Y. 2006. Optimization of reaction conditions for preparing carboxymethyl cellulose from sago waste. *Carbohydrate polymers,* 64, 312-318.

PUTRO, P. A., SUMARDI, T., SULAEMAN, A. S., ROZA, L., RAMZA, H. & ANUGRAH, D. S. B. 2023. Synthesizing cellulose and its derivatives from pineapple peel: A systematic literature review. *Biointerface Research in Applied Chemistry,* 13, 575.

RAHMAN, M. S., HASAN, M. S., NITAI, A. S., NAM, S., KARMAKAR, A. K., AHSAN, M. S., SHIDDIKY, M. J. & AHMED, M. B. 2021. Recent developments of carboxymethyl cellulose. *Polymers,* 13, 1345.

RANGANAGOWDA, R., KAMATH, S. & BENNEHALLI, B. 2019. Extraction and characterization of cellulose from natural areca fiber. *Material Science Research,* 16, 86-93.

RASHID, S., DUTTA, H., 2022. Physicochemical characterization of carboxymethyl cellulose from differently sized rice husks and application as cake additive. *Lwt-Food Science Technology,* 154, 112630.

REDDY, N. & YANG, Y. 2005. Properties and potential applications of natural cellulose fibers from cornhusks. *Green Chemistry,* 7, 190-195.

REDDY, N. & YANG, Y. 2006. Properties of high-quality long natural cellulose fibers from rice straw. *Journal of agricultural and food chemistry,* 54, 8077-8081.

ROMINIYI, O., ADARAMOLA, B., IKUMAPAYI, O., OGINNI, O. & AKINOLA, S. 2017. Potential utilization of sawdust in energy, manufacturing and agricultural industry; waste to wealth. *World Journal of Engineering and Technology,* 5, 526-539.

ROSA, S. M., REHMAN, N., DE MIRANDA, M. I. G., NACHTIGALL, S. M. & BICA, C. I. 2012. Chlorine-free extraction of cellulose from rice husk and whisker isolation. *Carbohydrate Polymers,* 87, 1131-1138.

SAEEDI M, DALLALPOOR-MOHAMMADI N AND FARID D. (2003). Prevention of crystal growth in acetaminophen suspensions by the use of polyvinyl pyrrolidone and bovine serum albumin. *Carbohydrate polymers,* 11: 106-114.

SAELEE, K., YINGKAMHAENG, N., NIMCHUA, T. & SUKYAI, P. Extraction and characterization of cellulose from sugarcane bagasse by using environmentally friendly method. Proceedings of the 26th annual meeting of the thai society for biotechnology and international conference, Mae Fah Lunag University (School of Science), Thailand, 2014. 26-29.

SAHA, B. C. 2003. Hemicellulose bioconversion. *Journal of Industrial Microbiology and Biotechnology,* 30, 279-291.

SALAMA, A., ETRI, S., MOHAMED, S. A. & EL-SAKHAWY, M. 2018. Carboxymethyl cellulose prepared from mesquite tree: New source for promising nanocomposite materials. *Carbohydrate polymers,* 189, 138-144.

SAPUTRA, A. H., QADHAYNA, L. & PITALOKA, A. B. 2014. Synthesis and characterization of carboxymethyl cellulose (CMC) from water hyacinth using ethanol-isobutyl alcohol mixture as the solvents. *International Journal of Chemical Engineering and Applications,* 5, 36.

SCHELLER, H. V. & ULVSKOV, P. 2010. Hemicelluloses. *Annual Review of Plant Biology,* 61, 263-289.

SCHNEIDER, L., DONG, Y., HAVERINEN, J., JAAKKOLA, M. & LASSI, U. 2016. Efficiency of acetic acid and formic acid as a catalyst in catalytical and mechanocatalytical pretreatment of barley straw. *Biomass and Bioenergy,* 91, 134-142.

SCZOSTAK, A. Cotton linters: an alternative cellulosic raw material. Macromolecular Symposia, 2009. *Wiley Online Library*, 13, 45-53.

SHOGREN, R. L., PETERSON, S. C., EVANS, K. O. & KENAR, J. A. 2011. Preparation and characterization of cellulose gels from corn cobs. *Carbohydrate Polymers,* 86, 1351-1357.

SHOKRI, J. & ADIBKIA, K. 2013. Application of cellulose and cellulose derivatives in pharmaceutical industries. *Cellulose-medical, pharmaceutical and electronic applications,* 11, 98-116.

SINGH, R. K. & SINGH, A. K. 2013. Optimization of reaction conditions for preparing carboxymethyl cellulose from corn cobic agricultural waste. *Waste and Biomass Valorization,* 4, 129-137.

SUN, J., SUN, X., ZHAO, H. & SUN, R. 2004. Isolation and characterization of cellulose from sugarcane bagasse. *Polymer degradation and stability,* 84, 331-339.

SUN, R. & TOMKINSON, J. 2005. Separation and characterization of cellulose from wheat straw. *Separation science and technology,* 39, 391-411.

SUTHAR AM, AND PATEL MM. 2011. Formulation and evaluation of taste-masked suspension of metronidazole. *Carbohydrate Polymers,* 86, 1351-1357

TARCHOUN, A.F., TRACHE, D., KLAPÖTKE, T.M., 2019. Microcrystalline cellulose from Posidonia oceanica brown algae: Extraction and characterization. *Carbohydrate Polymers,* 54, 73-82.

TEJADA-TOVAR, C., VILLABONA-ORTÍZ, A., ORTEGA-TORO, R., MANCILLA-BONILLA, H. & ESPINOZA-LEÓN, F. 2021. Potential use of residual sawdust of Eucalyptus Globulus Labill in Pb (II) adsorption: Modelling of the kinetics and equilibrium. *Applied Sciences,* 11, 3125.

TOĞRUL, H. & ARSLAN, N. 2003. Production of carboxymethyl cellulose from sugar beet pulp cellulose and rheological behaviour of carboxymethyl cellulose. *Carbohydrate Polymers,* 54, 73-82.

United States Pharmacopeia. 35th revision. National Formulary 30th ed. (2012). United States Pharmacopeial Convention, Inc., meeting at Washington, D.C.

United States Pharmacopoeia 38th ed. National Formulary 33 ed. (USP 38/NF 33) (2015). The United States Pharmacopeial Convention 12601 Twinbrook Parkway, Rockville, MD 20852.

ÜNLÜ, C. H. 2013. Carboxymethylcellulose from recycled newspaper in aqueous medium. *Carbohydrate polymers,* 97, 159-164.

VALLEJOS, M. E., FELISSIA, F. E., AREA, M. C., EHMAN, N. V., TARRÉS, Q. & MUTJÉ, P. 2016. Nanofibrillated cellulose (CNF) from eucalyptus sawdust as a dry strength agent of unrefined eucalyptus handsheets. *Carbohydrate polymers,* 139, 99-105.

VARSHNEY, V., GUPTA, P., NAITHANI, S., KHULLAR, R., BHATT, A. & SONI, P. 2006. Carboxymethylation of α-cellulose isolated from Lantana camara with respect to degree of substitution and rheological behavior. *Carbohydrate polymers,* 63, 40-45.

VASSILEV, S. V., BAXTER, D., ANDERSEN, L. K. & VASSILEVA, C. G. 2010. An overview of the chemical composition of biomass. *Fuel,* 89, 913-933.

VEERAMACHINENI, A. K., SATHASIVAM, T., MUNIYANDY, S., JANARTHANAN, P., LANGFORD, S. J. & YAN, L. Y. 2016. Optimizing extraction of cellulose and synthesizing pharmaceutical grade carboxymethyl sago cellulose from malaysian sago pulp. *Applied Sciences,* 6, 170.

WANG, K., JIANG, J., XU, F. & SUN, R. 2009. Influence of steaming pressure on steam explosion pretreatment of Lespedeza stalks (Lespedeza crytobotrya): Part 1. Characteristics of degraded cellulose. *Polymer Degradation and Stability,* 94, 1379-1388

WHETTEN, R. & SEDEROFF, R. 1995. Lignin Biosynthesis. *The Plant Cell,* 7, 1001-1013.

WÜSTENBERG, T. 2014. *Cellulose and cellulose derivatives in the food industry: fundamentals and applications*, John Wiley & Sons.

Yang, H., Yan, R., Chen, H., Lee, D.H., Zheng, C., 2007. Characteristics of hemicellulose, cellulose and lignin pyrolysis. *Fuel* 86, 1781–1788.

YAŞAR, F., TOĞRUL, H. & ARSLAN, N. 2007. Flow properties of cellulose and carboxymethyl cellulose from orange peel. *Journal of food Engineering,* 81, 187-199.

YEASMIN, M. S. & MONDAL, M. I. H. 2015. Synthesis of highly substituted carboxymethyl cellulose depending on cellulose particle size. *International journal of biological macromolecules,* 80, 725-731.

YILDIRIM-YALCIN, M., TORNUK, F. & TOKER, O. S. 2022. Recent advances in the improvement of carboxymethyl cellulose-based edible films. *Trends in Food Science & Technology,* 129, 179-193.

ZAINI, L. H., JONOOBI, M., TAHIR, P. M. & KARIMI, S. 2013. Isolation and characterization of cellulose whiskers from kenaf (Hibiscus cannabinus L.) bast fibers. *International journal of biological macromolecules,* 80, 725-731.

ZENNIFER, A., SENTHILVELAN, P., SETHURAMAN, S. & SUNDARAMURTHI, D. 2021. Key advances of carboxymethyl cellulose in tissue engineering & 3D bioprinting applications. *Carbohydrate polymers,* 256, 117561.

ZHANG, G., ZHANG, L., DENG, H. & SUN, P. 2011. Preparation and characterization of sodium carboxymethyl cellulose from cotton stalk using microwave heating. *Journal of Chemical Technology & Biotechnology,* 86, 584-589.

ZHANG, J., SONG, H., LIN, L., ZHUANG, J., PANG, C. & LIU, S. 2012. Microfibrillated cellulose from bamboo pulp and its properties. *Biomass and Bioenergy,* 39, 78-83.